

FILAMENTS: FAD OR FUNDAMENTAL?

Alyssa A. Goodman
Harvard-Smithsonian Center for Astrophysics
Radcliffe Institute for Advanced Study
@aagie



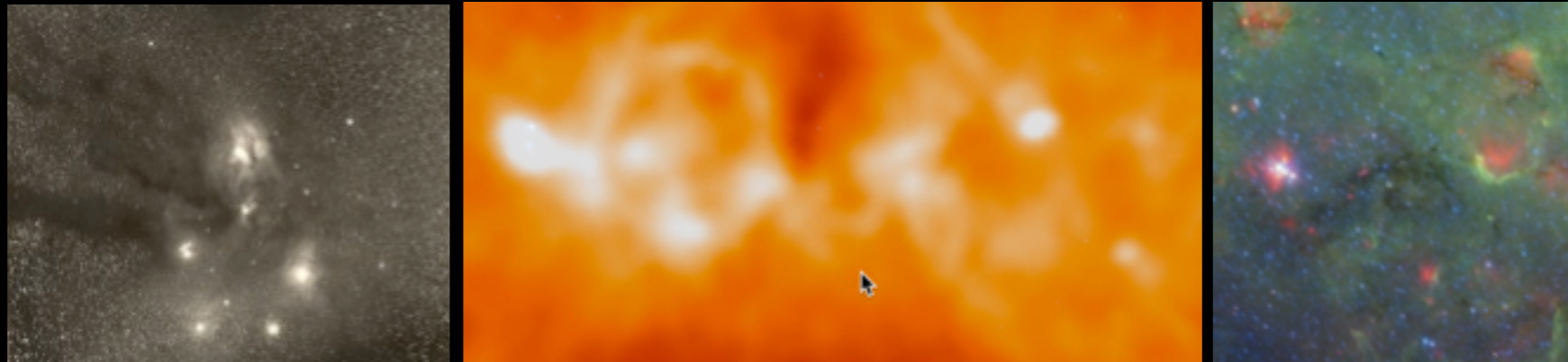
Ophiuchus, Barnard 1919



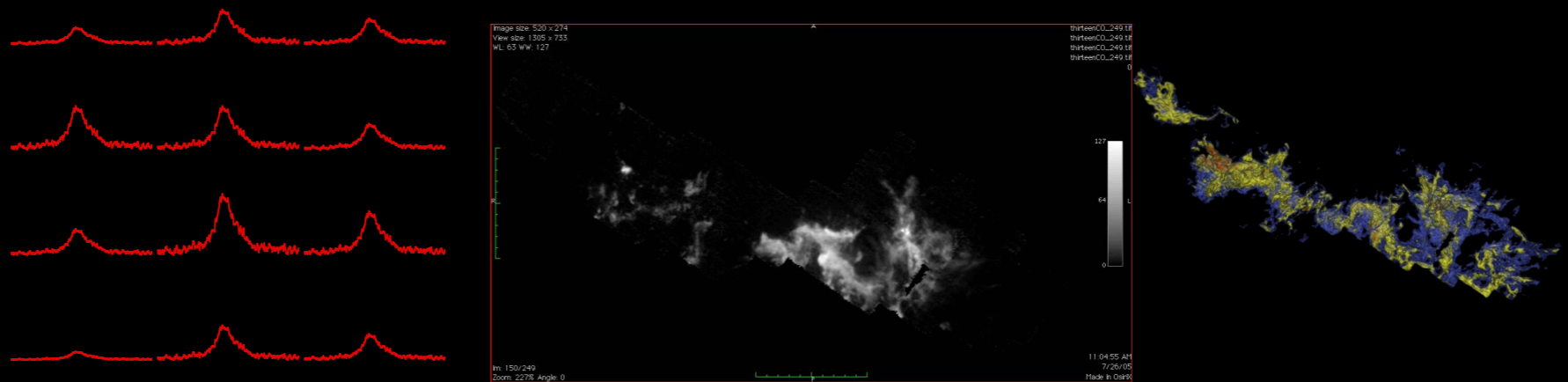
Ophiuchus, Barnard 1919

WHAT CAN WE SEE

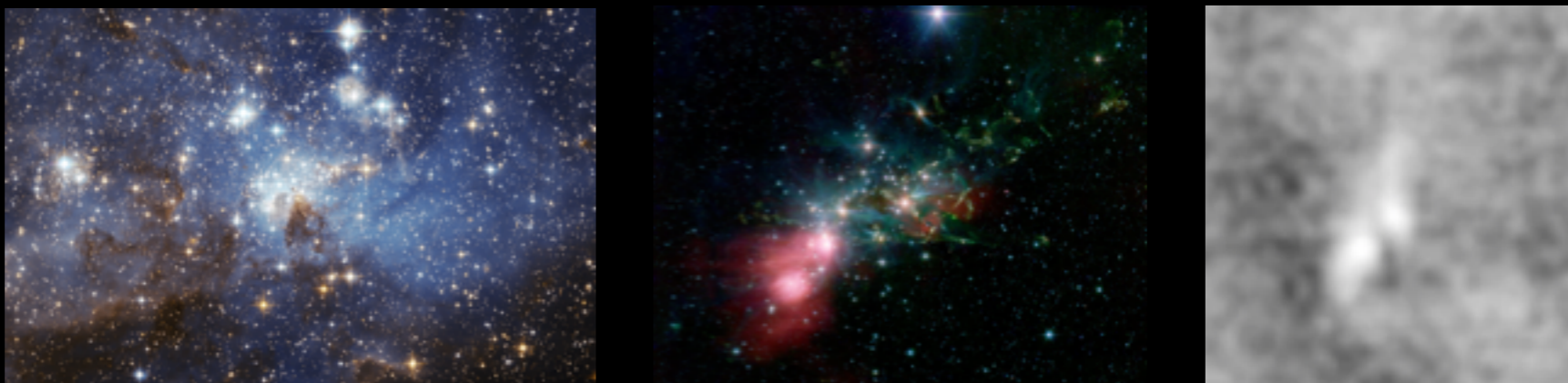
Dust



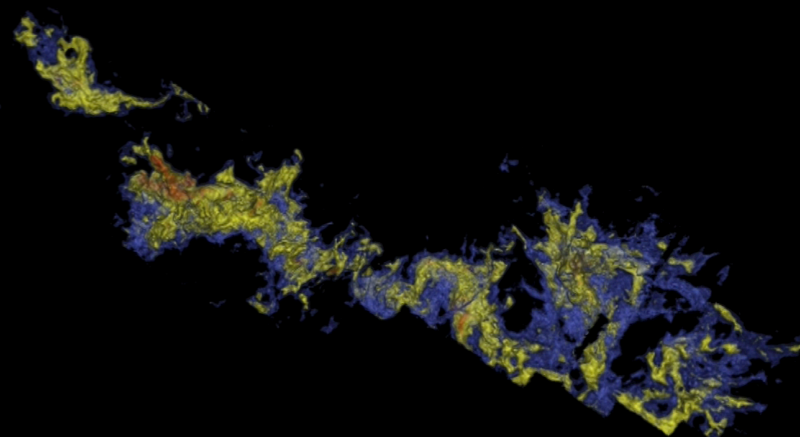
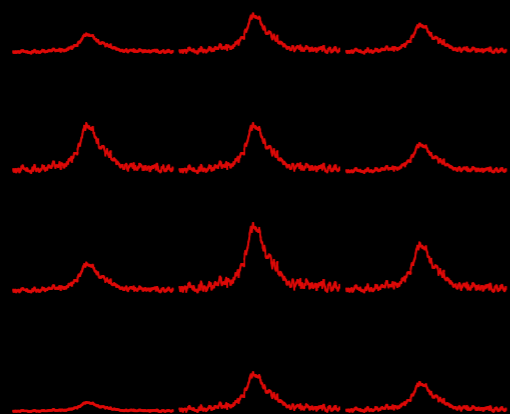
Gas



"Stars"



HOW WE "SEE"



IN 3D

Atomic Gas

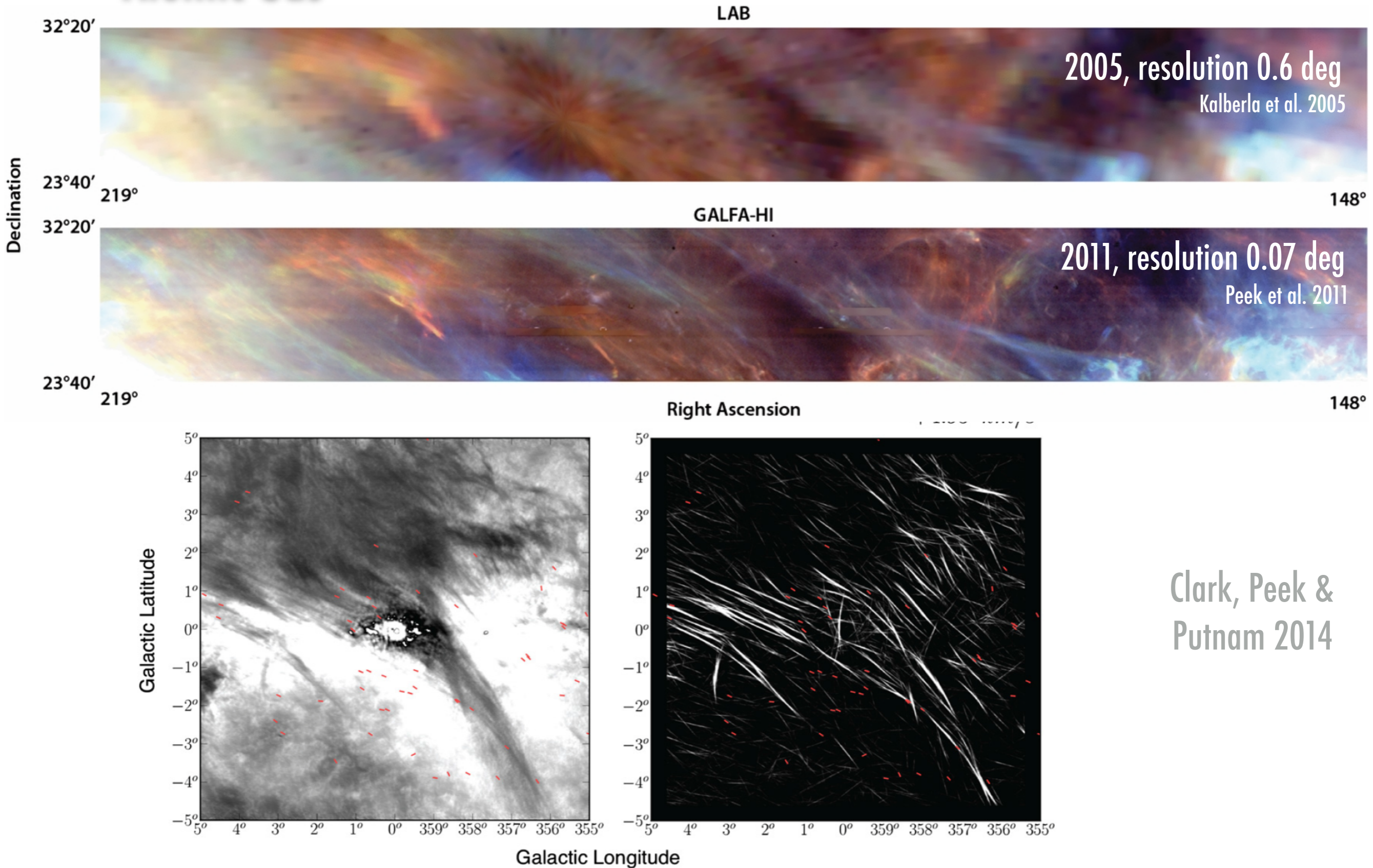
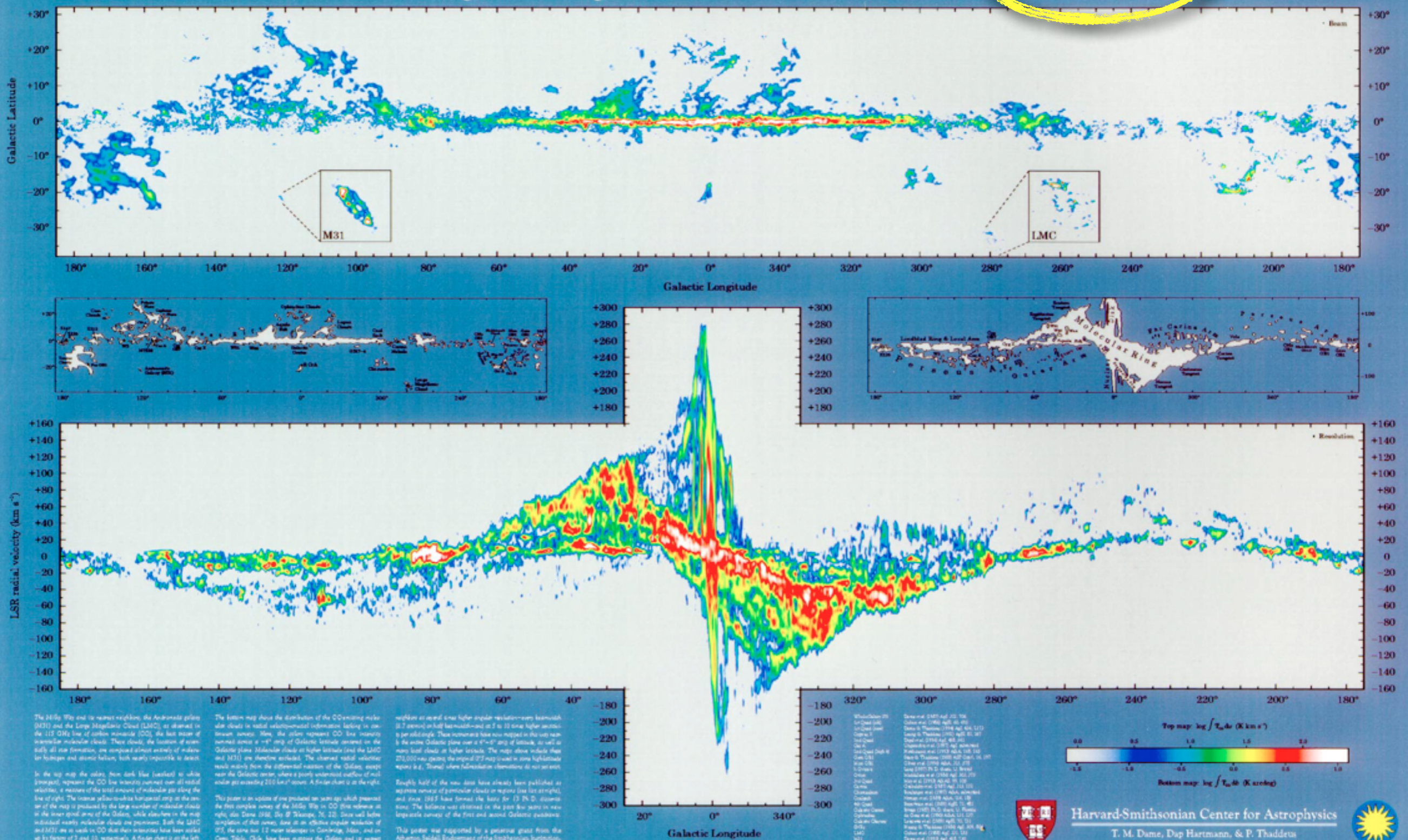


Figure 10. Riegel–Crutcher cloud (Section 6) in H I absorption (left) and RHT backprojection (right). Overlaid pseudovectors represent polarization angle measurements from the Heiles (2000) compilation. In the left panel, the intensity scale is linear from -20 K (white) to -120 K (black).

(A color version of this figure is available in the online journal.)

Clark, Peek &
Putnam 2014

The Milky Way in Molecular Clouds



The Milky Way and its nearest neighbors, the Andromeda galaxy (M31) and the Large Magellanic Cloud (LMC), as observed in the 115 GHz line of carbon monoxide (CO), the best tracer of interstellar molecular clouds. These clouds, the location of essentially all star formation, are composed almost entirely of molecular hydrogen and atomic helium, both nearly impossible to detect.

In the top map the colors from dark blue (weakest) to white (strongest) represent the CO line intensity summed over all radial velocities, a measure of the total amount of molecular gas along the line of sight. The intense yellow-white horizontal strip at the center of the map is produced by the large number of molecular clouds in the inner spiral arm of the Galaxy, while elsewhere in the map individual nearby molecular clouds are prominent. Both the LMC and M31 are in view in CO but their molecules have been excited up by beams of 2 and 23, respectively. A finer chart is on the left.

The bottom map shows the distribution of the CO emitting molecular clouds in radial velocity-bin-by-bin observations lacking in common sources. Here, the yellow represents CO line intensity summed across a 4° strip of Galactic latitude centered on the Galactic plane. Molecular clouds at higher latitudes (and the LMC and M31) are otherwise excluded. The observed radial velocity results mainly from the differential rotation of the Galaxy, except near the Galactic center, where a poorly understood outflow of molecular gas exceeding 200 km/s occurs. A finer chart is on the right.

This paper is an update of one produced ten years ago which presented the first complete survey of the Milky Way in CO line emission at night, also Dame 1990, *City of Stars*, p. 22. Data well before completion of that survey, done at an effective angular resolution of 95", the stars had 12 major colleagues in Cambridge, Mass., and on Oahu, Hawaii, Ohio, have been mapping the Galaxy and its nearest

neighbors at several times higher angular resolution—now least-much 3.7 arcmin on half-beamwidth—and at 2 to 20 times higher accuracy per solid angle. These surveys have now merged in this way nearly the entire Galactic plane over a 6°-6° strip of latitude, as well as many local clouds at higher latitudes. The maps above indicate that 270,000 new objects the original 277 map revealed in some high-latitude regions (e.g., Theta) where full-resolution observations do not penetrate.

Tenfold half of the new data have already been published as separate surveys of particular clouds or regions (see list at right), and since 1993 have formed the basis for 13 Ph.D. dissertations. The follow-up was obtained in the past few years in new large-scale surveys of the first and second Galactic quadrants.

This paper was supported by a postdoctoral grant from the Ad Astra Fund, Endowment of the Smithsonian Institution.

Whitcomb (1993), Dame et al. (1993), Dame et al. (1994), Dame et al. (1995), Dame et al. (1996), Dame et al. (1997), Dame et al. (1998), Dame et al. (1999), Dame et al. (2000), Dame et al. (2001), Dame et al. (2002), Dame et al. (2003), Dame et al. (2004), Dame et al. (2005), Dame et al. (2006), Dame et al. (2007), Dame et al. (2008), Dame et al. (2009), Dame et al. (2010), Dame et al. (2011), Dame et al. (2012), Dame et al. (2013), Dame et al. (2014), Dame et al. (2015), Dame et al. (2016), Dame et al. (2017), Dame et al. (2018), Dame et al. (2019), Dame et al. (2020), Dame et al. (2021), Dame et al. (2022), Dame et al. (2023), Dame et al. (2024), Dame et al. (2025).

Dame et al. (1987) *AJ*, 92, 106
 Dame et al. (1988) *AJ*, 95, 49
 Dame et al. (1989) *AJ*, 98, 1213
 Dame et al. (1990) *AJ*, 100, 40
 Dame et al. (1991) *AJ*, 102, 40
 Dame et al. (1992) *AJ*, 104, 40
 Dame et al. (1993) *AJ*, 106, 40
 Dame et al. (1994) *AJ*, 108, 40
 Dame et al. (1995) *AJ*, 110, 40
 Dame et al. (1996) *AJ*, 112, 40
 Dame et al. (1997) *AJ*, 114, 40
 Dame et al. (1998) *AJ*, 116, 40
 Dame et al. (1999) *AJ*, 118, 40
 Dame et al. (2000) *AJ*, 120, 40
 Dame et al. (2001) *AJ*, 122, 40
 Dame et al. (2002) *AJ*, 124, 40
 Dame et al. (2003) *AJ*, 126, 40
 Dame et al. (2004) *AJ*, 128, 40
 Dame et al. (2005) *AJ*, 130, 40
 Dame et al. (2006) *AJ*, 132, 40
 Dame et al. (2007) *AJ*, 134, 40
 Dame et al. (2008) *AJ*, 136, 40
 Dame et al. (2009) *AJ*, 138, 40
 Dame et al. (2010) *AJ*, 140, 40
 Dame et al. (2011) *AJ*, 142, 40
 Dame et al. (2012) *AJ*, 144, 40
 Dame et al. (2013) *AJ*, 146, 40
 Dame et al. (2014) *AJ*, 148, 40
 Dame et al. (2015) *AJ*, 150, 40
 Dame et al. (2016) *AJ*, 152, 40
 Dame et al. (2017) *AJ*, 154, 40
 Dame et al. (2018) *AJ*, 156, 40
 Dame et al. (2019) *AJ*, 158, 40
 Dame et al. (2020) *AJ*, 160, 40
 Dame et al. (2021) *AJ*, 162, 40
 Dame et al. (2022) *AJ*, 164, 40
 Dame et al. (2023) *AJ*, 166, 40
 Dame et al. (2024) *AJ*, 168, 40
 Dame et al. (2025) *AJ*, 170, 40

Molecular Gas "Clouds"

Rice et al. 2016

video: Matt Pasquini



THE ASTROPHYSICAL JOURNAL, 822:52 (27pp), 2016 May 1
© 2016. The American Astronomical Society. All rights reserved.

doi:10.3847/0004-637X/822/1/52



A UNIFORM CATALOG OF MOLECULAR CLOUDS IN THE MILKY WAY

THOMAS S. RICE¹, ALYSSA A. GOODMAN², EDWIN A. BERGIN¹, CHRISTOPHER BEAUMONT³, AND T. M. DAME²

¹Department of Astronomy, University of Michigan, 311 West Hall, 1085 South University Avenue, Ann Arbor, MI 48109, USA; tsrice@umich.edu

²Harvard-Smithsonian Center for Astrophysics, 60 Garden Street, Cambridge, MA 02138, USA

³Counsyl, 180 Kimball Way, South San Francisco, CA 94080, USA

Received 2015 July 14; accepted 2016 February 4; published 2016 May 3

ABSTRACT

The all-Galaxy CO survey of Dame et al. is by far the most uniform, large-scale Galactic CO survey. Using a dendrogram-based decomposition of this survey, we present a catalog of 1064 massive molecular clouds throughout the Galactic plane. This catalog contains 2.5×10^8 solar masses, or $25^{+10.7}_{-5.8}$ % of the Milky Way's estimated H_2 mass. We track clouds in some spiral arms through multiple quadrants. The power index of Larson's first law, the size-linewidth relation, is consistent with 0.5 in all regions—possibly due to an observational bias—but clouds in the inner Galaxy systematically have significantly ($\sim 30\%$) higher linewidths at a given size, indicating that their linewidths are set in part by the Galactic environment. The mass functions of clouds in the inner Galaxy versus the outer Galaxy are both qualitatively and quantitatively distinct. The inner Galaxy mass spectrum is best described by a truncated power law with a power index of $\gamma = -1.6 \pm 0.1$ and an upper truncation mass of $M_0 = (1.0 \pm 0.2) \times 10^7 M_\odot$, while the outer Galaxy mass spectrum is better described by a non-truncating power law with $\gamma = -2.2 \pm 0.1$ and an upper mass of $M_0 = (1.5 \pm 0.5) \times 10^6 M_\odot$, indicating that the inner Galaxy is able to form and host substantially more massive GMCs than the outer Galaxy. Additionally, we have simulated how the Milky Way would appear in CO from extragalactic perspectives, for comparison with CO maps of other galaxies.

Key words: Galaxy: general – ISM: clouds – ISM: molecules

Supporting material: machine-readable table

THE ASTROPHYSICAL JOURNAL, 822:52 (27pp), 2016 May 1

RICE ET AL.

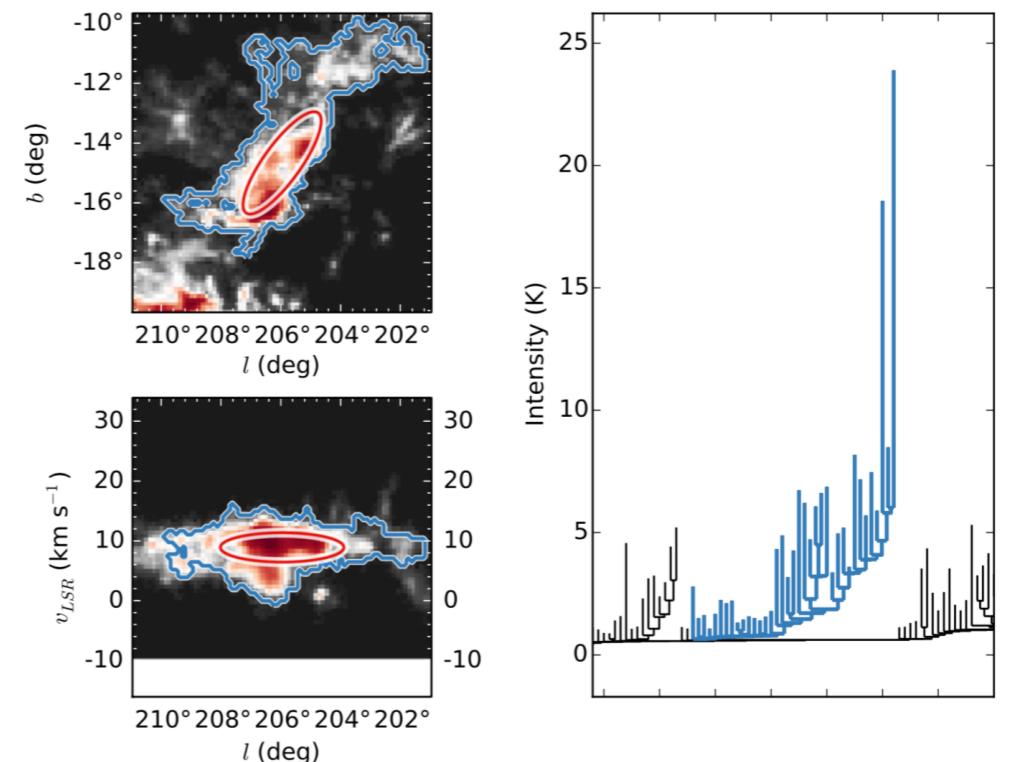
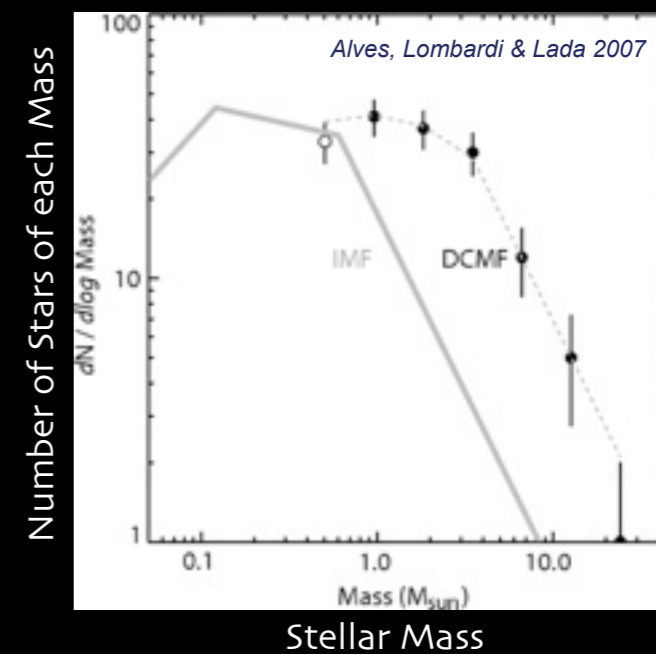
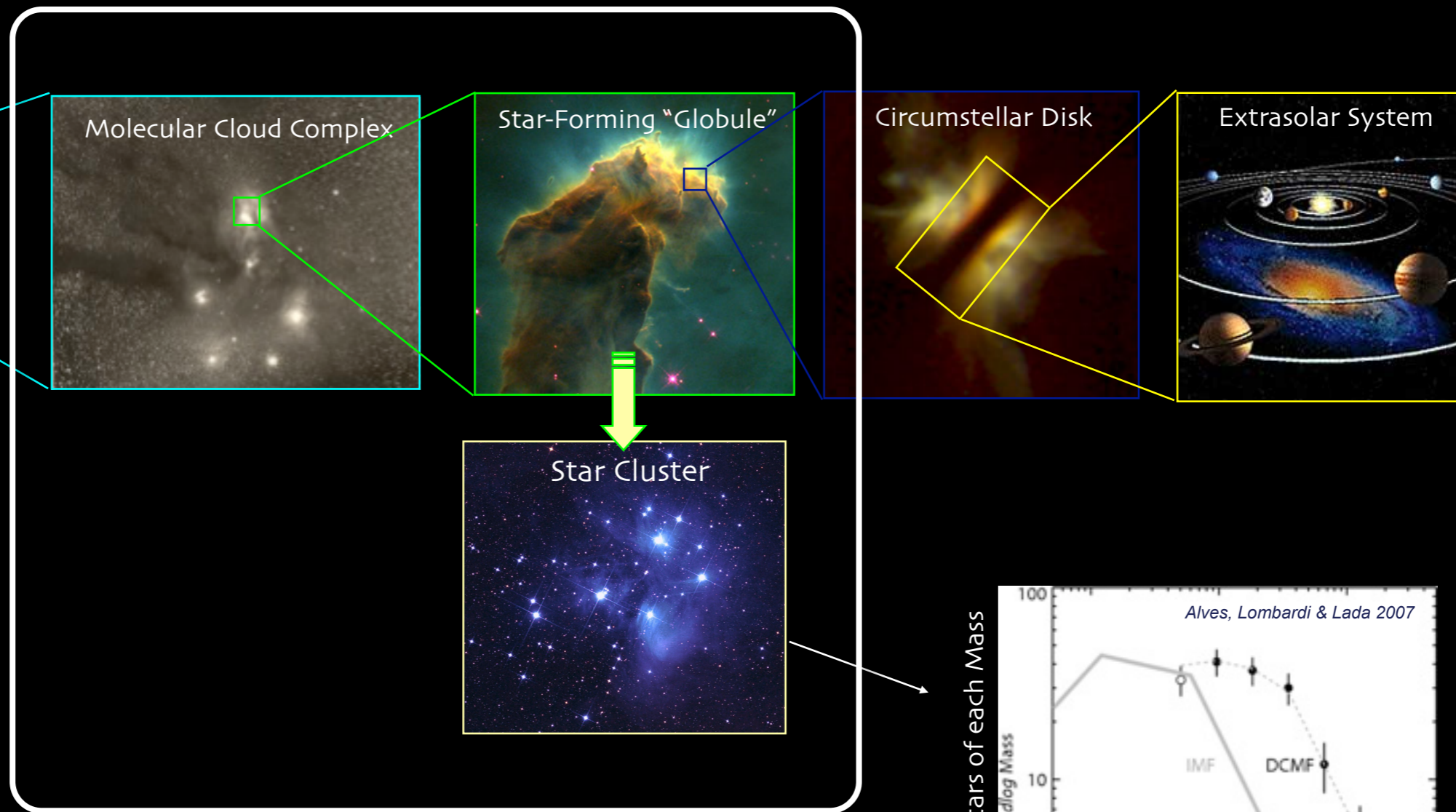
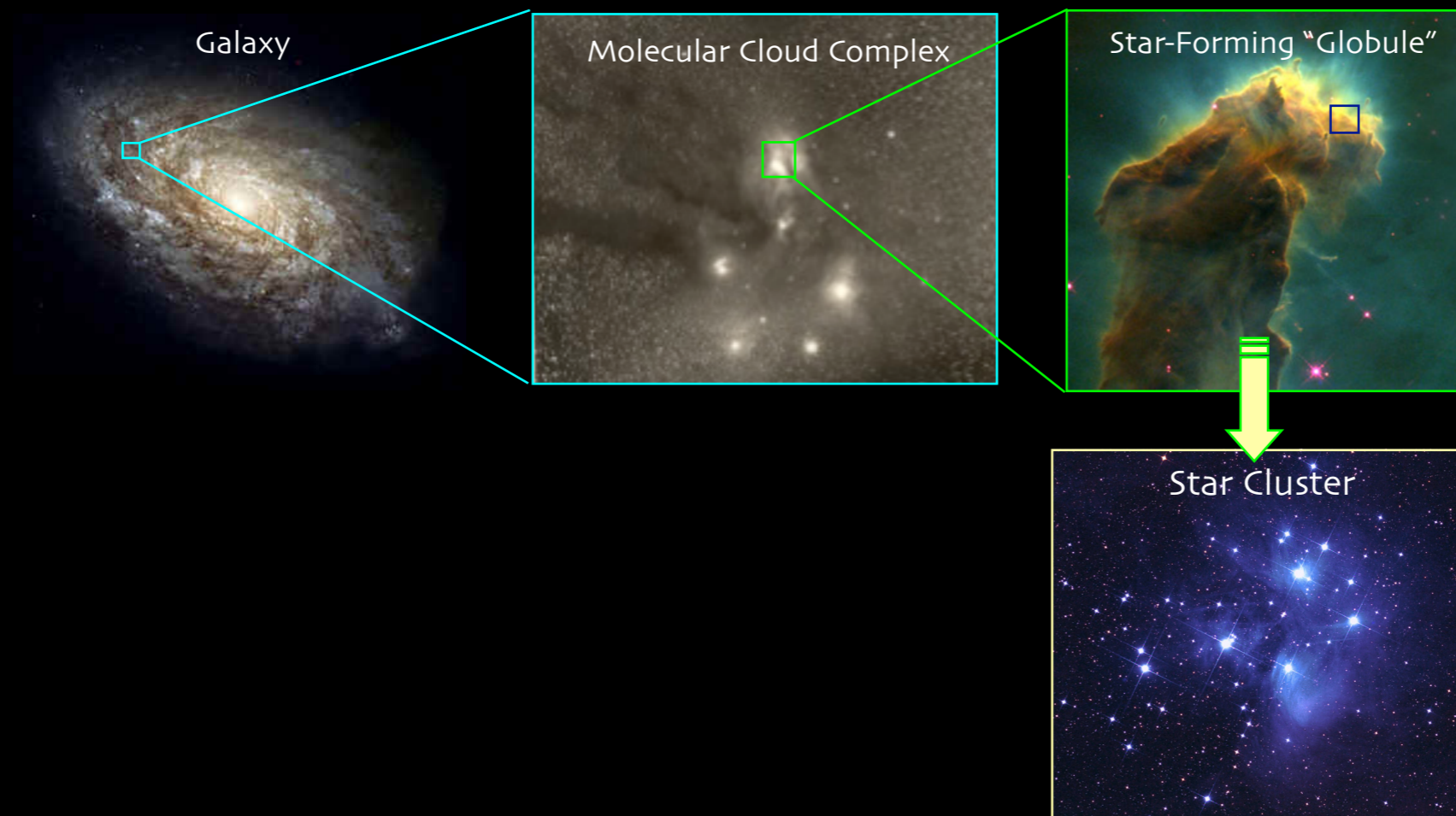
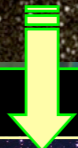
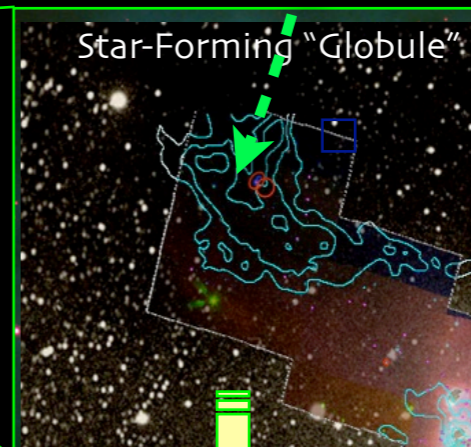
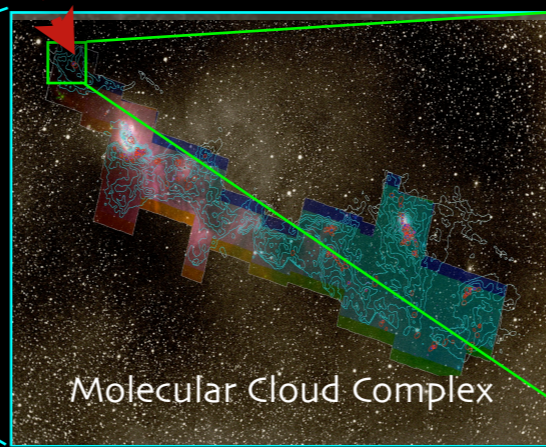
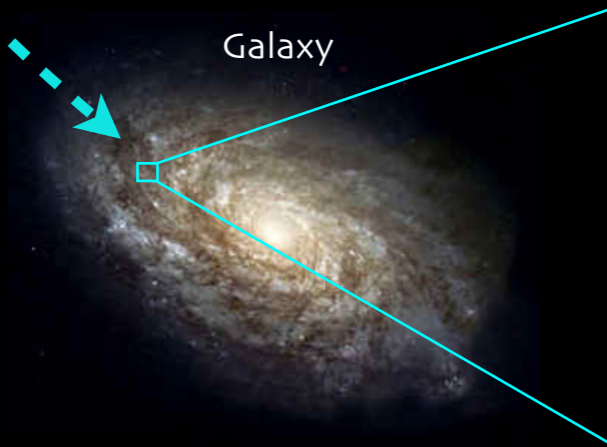
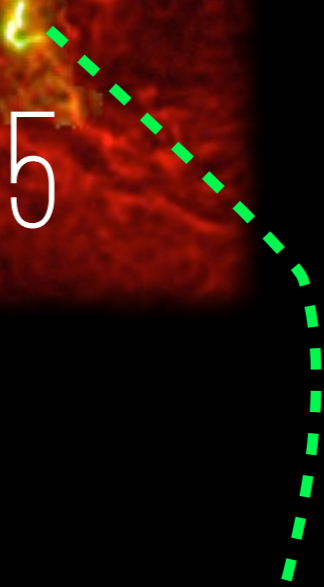
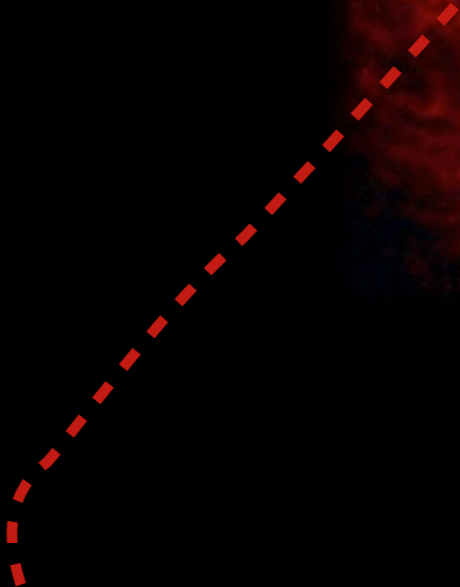
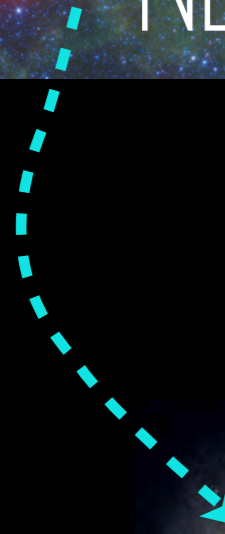
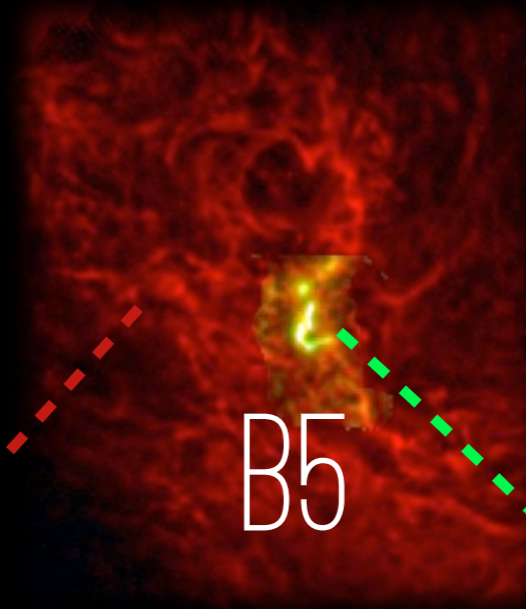


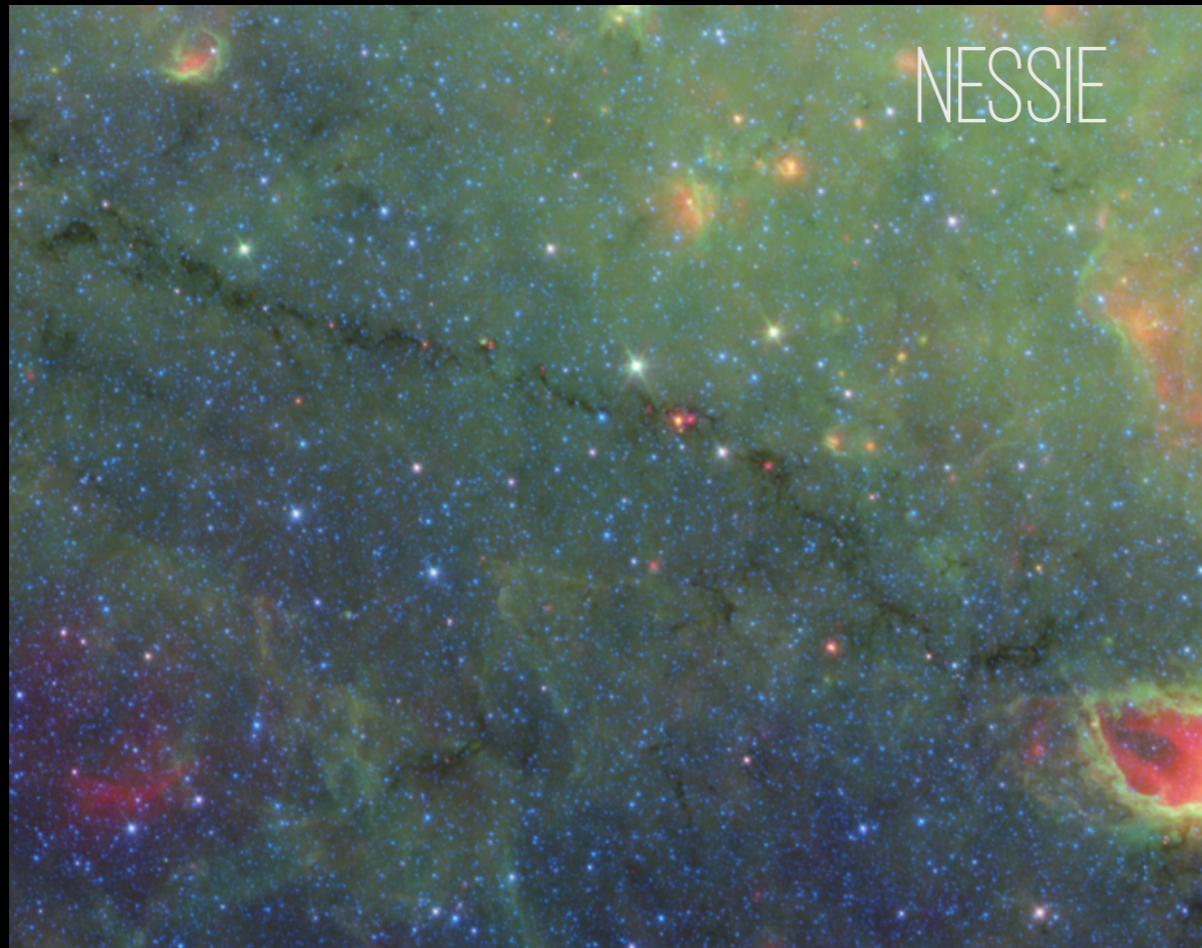
Figure 2. Example dendrogram extraction of Orion B: a nearby, well-studied giant molecular cloud. Top left: (l, b) thumbnail of the cloud and its neighboring region as seen on the sky. Bottom left: (l, v) thumbnail of the same region. Right: dendrogram cutout, with Orion B's structures highlighted in blue. The pixels corresponding to the highlighted dendrogram structures are outlined in the blue contour (in projection); a representative ellipse is drawn in red, with semimajor axis length equal to the second moment along each relevant dimension (as calculated in Section 2.2). Data come from DHT Survey #27 (the Orion complex).

HOW STARS FORM



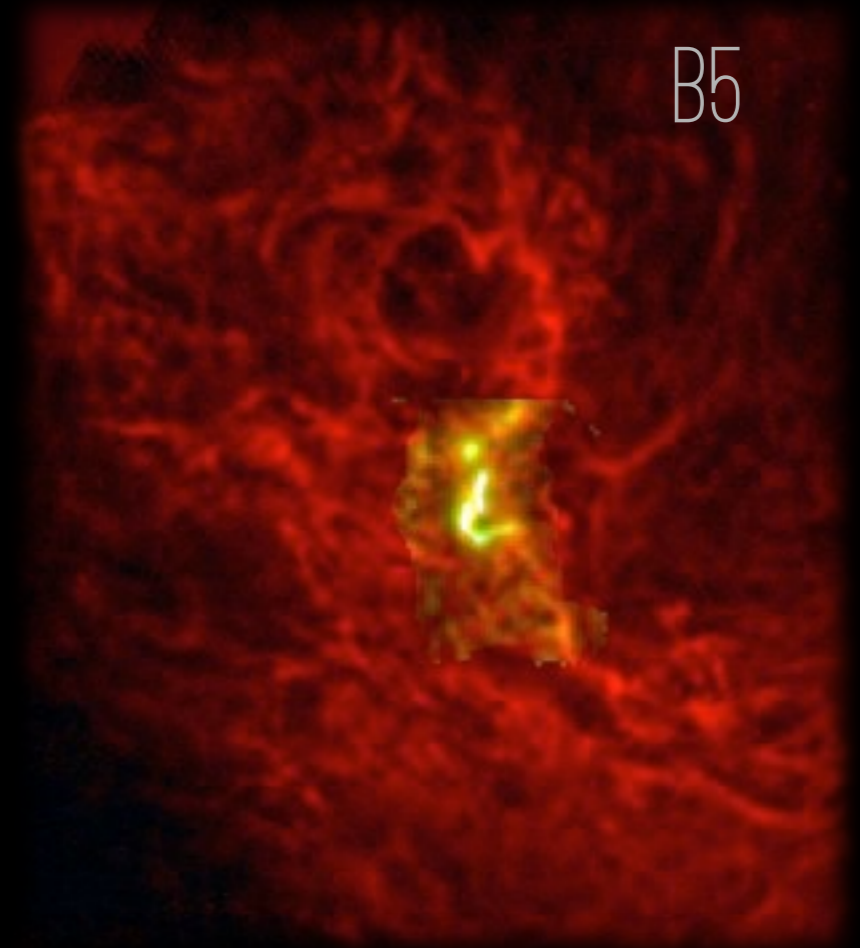






NESSIE

>100 pc



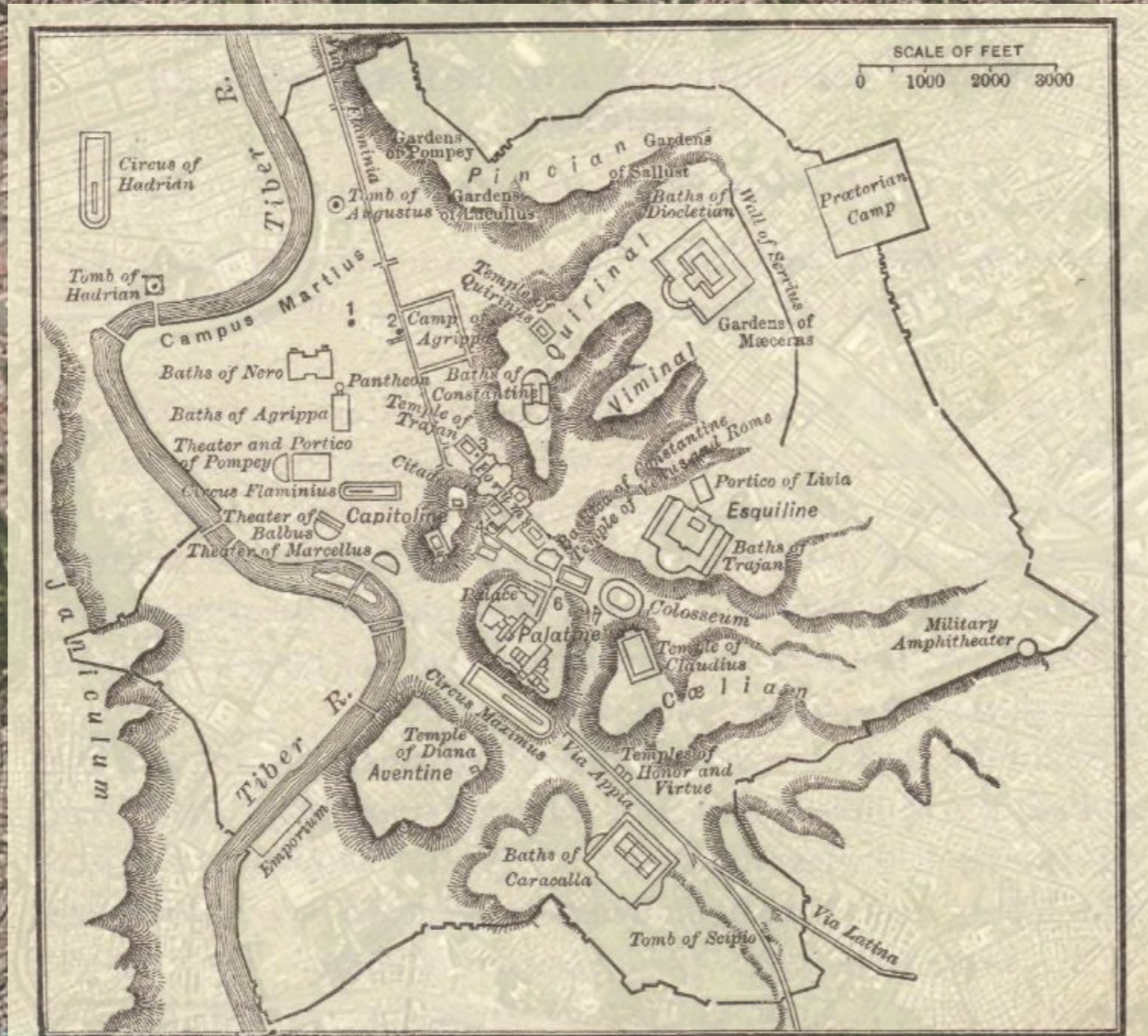
B5

~ 0.01 to 10 pc

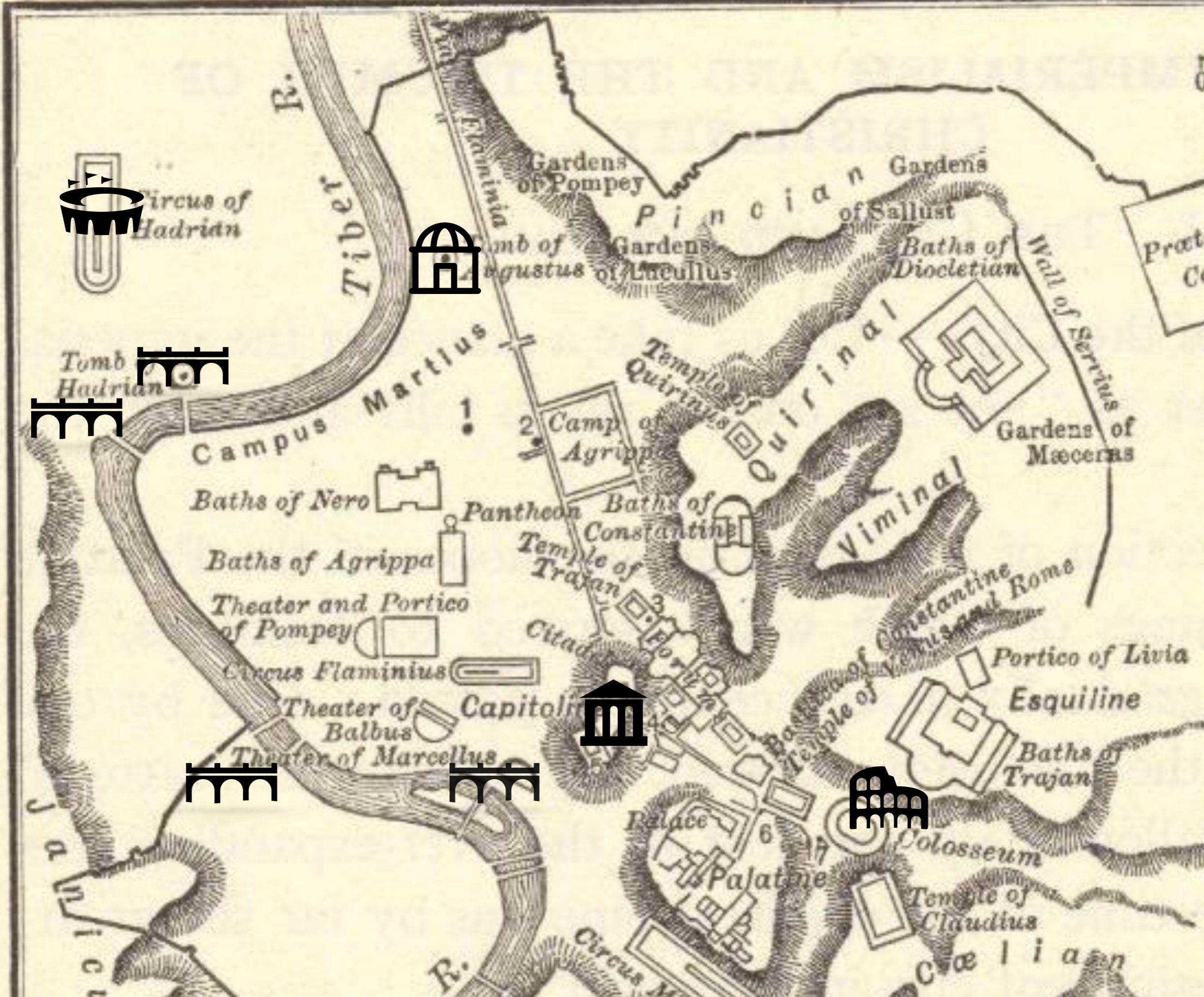
An aerial photograph of Rome, Italy, showing the Tiber River winding through the city. The image captures a dense urban landscape with a mix of historic and modern buildings, green spaces, and infrastructure. The Tiber River is a prominent feature, curving through the center of the city. The overall scene is a detailed view of the city's layout and its relationship with the river.

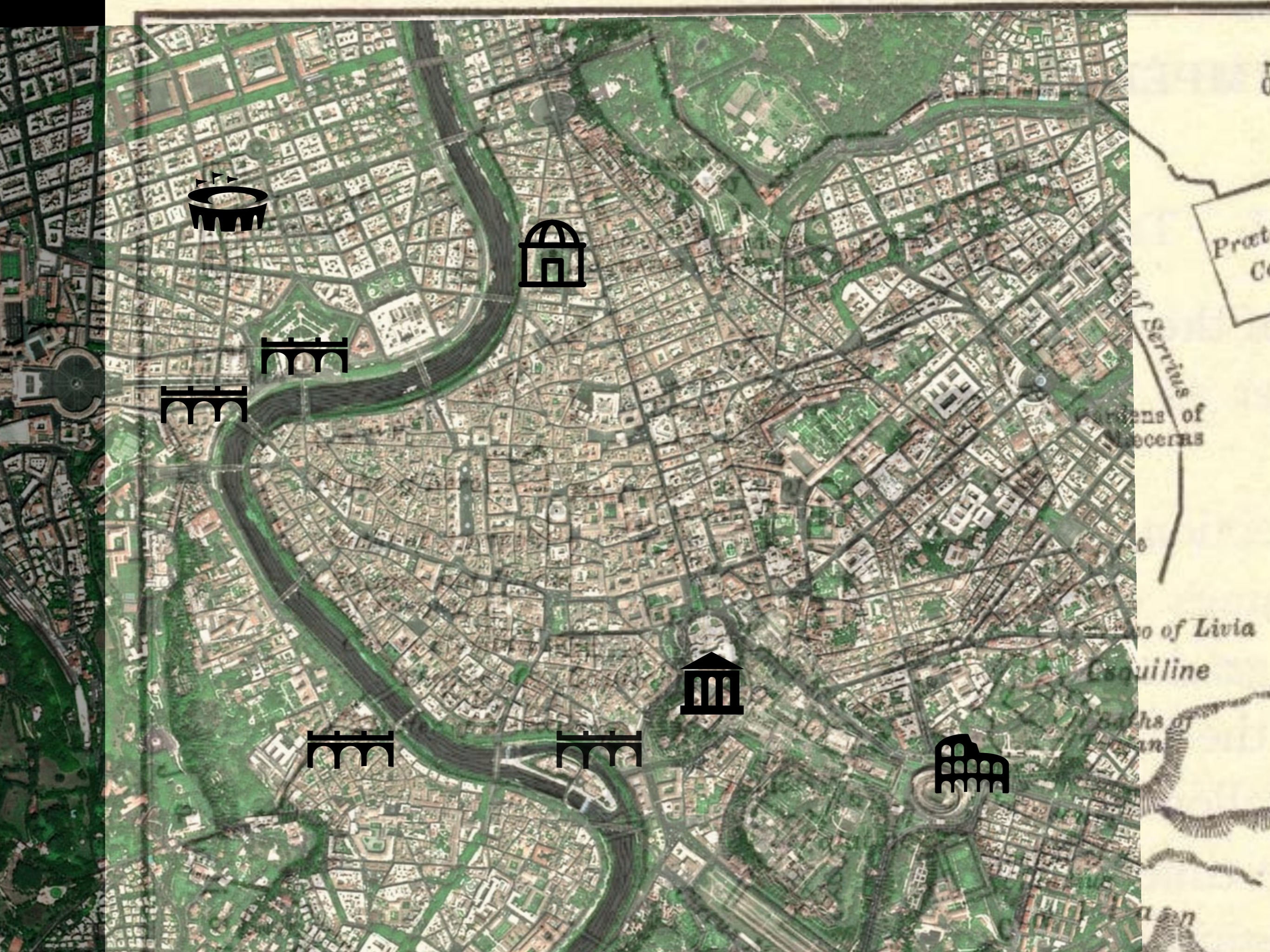
ROME 2016 AD

2000 YEARS AGO...



2000 YEARS AGO...





Praet
Co

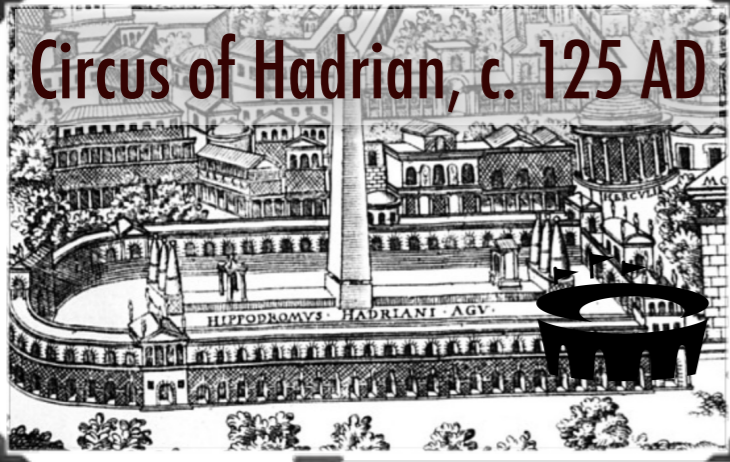
Servius
of
Livia
Cauline

of Livia
Cauline

Baths of
Livia

Livia

Circus of Hadrian, c. 125 AD



Mausoleum of Augustus, 28 BC



ALL STONE ALL IN ROME

Ponte Sant'Angelo, 134 (Hadrian)



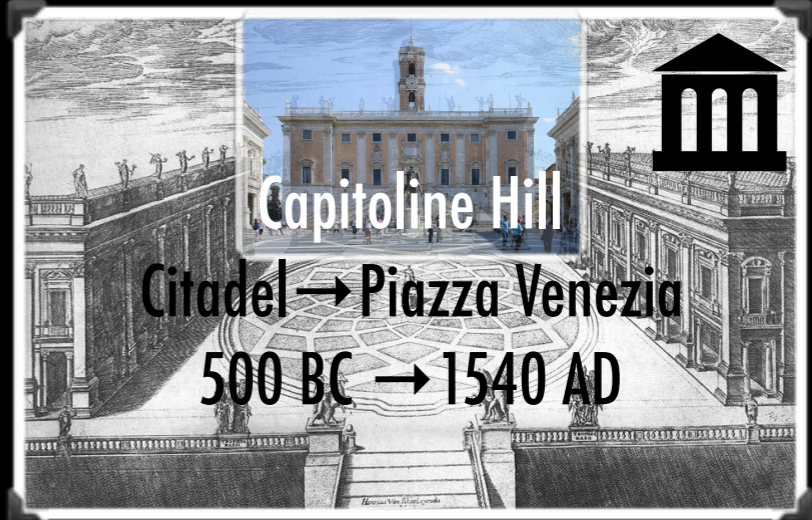
Pons Neronianus, c. 50 AD,
under Ponte Sant'Angelo

Ponte Vittorio Emanuele II, 1886



Capitoline Hill

Citadel → Piazza Venezia
500 BC → 1540 AD

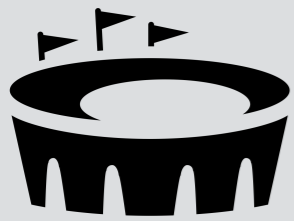


Pons Fabricius, 62 BC
(oldest in Rome)



Colosseum, 90 AD





≠



≠



≠

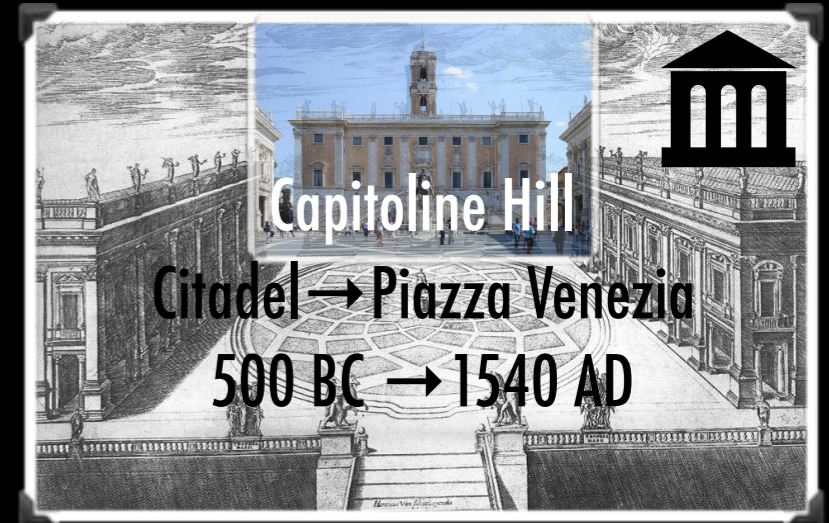


≠

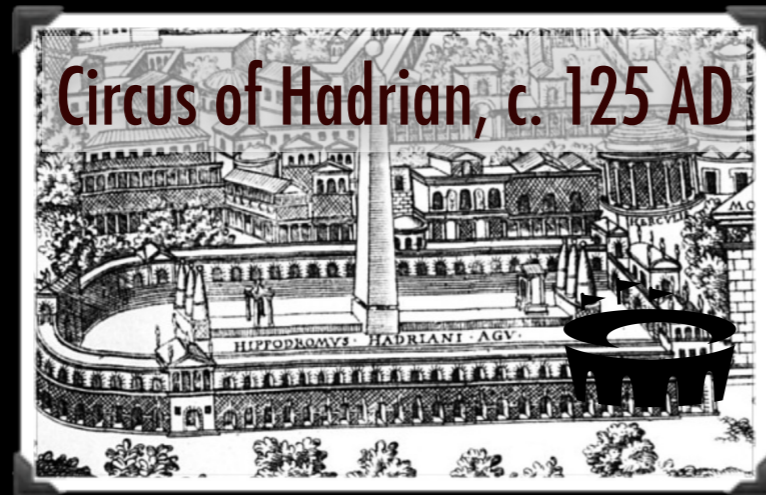


A SEQUENCE...
BUT NOT OF TIME
...OR OF TYPE

Replaced



Erased



Extant



Disappearing



New



ROME

is a mixture of



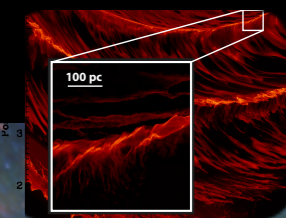
Erased

Disappearing

Replaced*

Extant

New



and so is

THE STAR-FORMING ISM

*Recycled?

What are the *destructive*/*constructive* forces?

Any structure's longevity is affected by which influences govern it.

How (*long*) do structures live?

ONLY SIMULATIONS ALLOW US TO BUILD, DESTROY & TIME TRAVEL

C. 80 AD

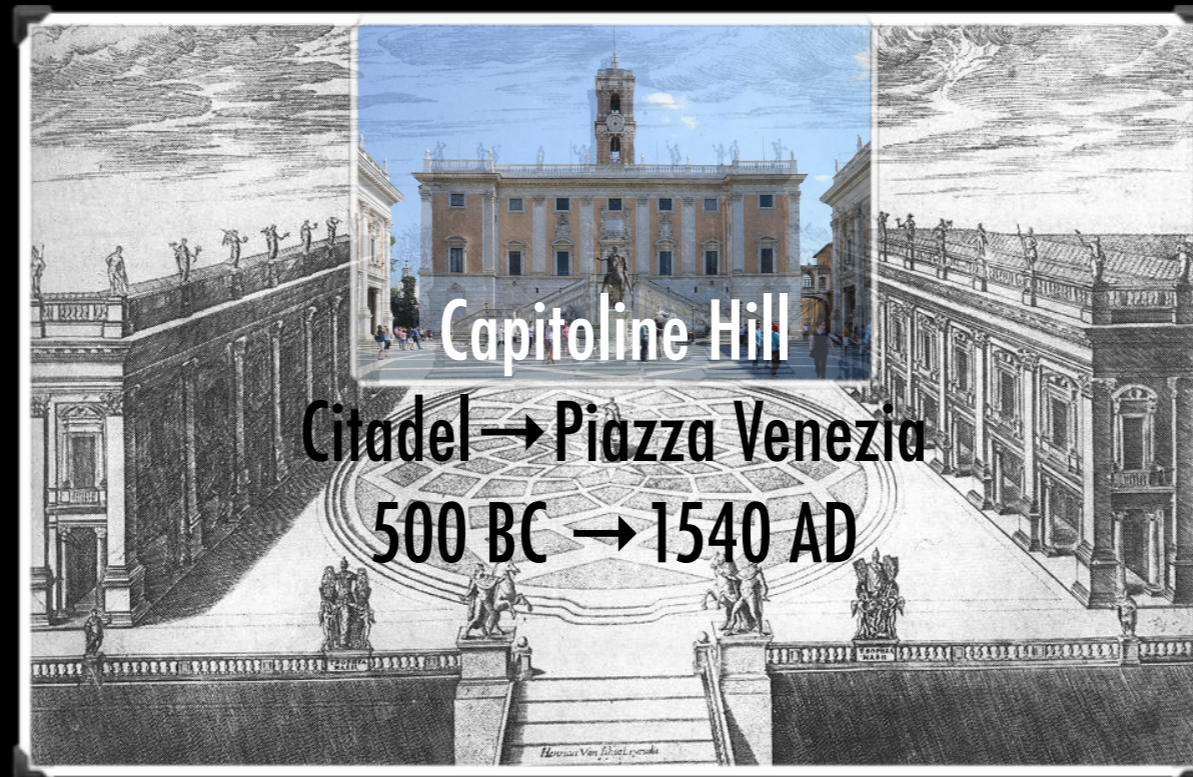


2016



+“observed” simulations are best

ARE SOME PLACES SPECIAL?

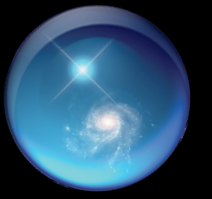


What are “special” places in ISM & how long do they last?

How do “influences” change what is special?

The mid-plane of a spiral galaxy is a special place.

"Is Nessie Parallel to the Galactic Plane?" -A. Burkert, 2012

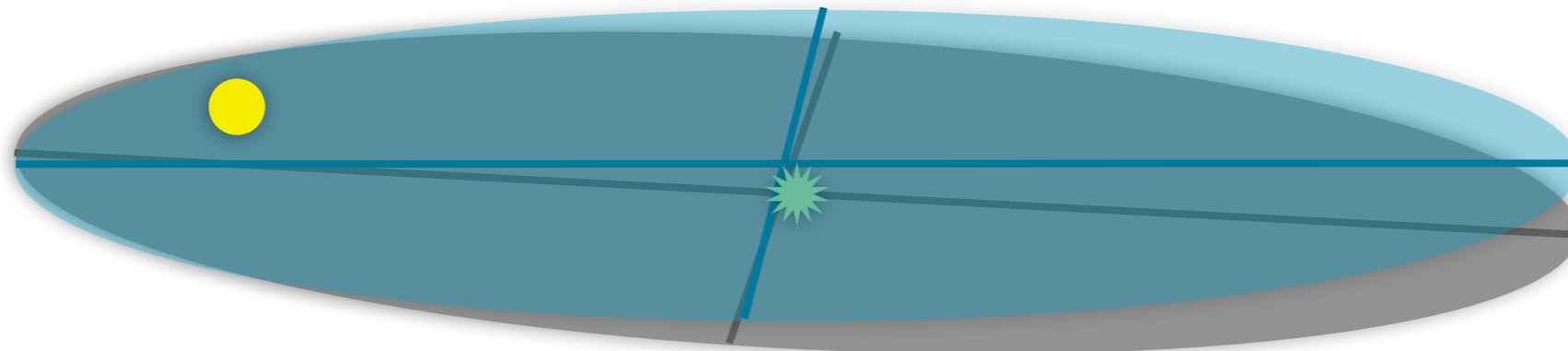


↑
Celestial
North

Yes but why not at Zero of Latitude ($b=0$)?

Where are we, really?

“IAU Milky Way”, est. 1959



True Milky Way, modern

The equatorial plane of the new co-ordinate system must of necessity pass through the sun. It is a fortunate circumstance that, within the observational uncertainty, both the sun and Sagittarius A lie in the mean plane of the Galaxy as determined from the hydrogen observations. If the sun had not been so placed, points in the mean plane would not lie on the galactic equator. *[Blaauw et al. 1959]*

Sun is
~25 pc
“above” the
IAU Milky Way
Plane

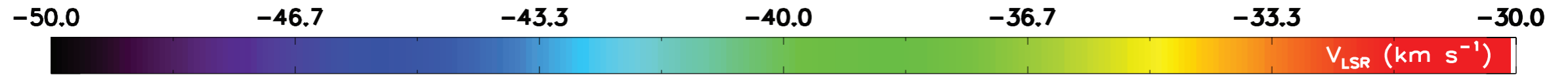
+

Galactic
Center is
~7 pc offset from the
IAU Milky Way
Center

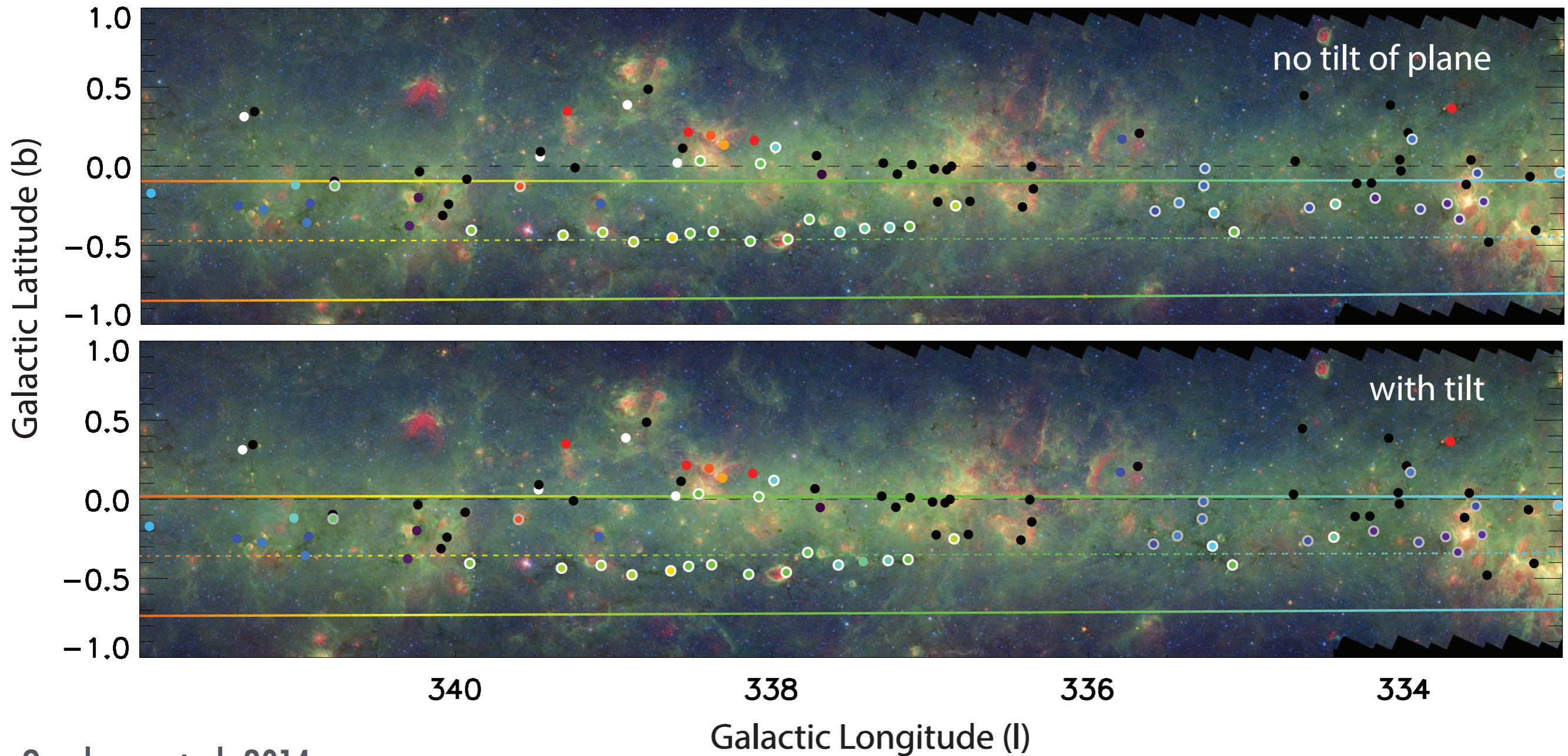
=

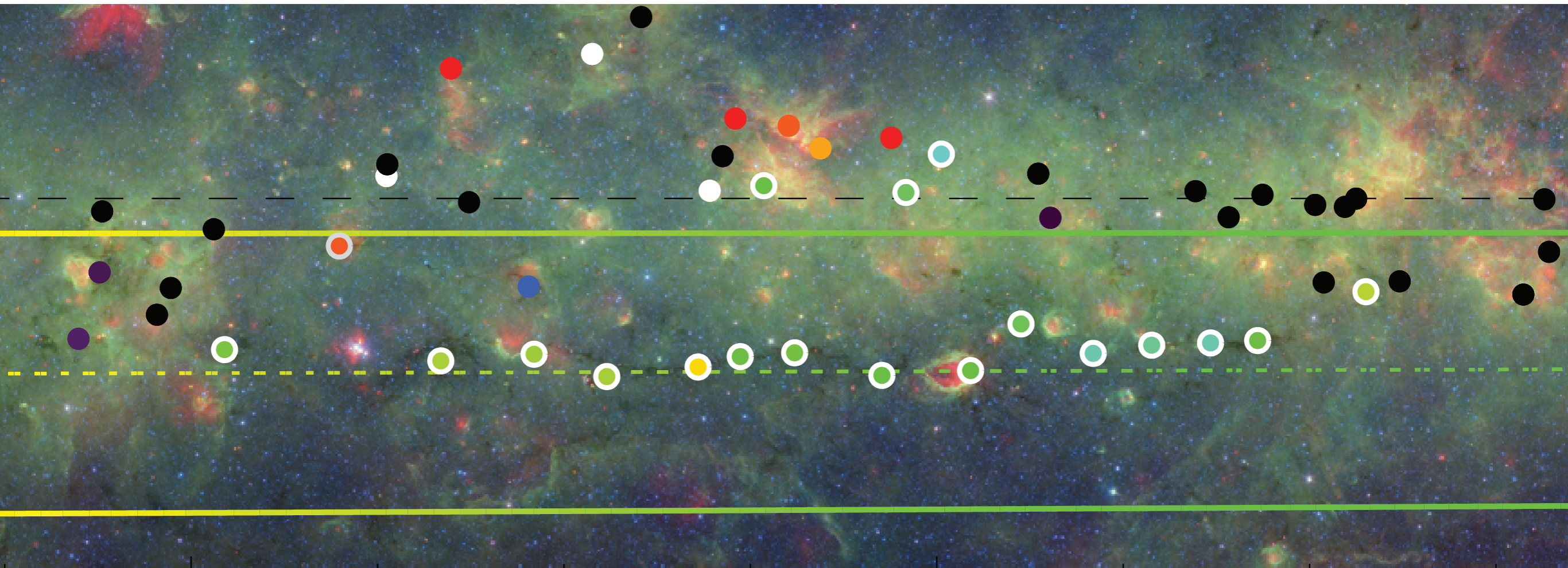
The **Galactic Plane is not quite
where you’d think it is**
when you look at the sky

In the plane! And at distance of spiral arm!



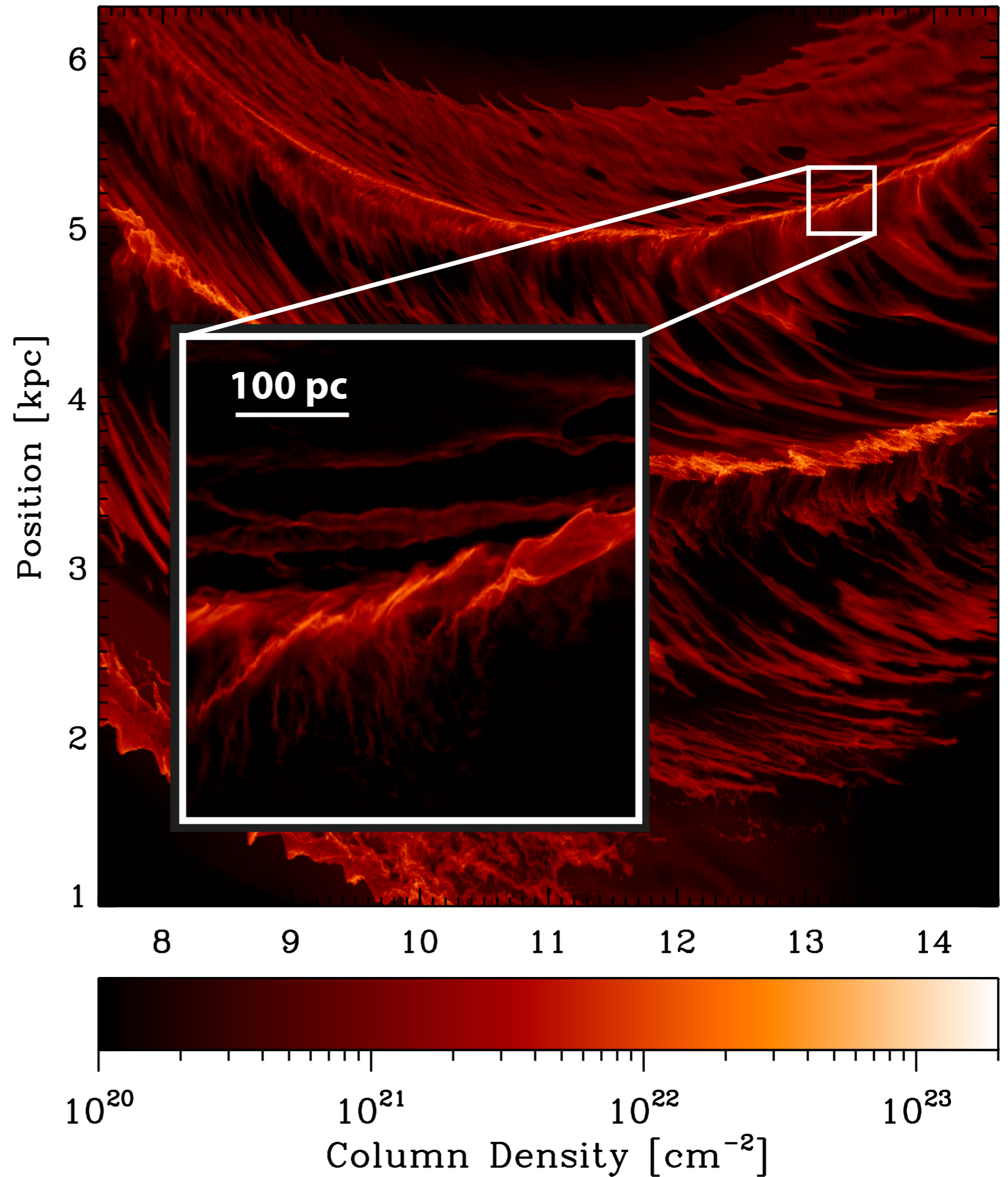
$[Z_0=25.0 \text{ pc}, R_0=8.5 \text{ kpc}, \Theta_0=220 \text{ km/s}]$





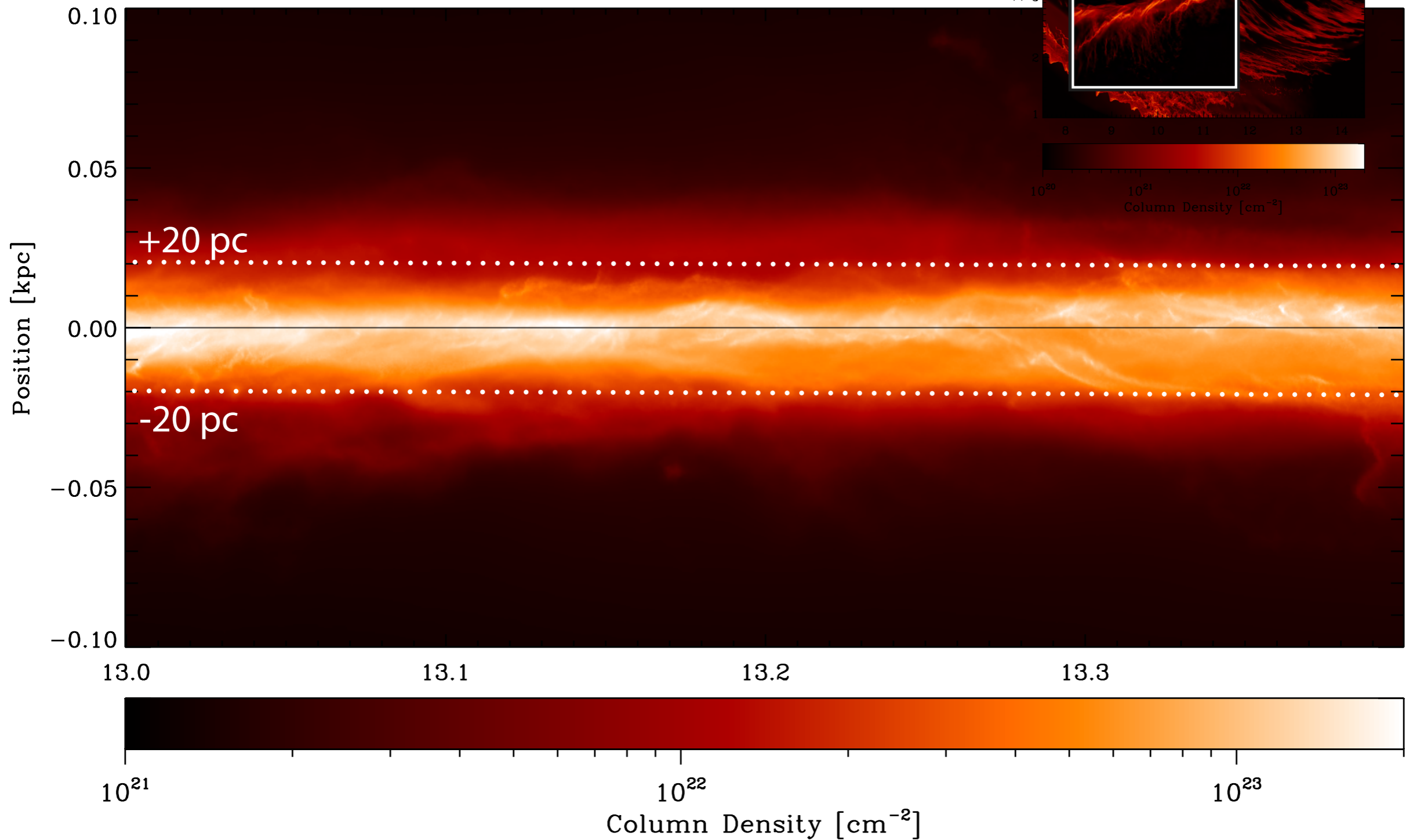
...eerily precisely...

2014 Simulation



Smith et al. 2014, using AREPO

2014 Simulation



Smith et al. 2014, using AREPO (hydro+chemistry, imposed potential, no B-fields, no local (self-)gravity, no feedback)



The Physical Properties of Large-Scale Galactic Filaments

Catherine Zucker, Alyssa Goodman, Cara Battersby
Harvard-Smithsonian Center for Astrophysics

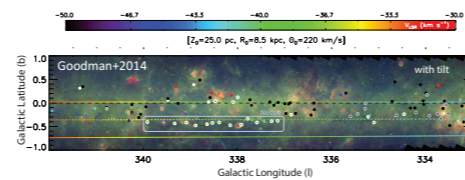


catherine.zucker@cfa.harvard.edu

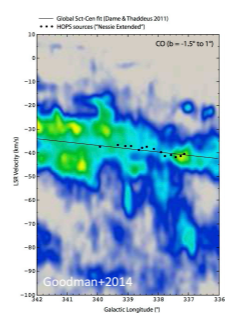
Nessie is a "Bone" of the Milky Way



1 The infrared dark cloud "Nessie" seen in extinction. Its length (160+ pc) and aspect ratio (>300:1) suggests its formation is due to the global spiral potential of the Galaxy.

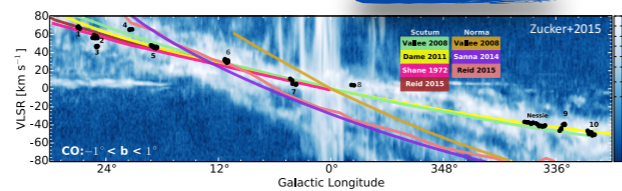


2 Nessie lies within 3 pc of the physical Galactic midplane (dashed colored line), at $d=3.1$ kpc

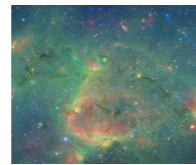


3 Nessie's velocity gradient exactly matches the global spiral fit to the Scutum Centaurus Arm in p-v space

And it may have friends!



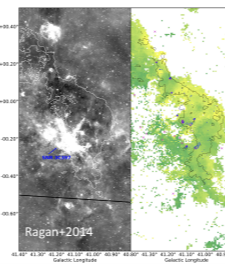
4 Milky Way Bones: Ultra-dense, high aspect ratio Nessie analogs that may form the "Skeleton" of the Milky Way. Analogs must satisfy quantitative Bone criteria (Zucker+2015)



Nessie Analog from Zucker+2015

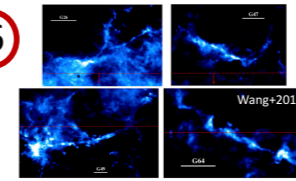
2.3 Establishing "Bone" Criteria
After narrowing down our list to 10 filaments with kinematic structure consistent with existing spiral arm models, we develop a set of criteria for an object to be called a "bone".

1. Largely continuous mid-infrared extinction feature
2. Parallel to the Galactic plane, to within 30°
3. Within 20 pc of the physical Galactic mid-plane, assuming a flat galaxy
4. Within 10 km s^{-1} of the global-log spiral fit to any Milky Way arm
5. No abrupt shifts in velocity (of more than 3 km s^{-1} per 10 pc) within extinction feature
6. Projected aspect ratio $\geq 50:1$



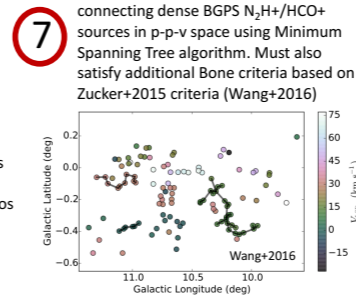
Ragan+2014

6 Large-Scale Herschel Filaments: Dense, cold filaments (aspect ratios $\gg 10$) chosen through visual inspection of Hi-GAL images. Confirmed velocity contiguous through ^{13}CO GRS data (Wang+2015)



Wang+2015

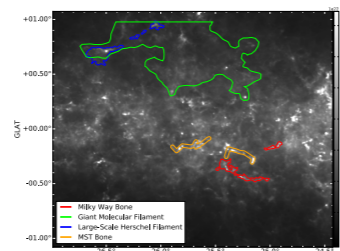
5 Giant Molecular Filaments: $70+$ pc lower density filaments traced mainly by ^{13}CO , with typical aspect ratios between 5:1-10:1 (Ragan+2014, Abreu-Vicente+2016)



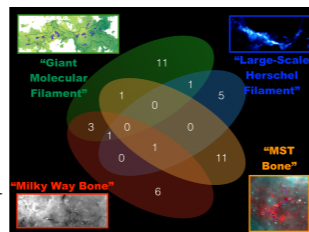
7 MST Bones: Filaments created by connecting dense BGPS $\text{N}_2\text{H}^+/\text{HCO}^+$ sources in p-p-v space using Minimum Spanning Tree algorithm. Must also satisfy additional Bone criteria based on Zucker+2015 criteria (Wang+2016)

But they have different properties and utility in tracing spiral structure

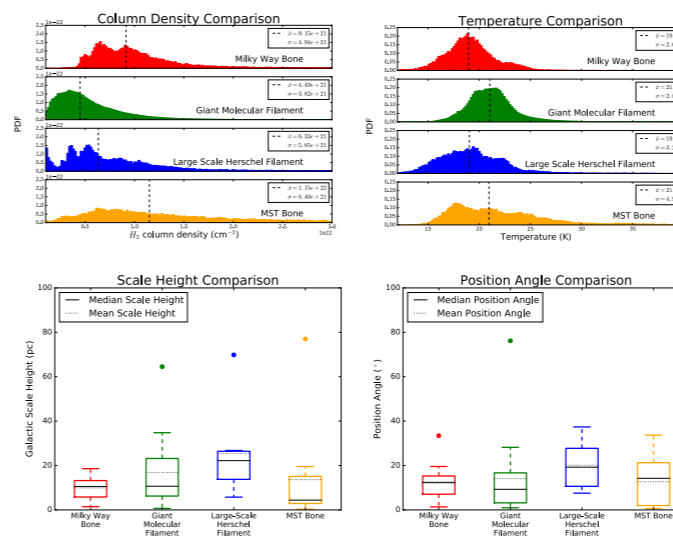
8 Size Scale Comparison of Large-Scale Filament Catalogs: Herschel column density map with filament outlines overlaid



9 Filament Venn Diagram: Only 18% of large-scale filaments share any overlap with other large-scale filament catalogs



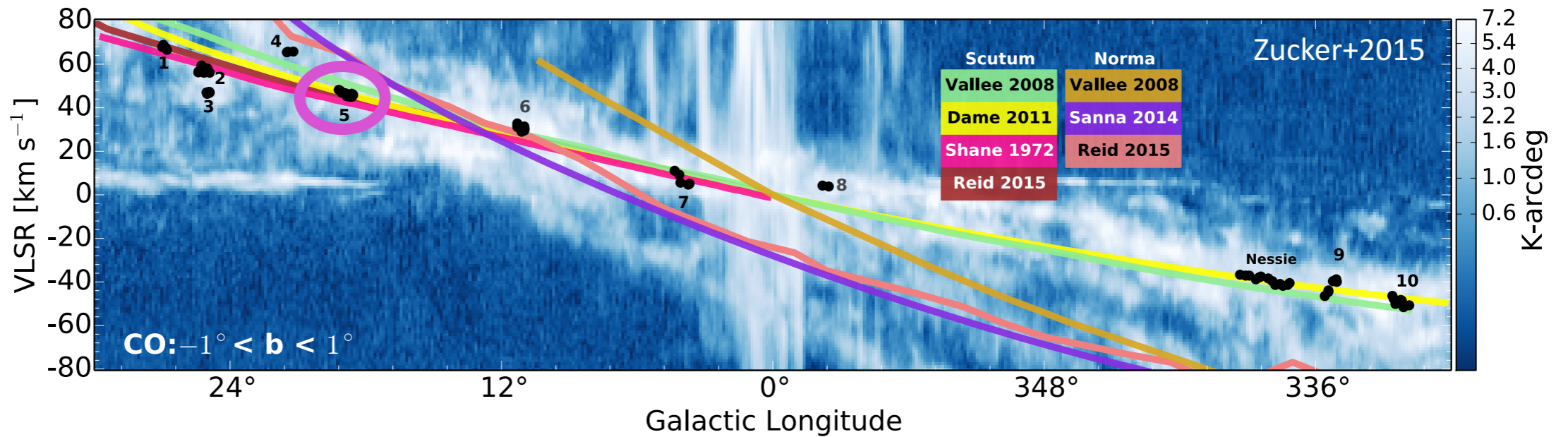
10 Systematic offsets in column density (top left), temperature (top right), scale height (bottom left) and position angle (bottom right) among different classes



formation is due to the global spiral potential of the Galaxy.



And it may have friends!



4

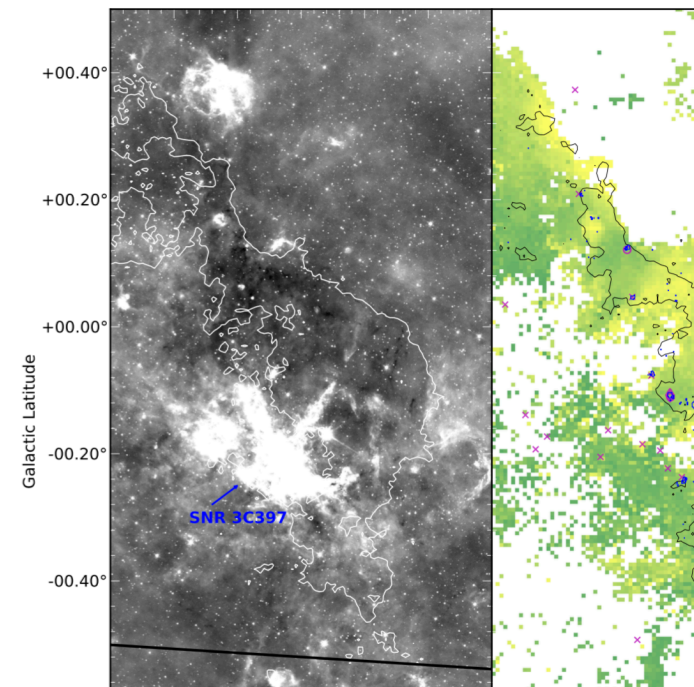
Milky Way Bones: Ultra-dense, high aspect ratio Nessie analogs that may form the “Skeleton” of the Milky Way. Analogs must satisfy quantitative Bone criteria (Zucker+2015)



2.3. Establishing “Bone” Criteria

After narrowing down our list to 10 filaments with kinematic structure consistent with existing spiral arm models, we develop a set of criteria for an object to be called a “bone”:

1. Largely continuous mid-infrared extinction feature
2. Parallel to the Galactic plane, to within 30°
3. Within 20 pc of the physical Galactic mid-plane, assuming a flat galaxy
4. Within 10 km s⁻¹ of the global-log spiral fit to any Milky Way arm

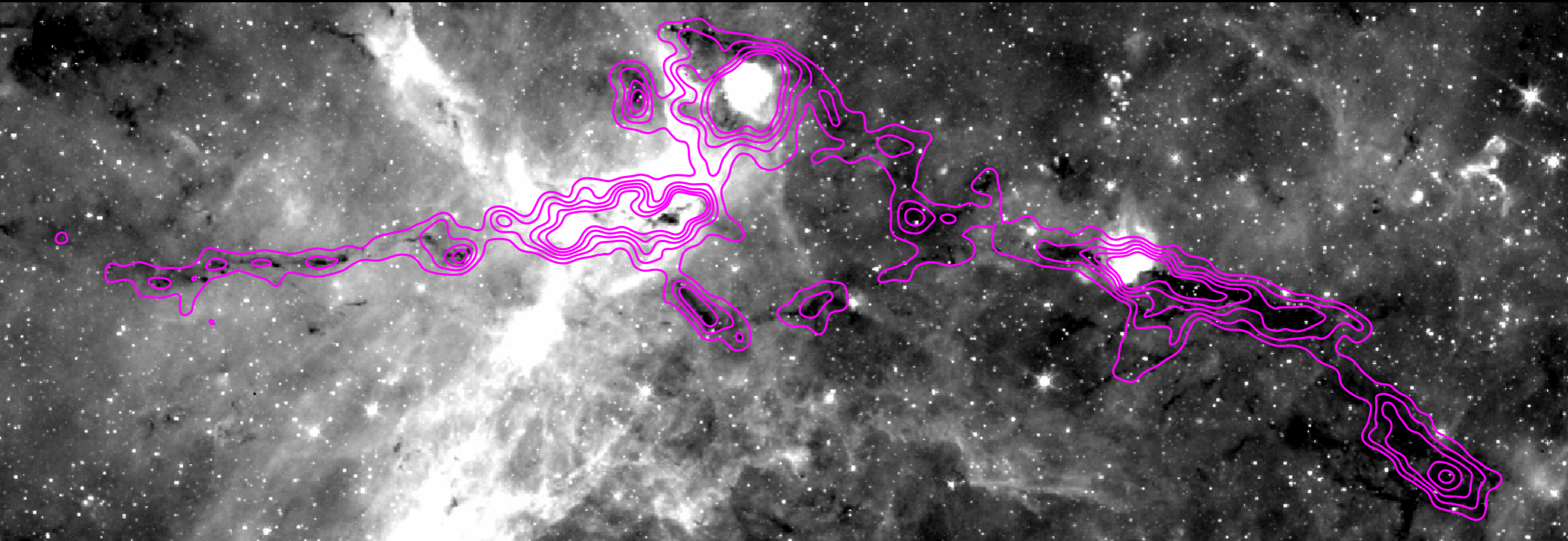


○ "FILAMENT 5"



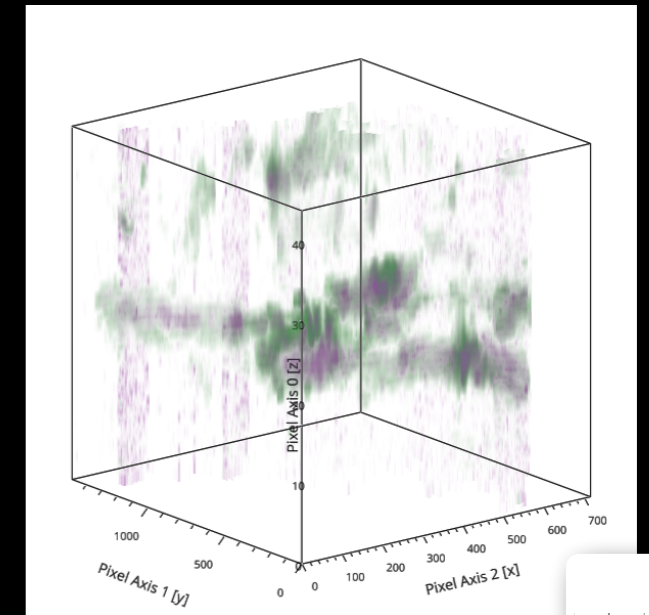
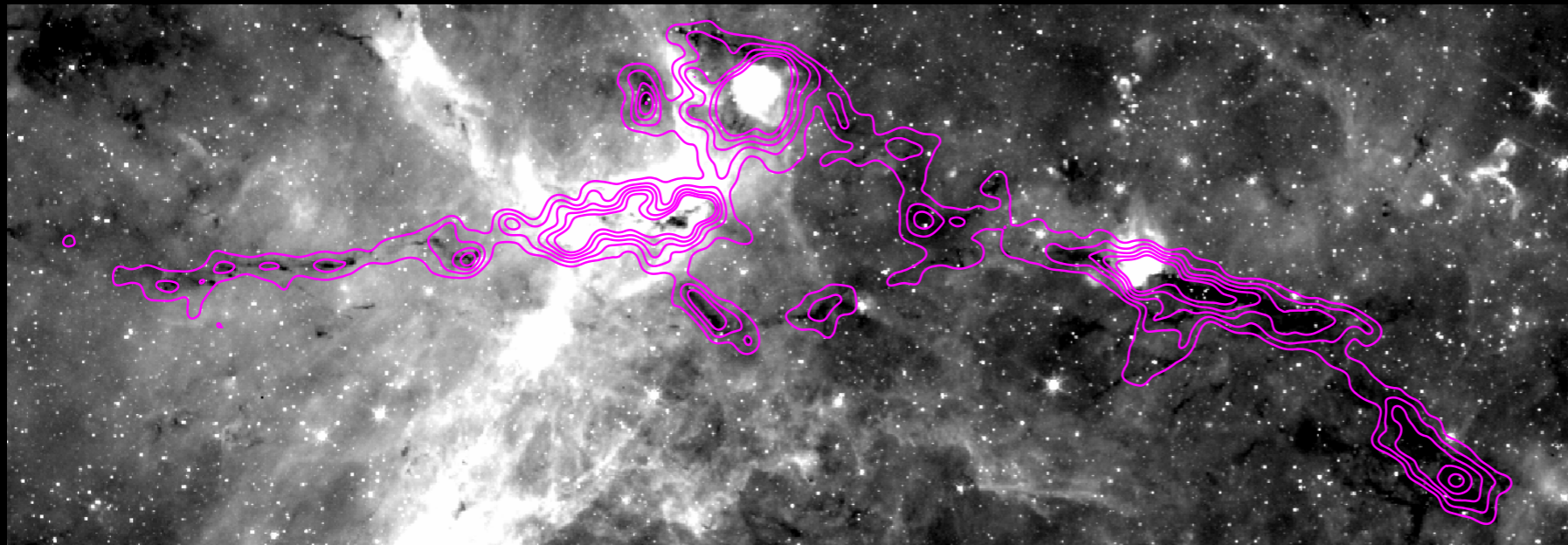
Battersby, Goodman, Zucker et al. in prep.

"FILAMENT 5" WITH THE 30-M



Battersby, Goodman, Zucker et al. in prep.

"FILAMENT 5" WITH THE 30-M



glue 3-D volume rendering of ^{13}CO and C^{18}O



Battersby, Goodman, Zucker et al. in prep.



The Physical Properties of Large-Scale Galactic Filaments

Catherine Zucker, Alyssa Goodman, Cara Battersby
Harvard-Smithsonian Center for Astrophysics

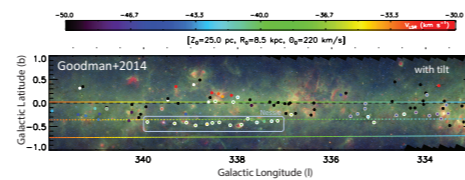


catherine.zucker@cfa.harvard.edu

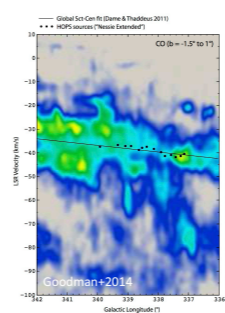
Nessie is a "Bone" of the Milky Way



1 The infrared dark cloud "Nessie" seen in extinction. Its length (160+ pc) and aspect ratio (>300:1) suggests its formation is due to the global spiral potential of the Galaxy.

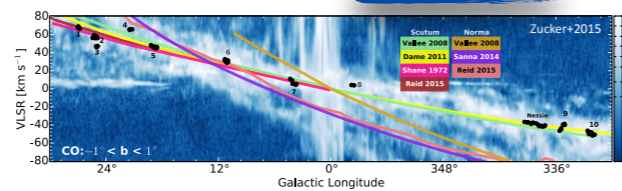


2 Nessie lies within 3 pc of the physical Galactic midplane (dashed colored line), at $d=3.1$ kpc

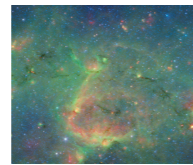


3 Nessie's velocity gradient exactly matches the global spiral fit to the Scutum Centaurus Arm in p-v space

And it may have friends!



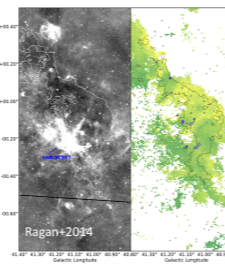
4 Milky Way Bones: Ultra-dense, high aspect ratio Nessie analogs that may form the "Skeleton" of the Milky Way. Analogs must satisfy quantitative Bone criteria (Zucker+2015)



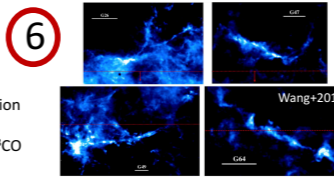
Nessie Analog from Zucker+2015

2.3 Establishing "Bone" Criteria
After narrowing down our list to 10 filaments with kinematic structure consistent with existing spiral arm models, we develop a set of criteria for an object to be called a "bone".

1. Largely continuous mid-infrared extinction feature
2. Parallel to the Galactic plane, to within 30°
3. Within 20 pc of the physical Galactic mid-plane, assuming a flat galaxy
4. Within 10 km s^{-1} of the global-log spiral fit to any Milky Way arm
5. No abrupt shifts in velocity (of more than 3 km s^{-1} per 10 pc) within extinction feature
6. Projected aspect ratio $\geq 50:1$

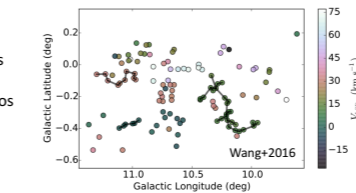


5 Giant Molecular Filaments: $70+$ pc lower density filaments traced mainly by ^{13}CO , with typical aspect ratios between 5:1-10:1 (Ragan+2014, Abreu-Vicente+2016)



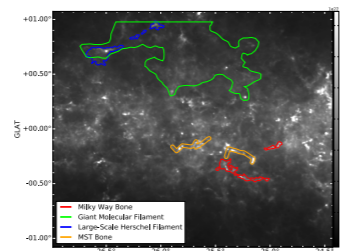
6 Large-Scale Herschel Filaments: Dense, cold filaments (aspect ratios $\gg 10$) chosen through visual inspection of Hi-GAL images. Confirmed velocity contiguous through ^{13}CO GRS data (Wang+2015)

7 MST Bones: Filaments created by connecting dense BGPS $\text{N}_2\text{H}^+/\text{HCO}^+$ sources in p-p-v space using Minimum Spanning Tree algorithm. Must also satisfy additional Bone criteria based on Zucker+2015 criteria (Wang+2016)

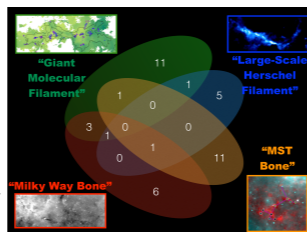


But they have different properties and utility in tracing spiral structure

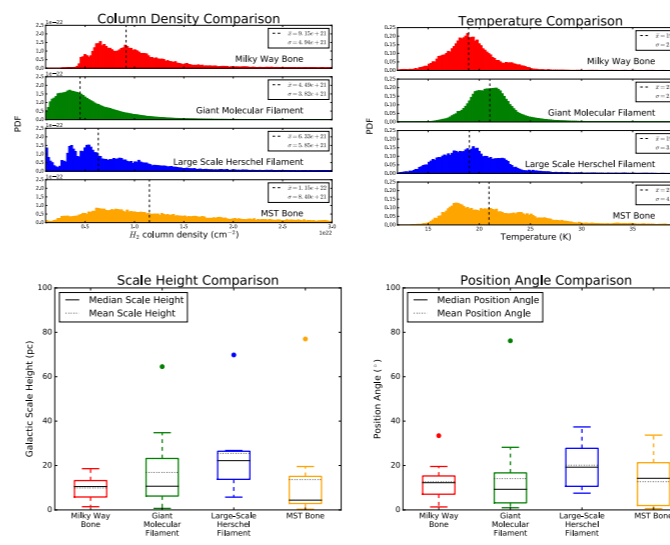
8 Size Scale Comparison of Large-Scale Filament Catalogs: Herschel column density map with filament outlines overlaid



9 Filament Venn Diagram: Only 18% of large-scale filaments share any overlap with other large-scale filament catalogs

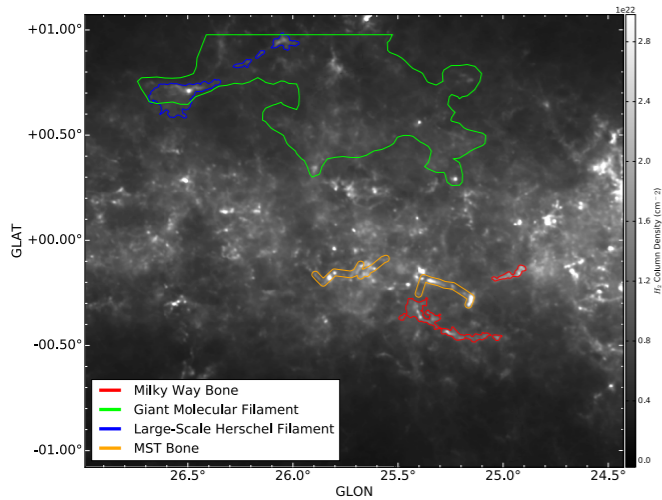


10 Systematic offsets in column density (top left), temperature (top right), scale height (bottom left) and position angle (bottom right) among different classes

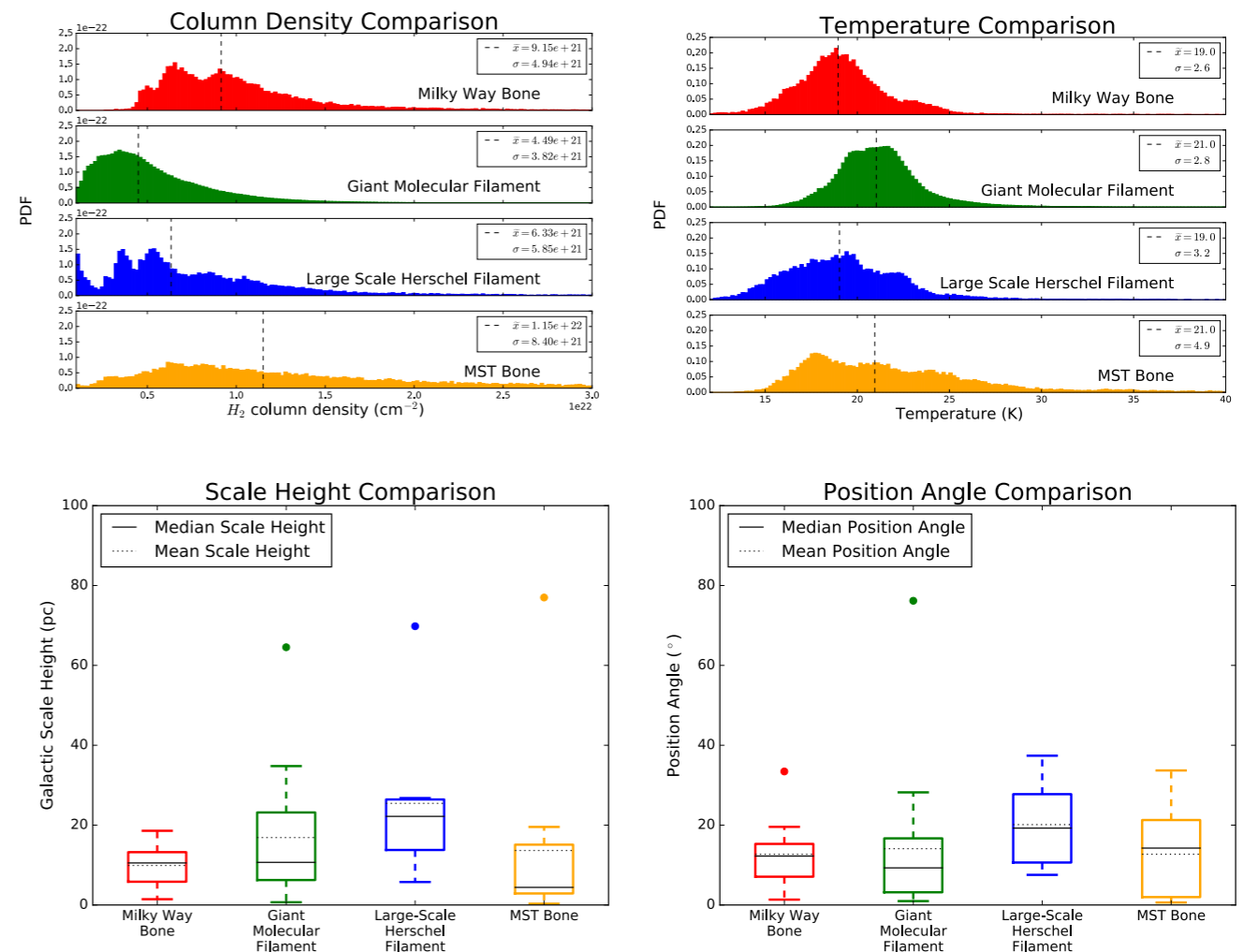


But they have different properties and utility in tracing spiral structure

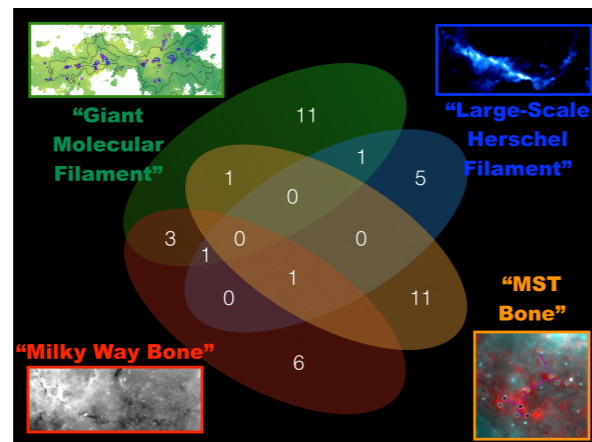
8 Size Scale Comparison of Large-Scale Filament Catalogs: Herschel column density map with filament outlines overlaid



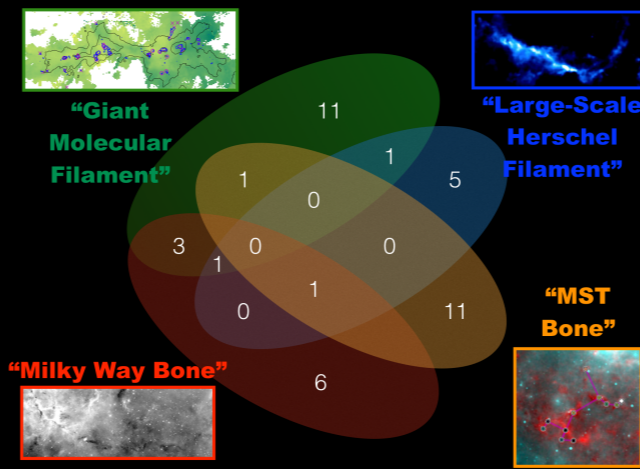
10 Systematic offsets in column density (top left), temperature (top right), scale height (bottom left) and position angle (bottom right) among different classes



9 Filament Venn Diagram: Only 18% of large-scale filaments share any overlap with other large-scale filament catalogs



"Bones" tend to be closest to mid-plane, closest to "horizontal," coldest, and densest.



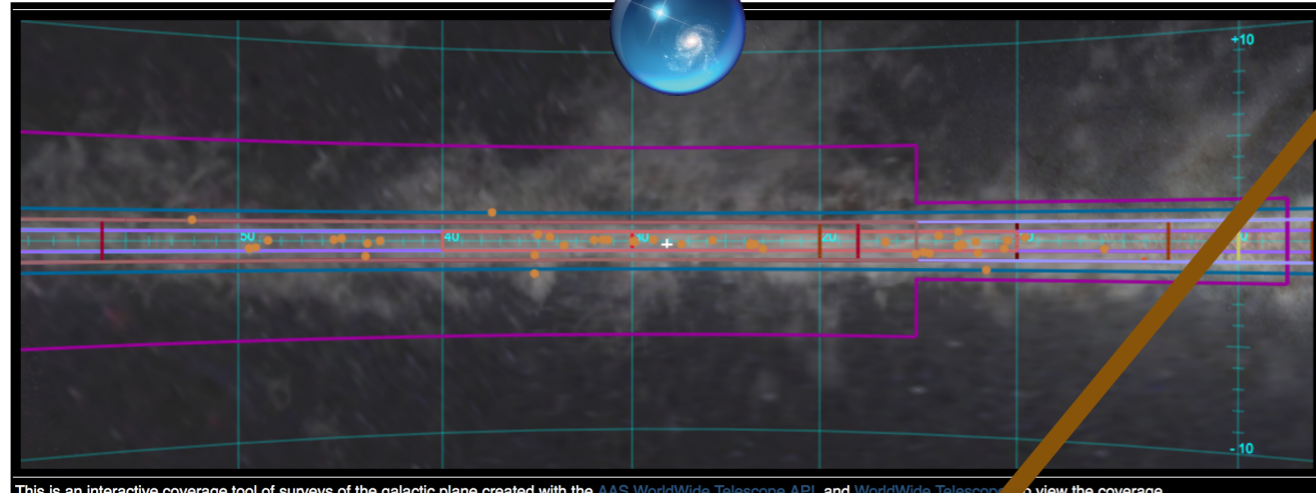
Filament Class	References	λ of Initial Detection	Velocity Reference	Spectral Lines	Velocity Contiguity Criterion	Aspect Ratio or Linearity Criterion	Min. Length	Spiral Arm Association Criterion	Spiral Arm Reference	Galactic scale height criterion	Position angle criterion
GMF	Ragan et al. 2014, Abreu-Vicente et	Mid-IR, Near-IR	GRS, ThrUMMS	^{13}CO	“Continuous” velocity gradient		1°	Intersects p - v fit within arm errors	Vallee 2008, Reid et al. 2014		
Herschel	Wang et al. 2015	Far-IR	GRS	^{13}CO	“Continuous, not broken” emission in p - v diagram	$\gg 10$		Intersects p - p fit within arm/	Reid et al. 2014		
Bone	Goodman et al. 2014, Zucker et	Mid-IR	HOPS, MALT90, BGPS, GRS,	NH_3 , N_2H^+ , HCO^+ , ^{13}CO	$\Delta v < 3$ km/s per 10 pc	$> 50:1$		Within 10 km/s of p - v fit	Dame et al. 2011, Reid et al. 2016	< 20 pc	$< 30^\circ$ from midplane
ATLASGAL	Li et al. 2016	Submm	HOPS, MALT90, BGPS, COHRS,	NH_3 , N_2H^+ , HCO^+ , ^{13}CO ,	Std. Dev. of clumps < 10 km/s	$> 3:1$		Within 10 km/s of p - v fit	Taylor & Cordes 1993		
MST	Wang et al. 2016	Radio	BGPS	N_2H^+ , HCO^+	$\Delta v < 2$ km/s between connected clumps	$\sigma_{\text{major}} / \sigma_{\text{minor}} > 1.5$	10 pc	Within 5 km/s of p - v fit	Reid et al. 2016	< 20 pc	$< 30^\circ$ from midplane

milkyway3d.org



Milky Way 3D Galactic Plane Coverage Tool

MilkyWay3D.org is a tool intended to organize and curate links to information about data sets relevant to our 3D understanding of the Milky Way. For any given longitude range, we provide the means to determine the available surveys, their overlapping footprint, and the type of data each provides. Information about each dataset, including how to access the data, their hallmark publications, and their principal investigators, is available at the [Milky Way 3D Dataverse](#). All the data can be loaded, "linked", and explored using the new 3D visualization software package Glueviz, available for download at [glueviz.org](#)!



This is an interactive coverage tool of surveys of the galactic plane created with the [AAS WorldWide Telescope API](#) and [WorldWide Telescope](#). To view the coverage of a region, click on the data in the region.

View Region	Link to Survey	Wavelength	Extended Observations		Catalogs and Pointed Surveys	
			Continuum (2D)	Spectral Line (3D)	Source-Based Lists	Spectral Line
<input checked="" type="checkbox"/>	THOR	21 cm, 300 mm, 174-186 mm		★		
<input checked="" type="checkbox"/>	BESSEL	1-3 cm			★	
<input checked="" type="checkbox"/>	RAMPS*	1 cm		★		
<input checked="" type="checkbox"/>	CORNISH*	60 mm	★		★	
<input checked="" type="checkbox"/>	HOPS	12 mm		★		★
<input checked="" type="checkbox"/>	GRS	3 mm		★		
<input checked="" type="checkbox"/>	MALT90	3 mm				★
<input checked="" type="checkbox"/>	THRUMMS	3 mm		★		
<input type="checkbox"/>	Dame CO	2.6 mm		★		
<input checked="" type="checkbox"/>	BGPS	1 mm	★		★	★
<input checked="" type="checkbox"/>	CHIMPS	1 mm		★		
<input checked="" type="checkbox"/>	COHRS	1 mm		★		
<input checked="" type="checkbox"/>	ATLASGAL	870 μm	★		★	
<input checked="" type="checkbox"/>	JCMT*	850 μm	★		★	
<input checked="" type="checkbox"/>	HIGAL*	70-500 μm	★			
<input checked="" type="checkbox"/>	MIPSGAL	24, 70 μm	★			
<input type="checkbox"/>	WISE	3.4, 4.6, 12, 22.0 μm	★			
<input type="checkbox"/>	GLIMPSE	3.6, 4.5, 5.8, 8.0 μm	★			
<input checked="" type="checkbox"/>	UKIDSS-GPS*	1.3, 1.6, 2.2 μm	★			
<input checked="" type="checkbox"/>	GPIPS*	1.6 μm				★



VIALACTEA Science Gateway

- Welcome ▾
- Workflow ▾
- Storage ▾
- Settings ▾
- Security ▾
- Statistics
- Information ▾
- Data Avenue**
- Help ▾
- End User ▾
- PBS Monitoring ▾

Data Avenue

DataAvenue

and coming soon!

- Two panel view
- Edit favorites
- History

Admin ▾ Alyssa Ann Goodman ▾

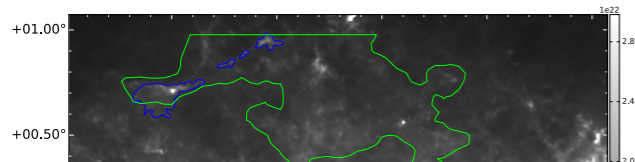
Powered By [Liferay](#)

Author Name
Simon Bihl (1)

But they have different properties and utility in tracing spiral structure

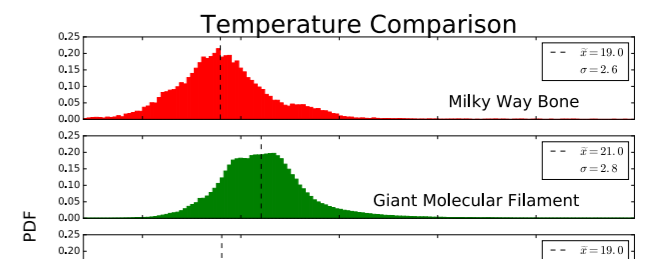
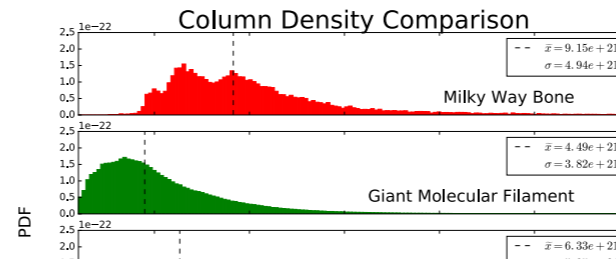
8

Size Scale Comparison of Large-Scale Filament Catalogs: Herschel column density map with filament outlines overlaid



10

Systematic offsets in column density (top left), temperature (top right)



≠



≠



≠

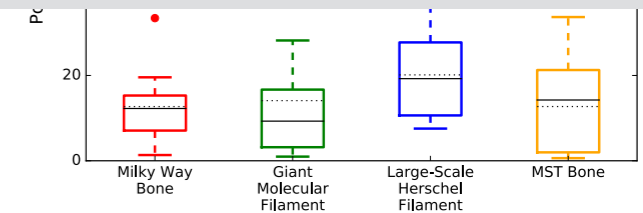
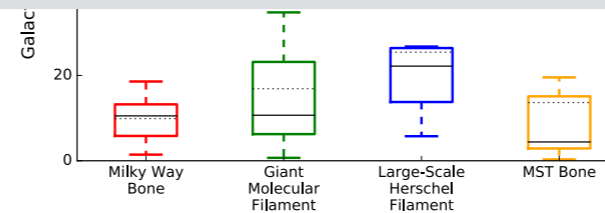


≠



Filament Venn Diagram

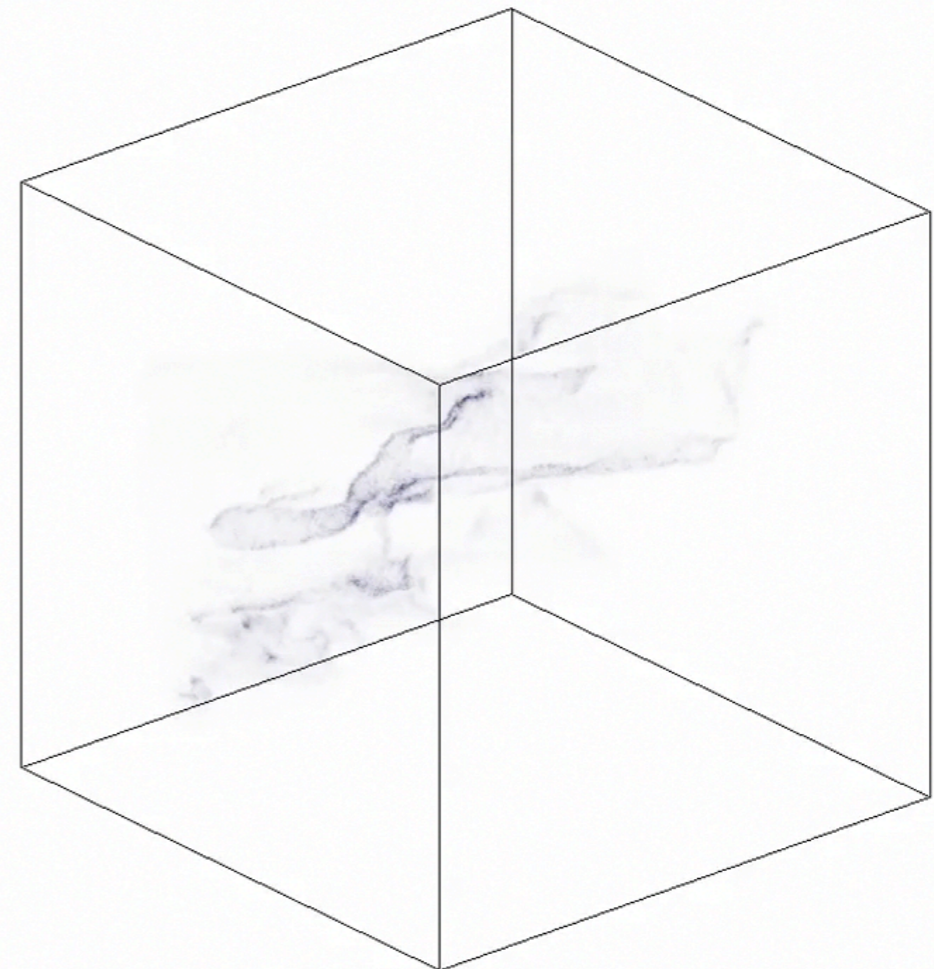
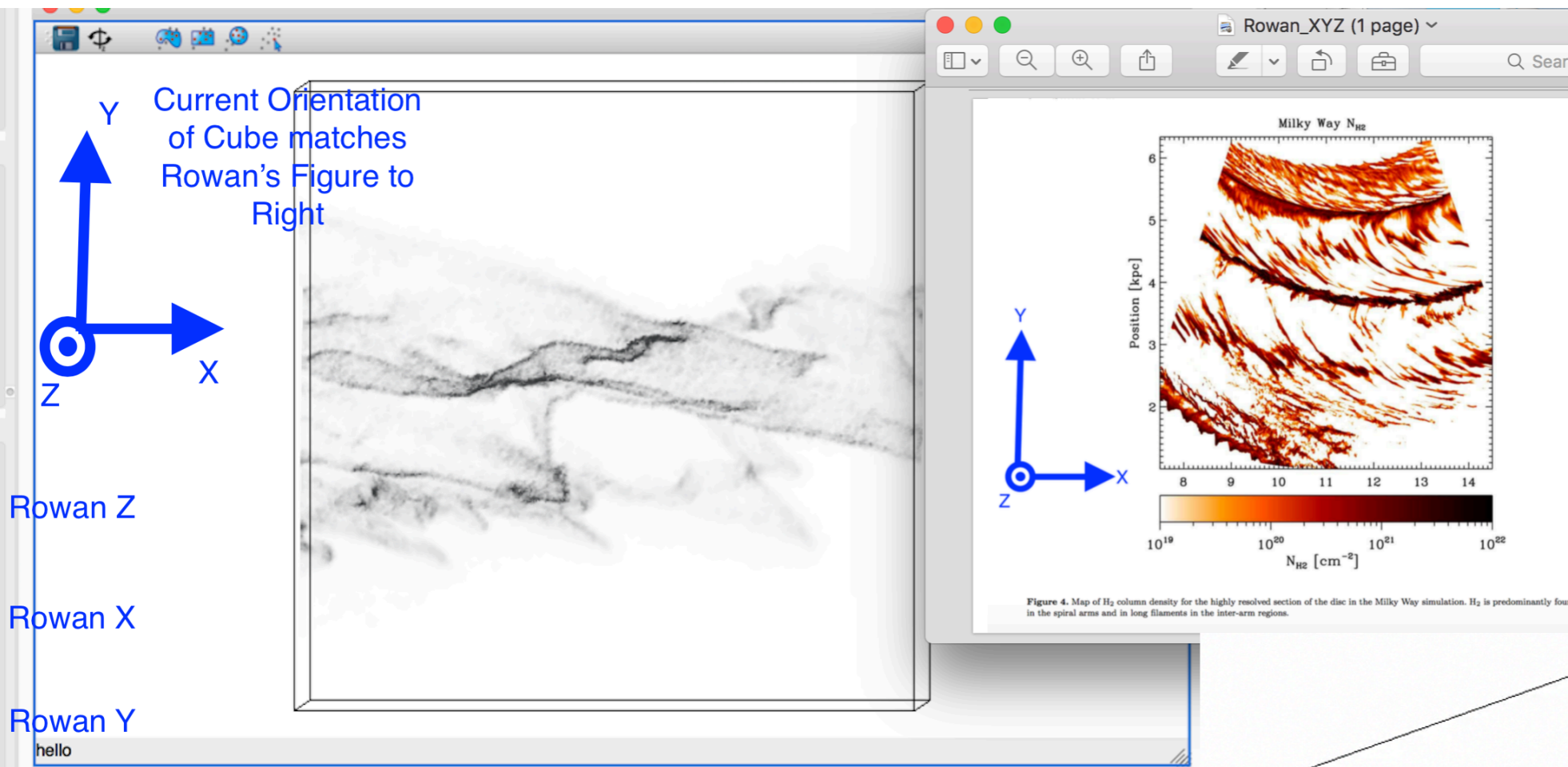
Diagram: Only 18% of large-scale filaments share any overlap with other large-scale filament catalogs



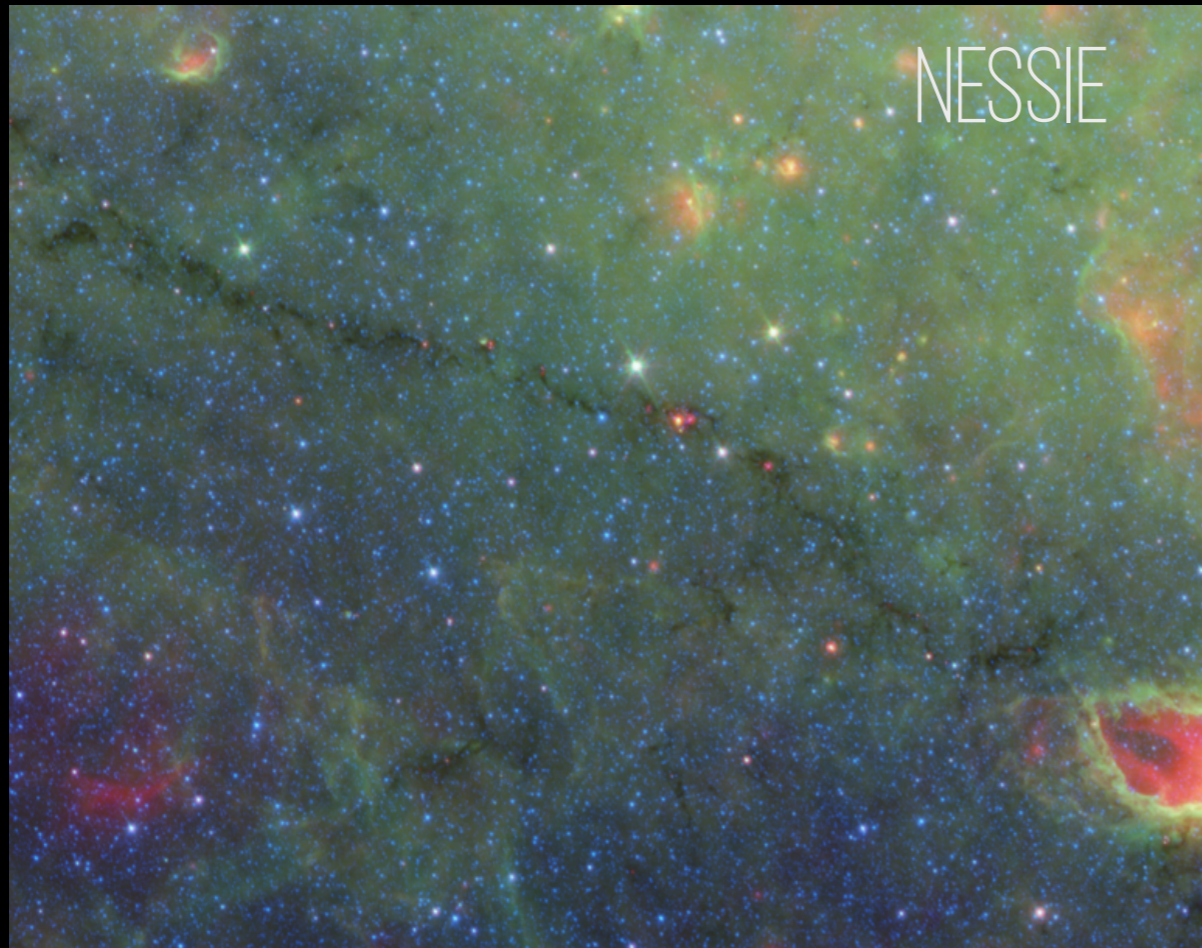
"Bones" are most likely to trace structure in/of the Galaxy's plane.

But what creates the Bones we observe?

brand new
AREPO work...look for
Zucker, Smith,
Battersby, Goodman
2017

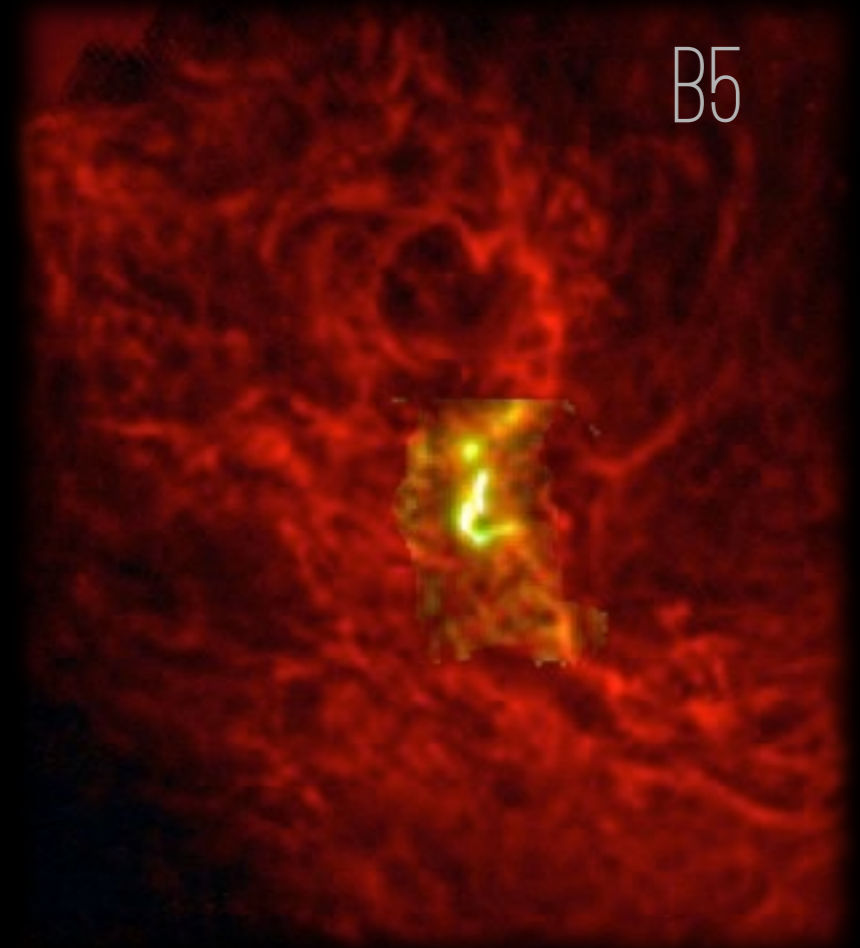


cf. simulation work by Moeckl & Burkert 2015, Duarte-Cabral & Dobbs 2016; + AREPO MHD simulation -ALMA polarimetry comparison from Hull et al. 2016, more...



NESSIE

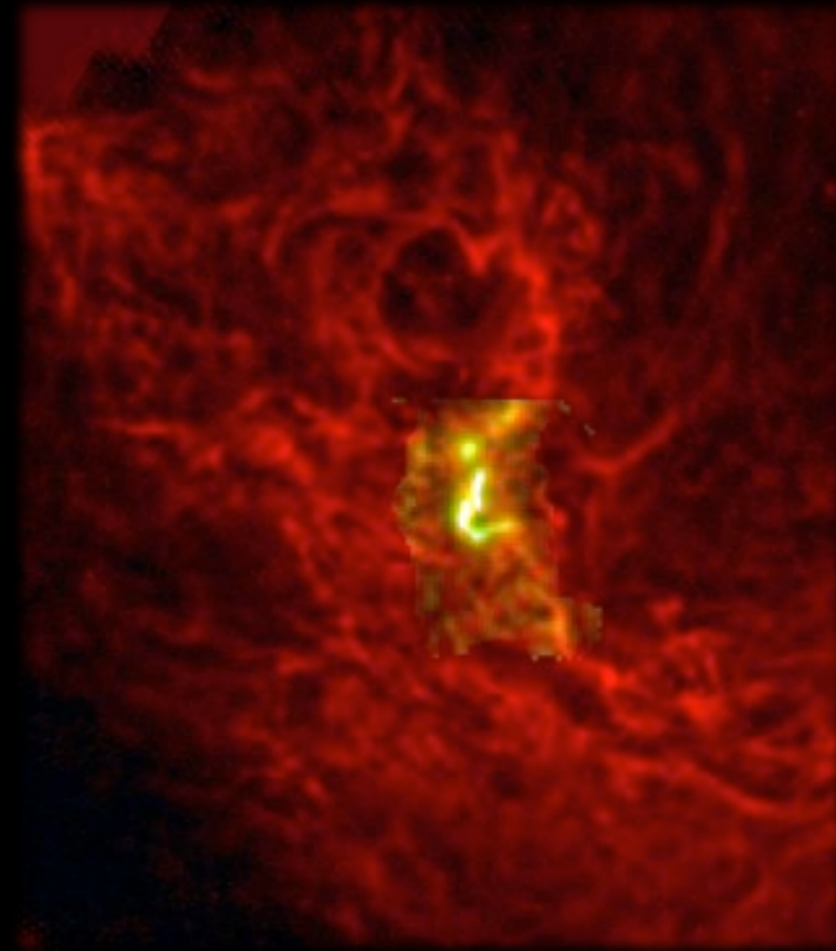
>100 pc



B5

~ 0.01 to 10 pc

COHERENT CORES ISLANDS OF CALM IN TURBULENT SEAS(?)



The 30-year story: Myers & Benson 1983, Goodman et al. 1998, Pineda et al. 2010, 2011, 2014

COHERENCE IN DENSE CORES. II. THE TRANSITION TO COHERENCE

ALYSSA A. GOODMAN¹

Harvard University Department of Astronomy, Cambridge, MA 02138; agoodman@cfa.harvard.edu

JOSEPH A. BARRANCO

Astronomy Department, University of California, Berkeley, Berkeley, CA 94720; barranco@ucbast.berkeley.edu

DAVID J. WILNER

Harvard-Smithsonian Center for Astrophysics, 60 Garden Street, Cambridge, MA 02138; dwilner@cfa.harvard.edu

AND

MARK H. HEYER

Five College Radio Astronomy Observatory, University of Massachusetts, Amherst, MA 01003; heyer@fcrao1.phast.umass.edu

Received 1997 June 17; accepted 1998 February 5

ABSTRACT

After studying how line width depends on spatial scale in low-mass star-forming regions, we propose that “dense cores” (Myers & Benson 1983) represent an inner scale of a self-similar process that characterizes larger scale molecular clouds.

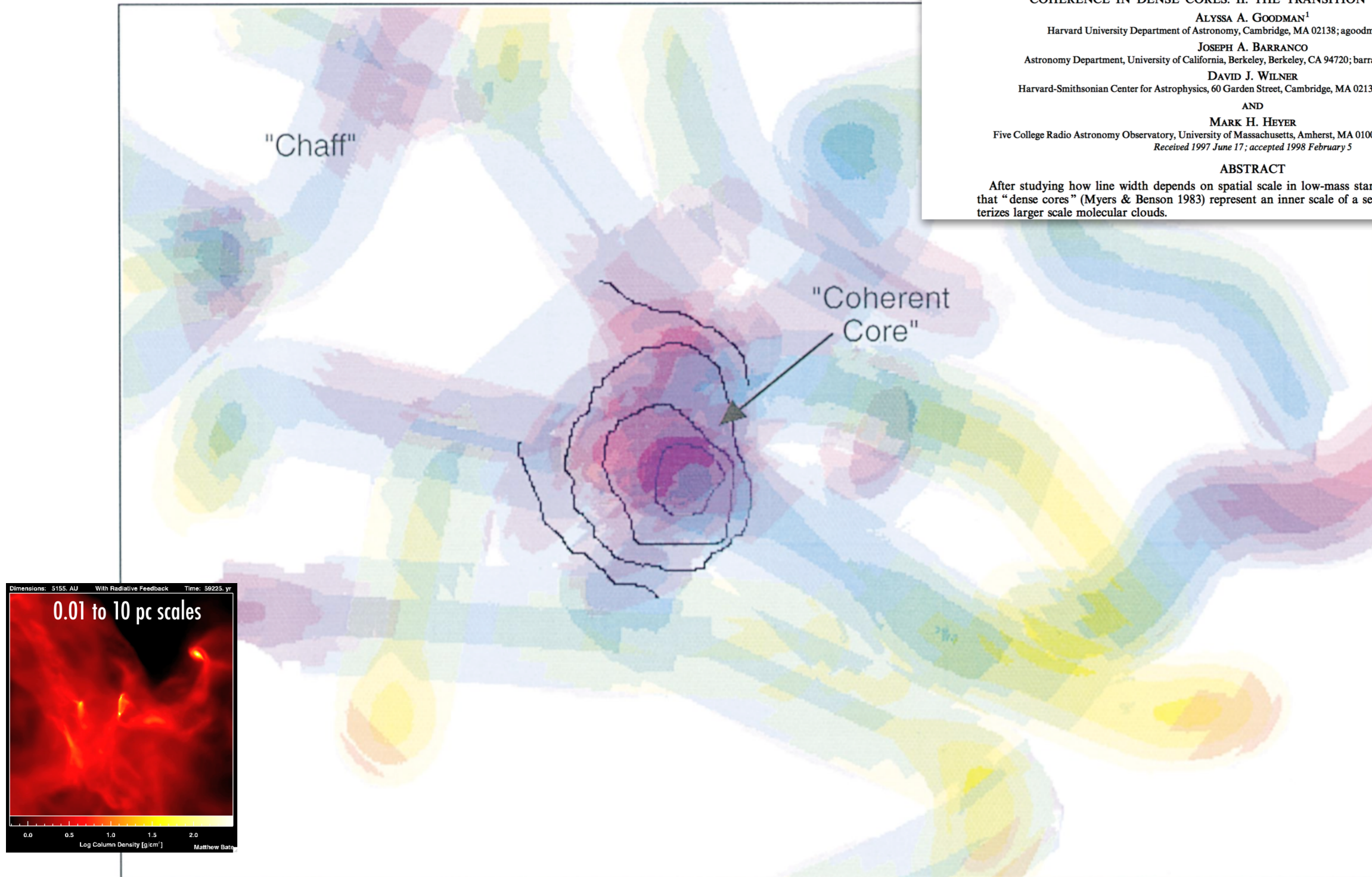
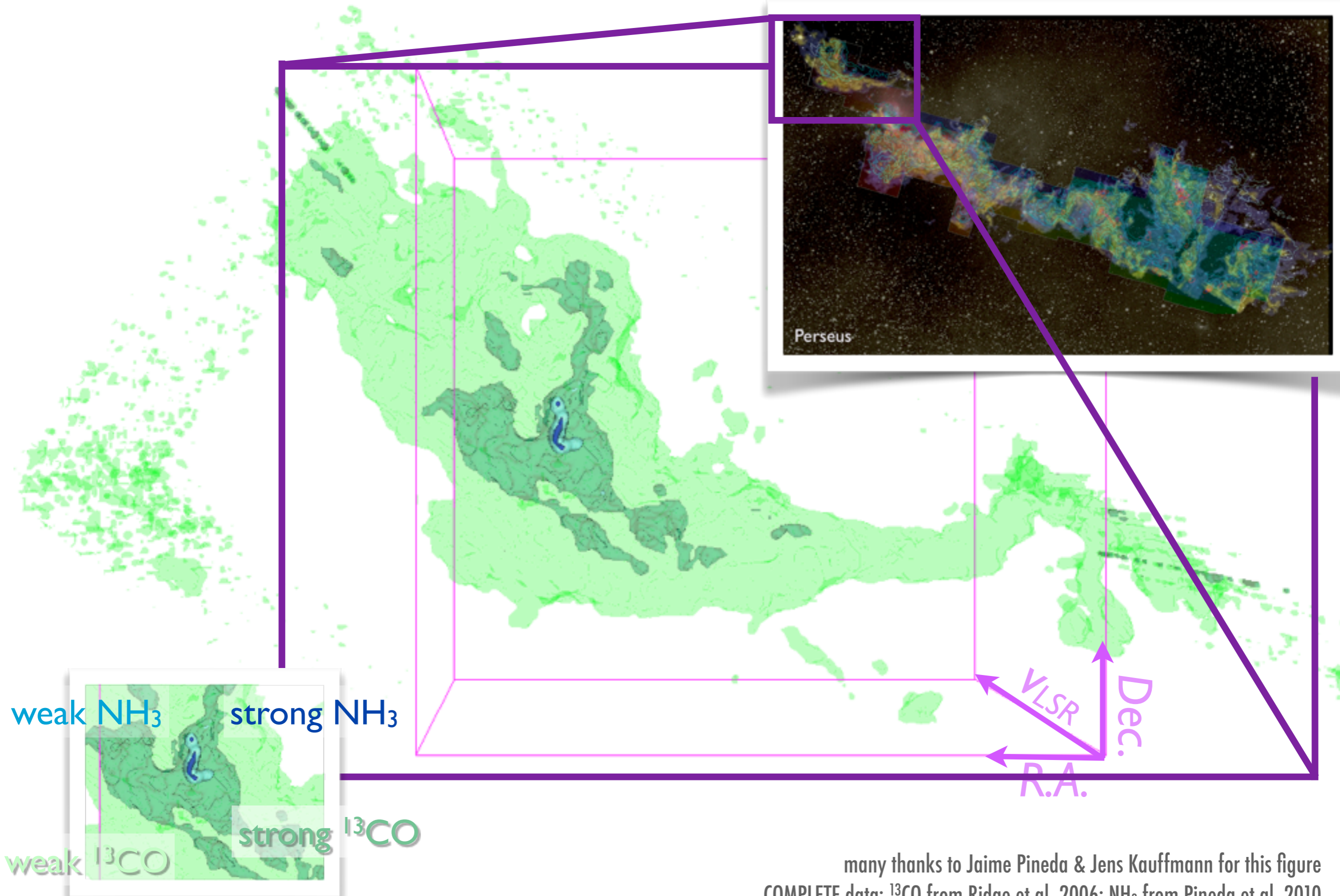


FIG. 10.—An illustration of the transition to coherence. Color and shading schematically represent velocity and density in this figure. On large scales, material (labeled chaff) is distributed in a self-similar fashion, and its filling factor is low. On scales smaller than some fiducial radius, the filling factor of gas increases substantially, and a coherent dense core, which is not self-similar, is formed. Due to limitations in the authors' drawing ability, the figure emphasizes a particular size scale in the chaff, which should actually exhibit self-similar structure on all scales ranging from the size of an entire molecular cloud complex down to a coherent core.



POSITION-VELOCITY STRUCTURE OF THE B5 REGION IN PERSEUS



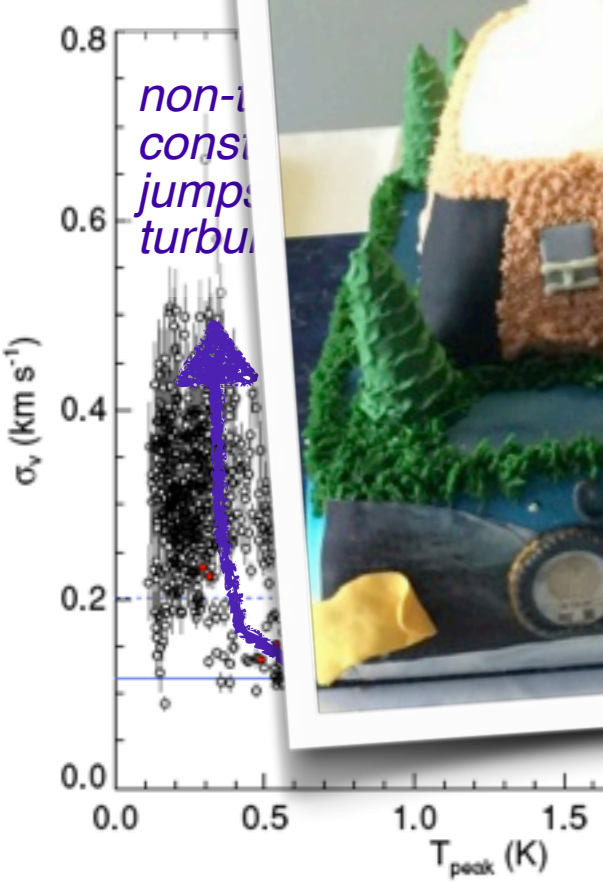
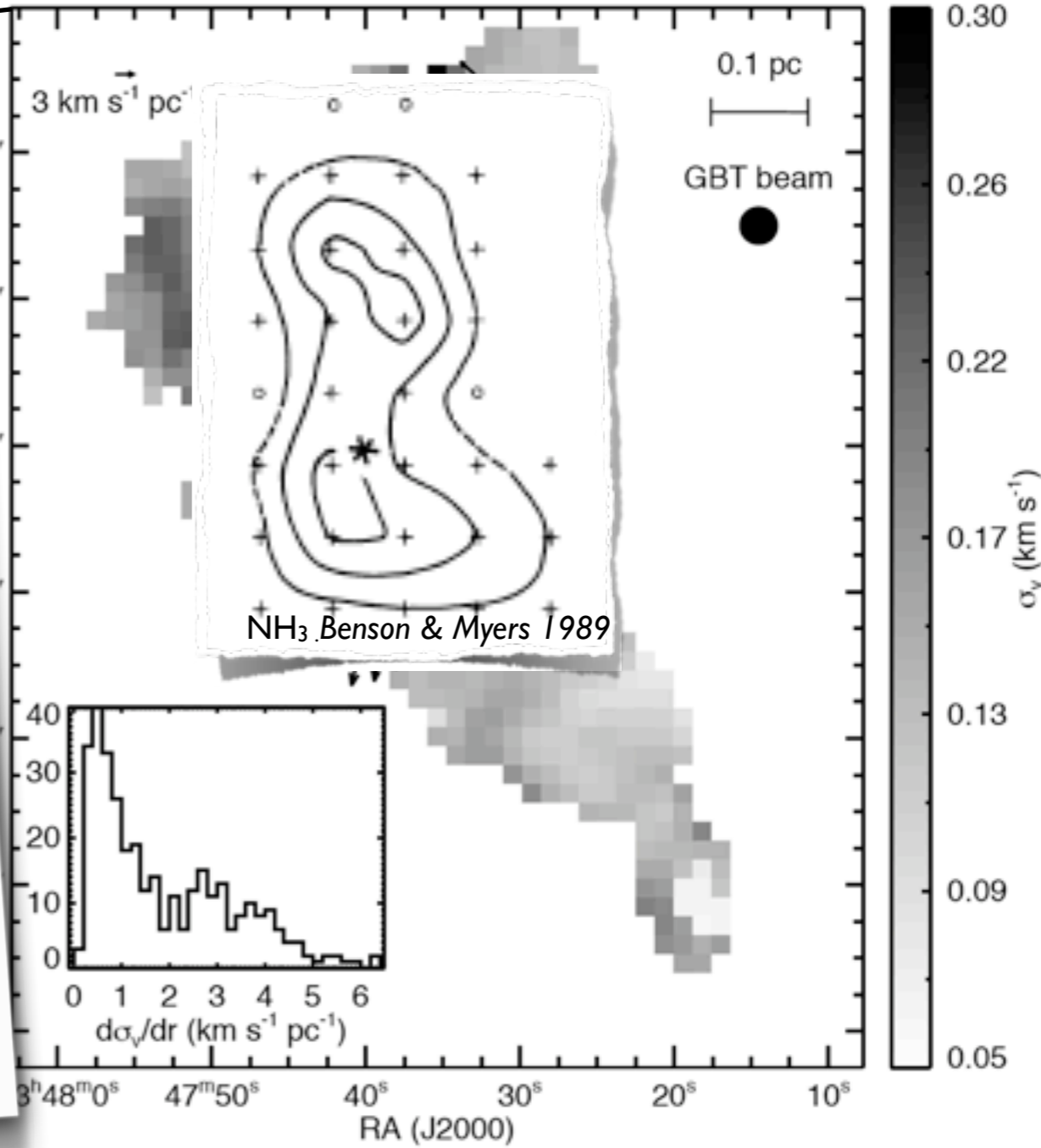
many thanks to Jaime Pineda & Jens Kauffmann for this figure
COMPLETE data: ^{13}CO from Ridge et al. 2006; NH_3 from Pineda et al. 2010

STRONG EVIDENCE FOR "VELOCITY COHERENCE" IN DENSE CORES

greyscale shows NH_3 velocity dispersion, arrows show gradient in dispersion

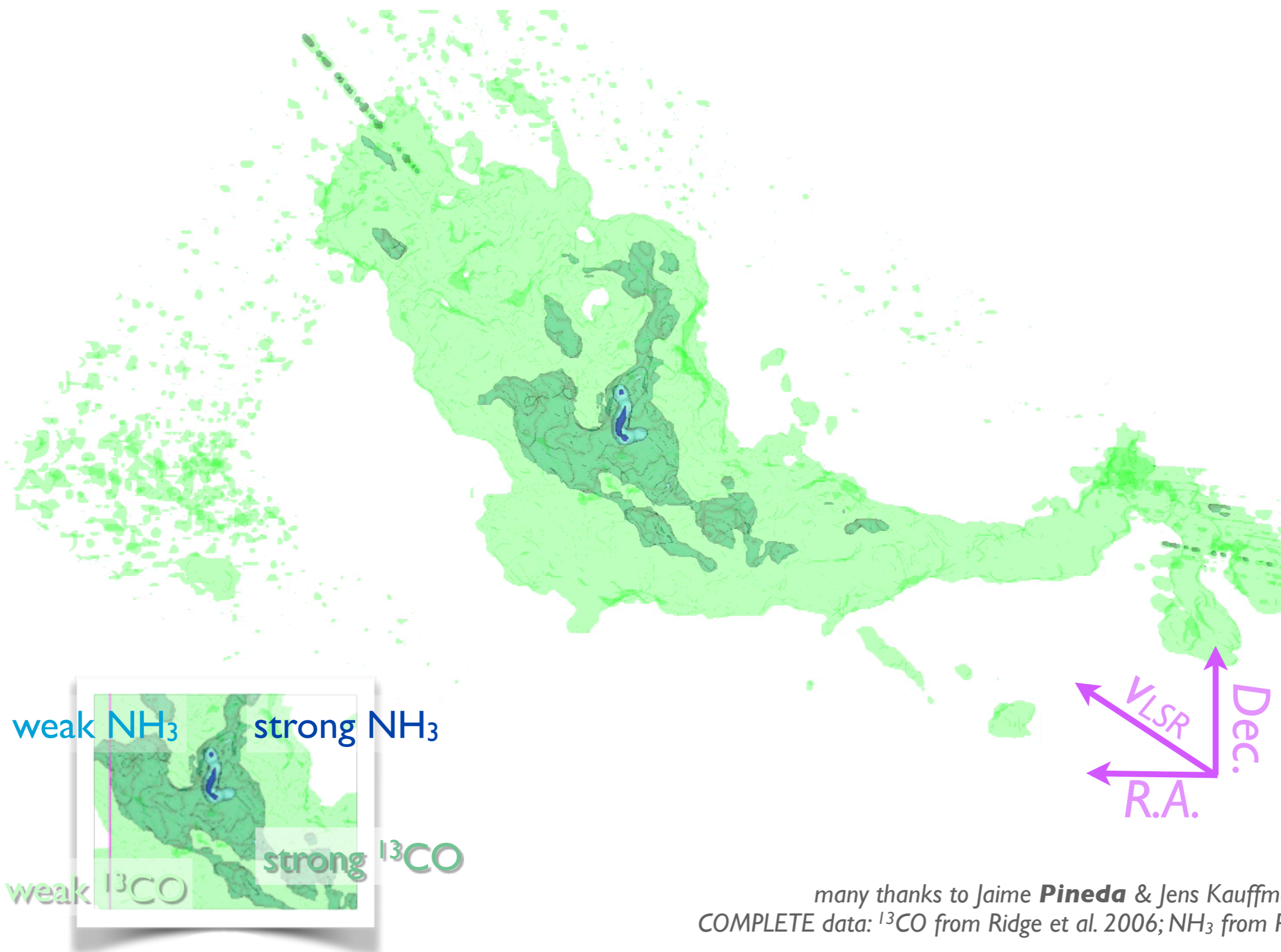
weak NH_3 strong NH_3

weak NH_3



GBT NH_3 observations of the B5 core (Pineda et al. 2010)

POSITION-VELOCITY STRUCTURE OF THE B5 REGION IN PERSEUS



many thanks to Jaime **Pineda** & Jens Kauffmann for this figure
COMPLETE data: ¹³CO from Ridge et al. 2006; NH₃ from Pineda et al. 2010

BUT THEN... WE FOUND SUB-STRUCTURE

THE ASTROPHYSICAL JOURNAL LETTERS, 739:L2 (5pp), 2011 September 20

PINEDA ET AL.

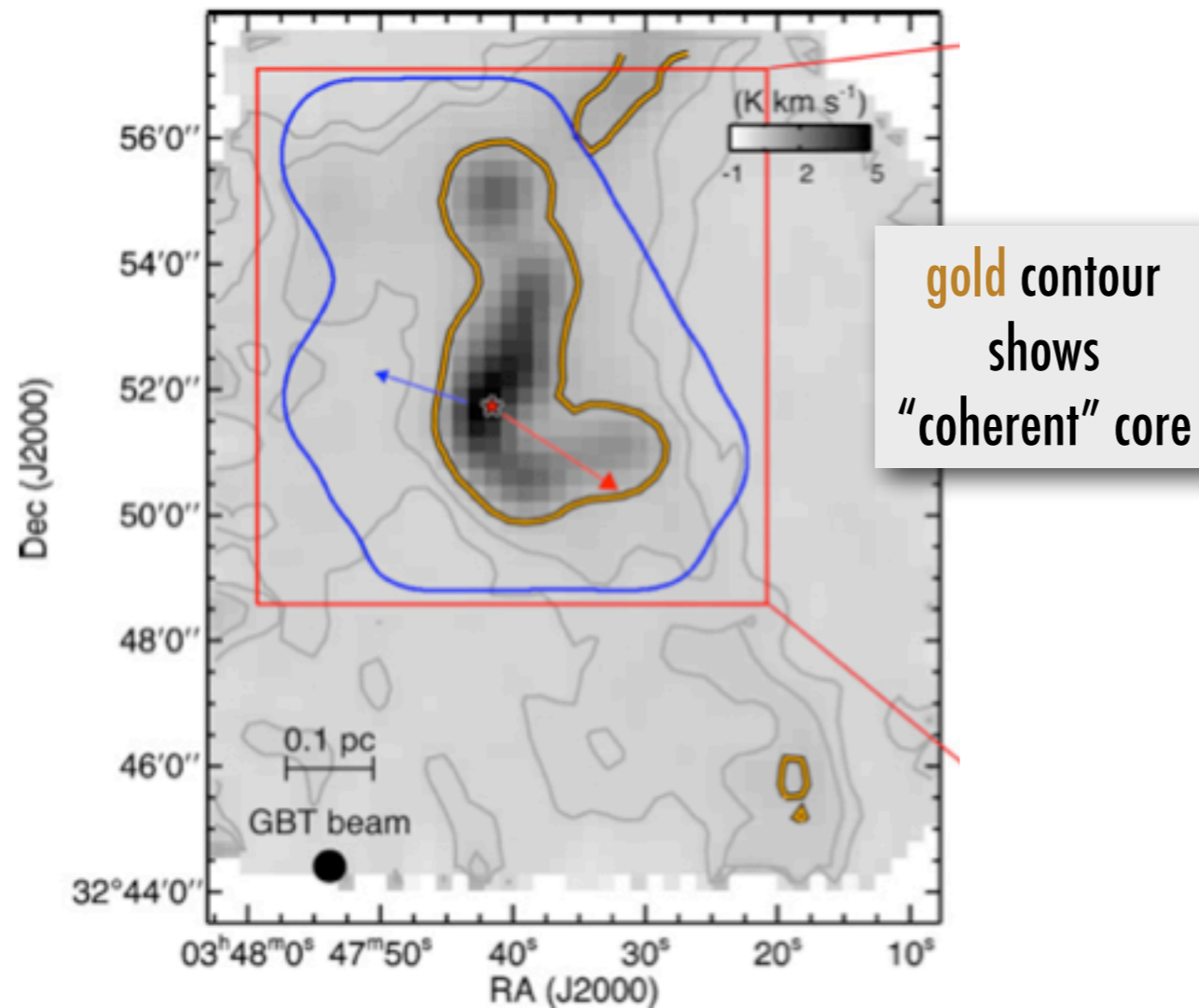
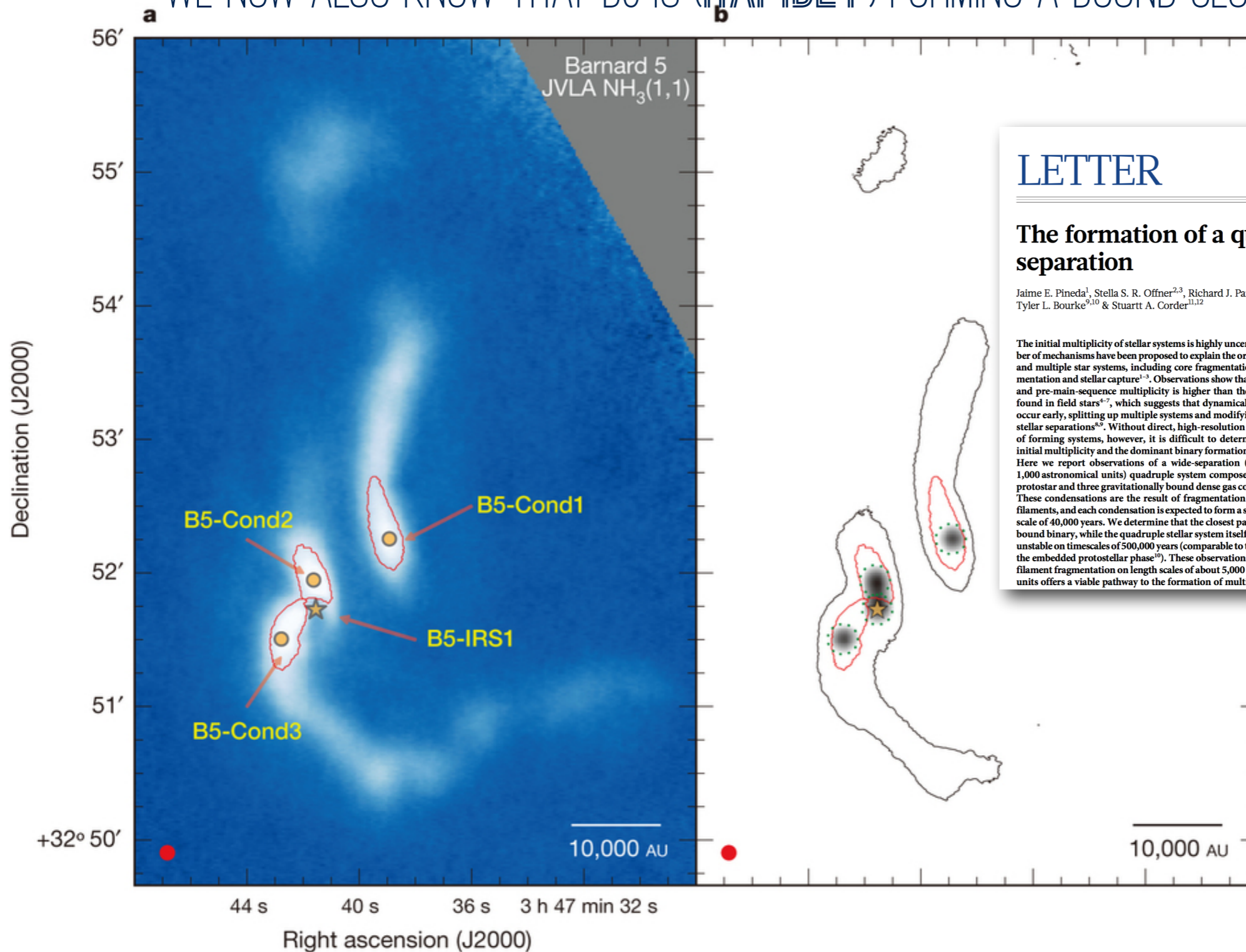


Figure 1. Left panel: integrated intensity map of B5 in NH₃ (1,1) obtained with GBT. Gray contours show the 0.15 and 0.3 K km s⁻¹ level in NH₃ (1,1) integrated intensity. The orange contours show the region in the GBT data where the non-thermal velocity dispersion is subsonic. The young star, B5-IRS1, is shown by the star in both panels. The outflow direction is shown by the arrows. The blue contour shows the area observed with the EVLA and the red box shows the area shown in the right panel. Right panel: integrated intensity map of B5 in NH₃ (1,1) obtained combining the EVLA and GBT data. Black contour shows the 50 mJy beam⁻¹ km s⁻¹ level in NH₃ (1,1) integrated intensity. The yellow box shows the region used in Figure 4. The northern starless condensation is shown by the dashed circle.

AND SUB-SUB STRUCTURE

WE NOW ALSO KNOW THAT B5 IS (RAPIDLY) FORMING A BOUND CLUSTER



LETTER

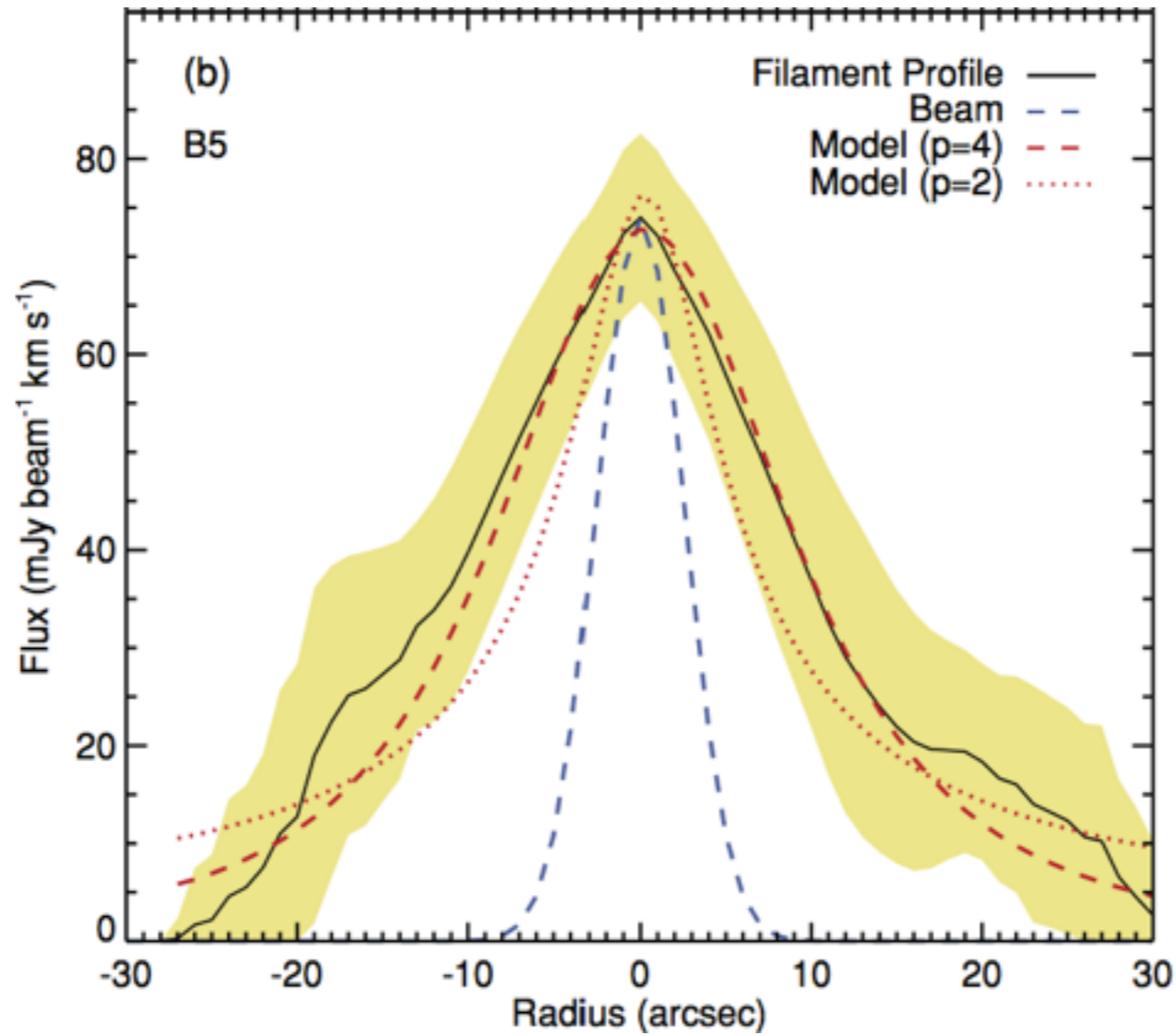
doi:10.1038/nature14166

The formation of a quadruple star system with wide separation

Jaime E. Pineda¹, Stella S. R. Offner^{2,3}, Richard J. Parker⁴, Héctor G. Arce⁵, Alyssa A. Goodman⁶, Paola Caselli⁷, Gary A. Fuller⁸, Tyler L. Bourke^{9,10} & Stuart A. Corder^{11,12}

The initial multiplicity of stellar systems is highly uncertain. A number of mechanisms have been proposed to explain the origin of binary and multiple star systems, including core fragmentation, disk fragmentation and stellar capture^{1–3}. Observations show that protostellar and pre-main-sequence multiplicity is higher than the multiplicity found in field stars^{4–7}, which suggests that dynamical interactions occur early, splitting up multiple systems and modifying the initial stellar separations^{8,9}. Without direct, high-resolution observations of forming systems, however, it is difficult to determine the true initial multiplicity and the dominant binary formation mechanism. Here we report observations of a wide-separation (greater than 1,000 astronomical units) quadruple system composed of a young protostar and three gravitationally bound dense gas condensations. These condensations are the result of fragmentation of dense gas filaments, and each condensation is expected to form a star on a time-scale of 40,000 years. We determine that the closest pair will form a bound binary, while the quadruple stellar system itself is bound but unstable on timescales of 500,000 years (comparable to the lifetime of the embedded protostellar phase¹⁰). These observations suggest that filament fragmentation on length scales of about 5,000 astronomical units offers a viable pathway to the formation of multiple systems.

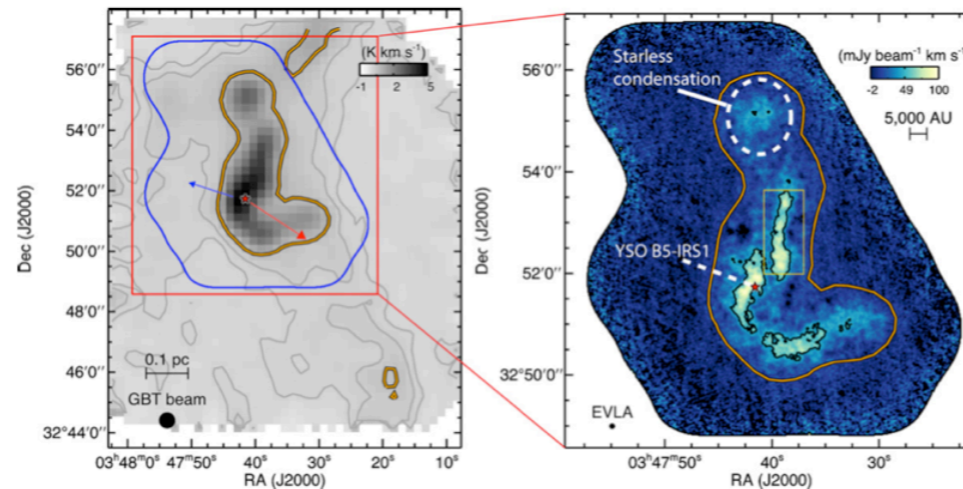
Detailed knowledge of the underlying distribution of dense gas is the key to determining which structures will go on to form stars. Here we identify the dense gas structures that are most likely to form stars using the dendrogram technique²¹. Dendrogram analysis is a hierarchical structure decomposition that uses isocontours to identify individual features, while also determining where these contours merge with adjacent structures to create a new parental structure. We refer to the smallest scale (and brightest) structures in the dendrogram as condensations. These are the most likely places for an individual star to form. Figure 1a shows the B5 region as seen in dense gas (number density of H_2 , $n_{H_2} \gtrsim 10^4 \text{ cm}^{-3}$), with the protostar and the identified gas condensations shown by a star and circles, respectively. The mass of the well known protostar B5-IRS1 is 0.1 solar masses (M_{Sun} ; ref. 22), while the masses of condensations B5-Cond1, B5-Cond2 and B5-Cond3 are $0.36 \pm 0.09 M_{\text{Sun}}$, $0.26 \pm 0.12 M_{\text{Sun}}$ and $0.30 \pm 0.13 M_{\text{Sun}}$, respectively. Uncertainty in these masses is dominated by the uncertainty in the temperature used to convert measured fluxes to masses. The radii of the three condensations are respectively 2,800 AU, 2,300 AU and 2,500 AU, while the projected separations between the same three condensations and the protostar are 3,300 AU, 5,100 AU and 11,400 AU (see Methods). The half-mass radii of the condensations are about half the condensation radii. This, combined with



isothermal,
hydrostatic filaments,
not turbulent ones?

THE ASTROPHYSICAL JOURNAL LETTERS, 739:L2 (5pp), 2011 September 20

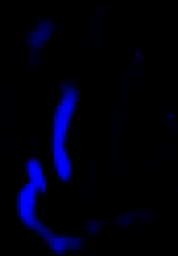
PINEDA ET AL.



Here's the fun/crazy part.

WHAT IF FILAMENTS CONTINUE ACROSS "CORE" BOUNDARIES?!

blue =VLA ammonia (high-density gas); **green**=GBT ammonia (lower-res high-density gas); **red**=Herschel 250 micron continuum (dust)





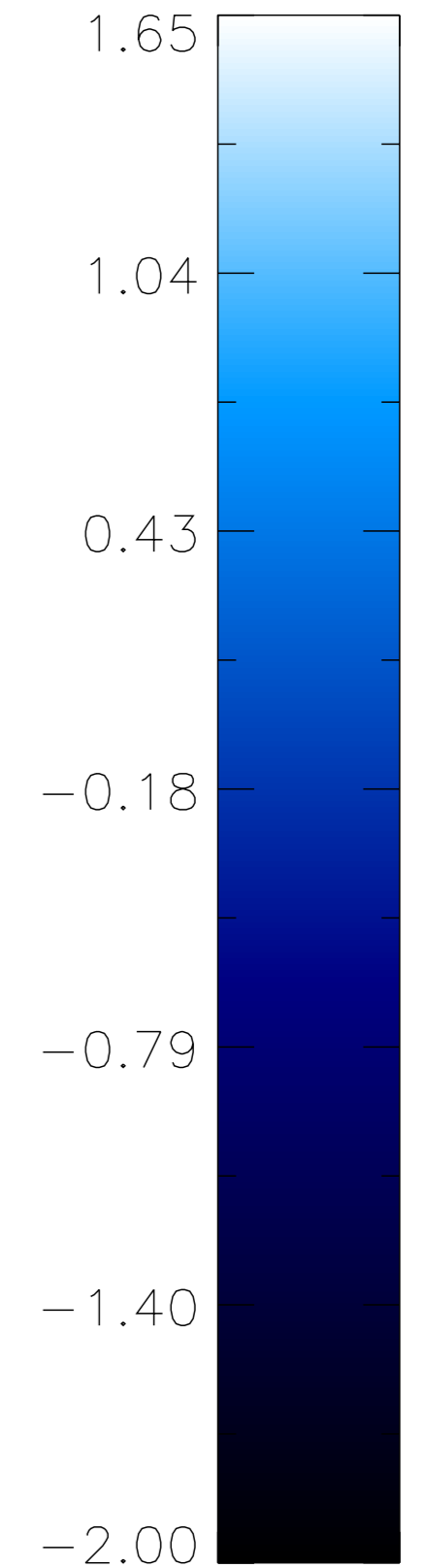
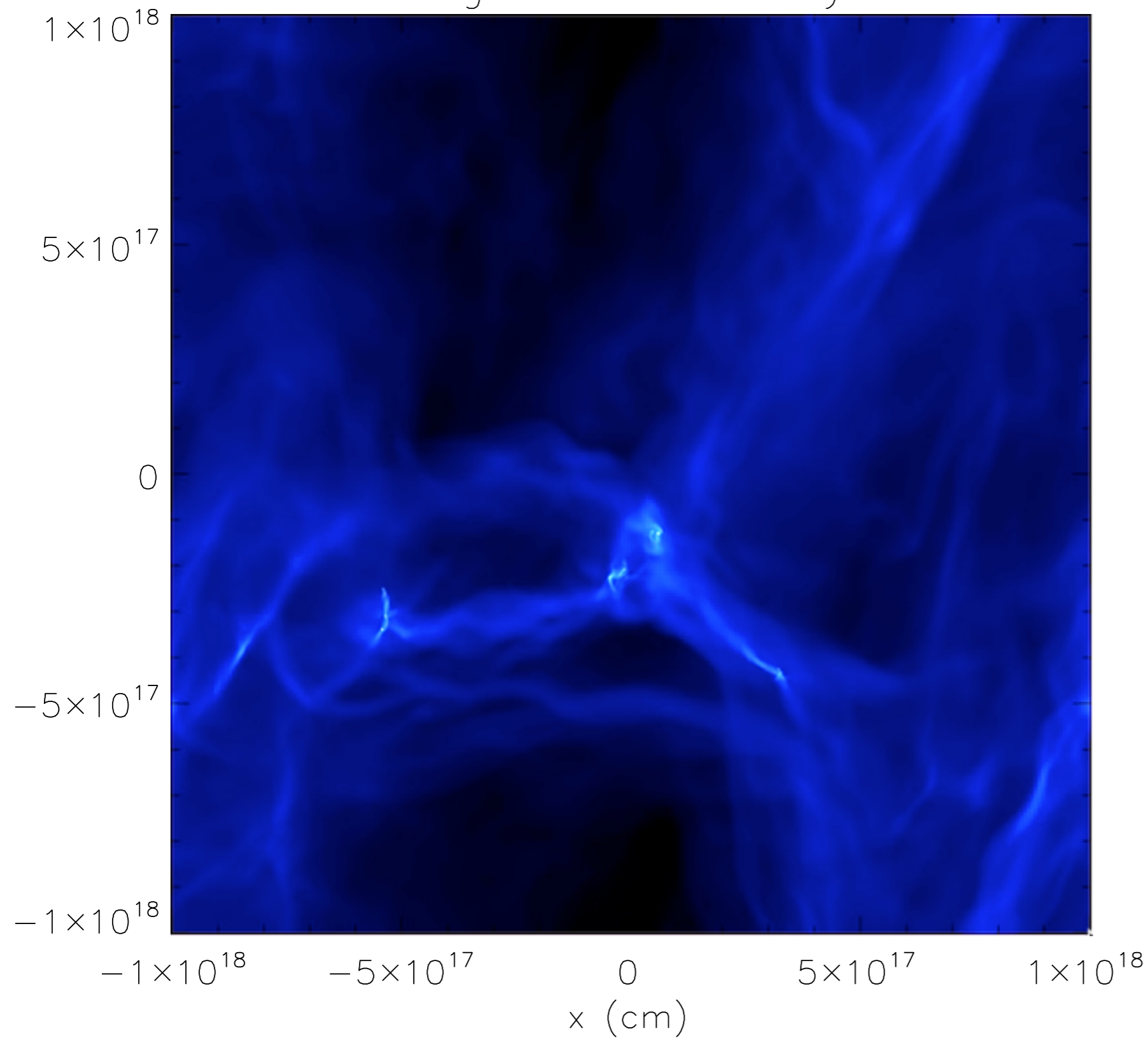
1998



2008

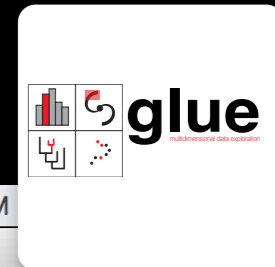
B5-ISH SIMULATION (NO MAGNETIC FIELD)

Log Column Density



Offner (priv. comm.)

B5/GLUE (NEW IRAM 30-M DATA)



Data Collection

- 4.9<=PRIMARY<5.6
- 5.6<=PRIMARY<6.3
- 6.3<=PRIMARY<7.0
- 12

12 (test)

Link Data

Plot Layers - 3D Volume Rendering

- 12 (combined_all_b5_13co_21_nc)
- 12 (combined_all_b5_c18o_21_nc)
- combined_all_b5_hcn_10_noise_1

Attribute: PRIMARY

Min: 0 Max: 5.004

Color: [white box]

Alpha: [slider]

Subset: Data Outline

Plot Options - 3D Volume Rendering

x axis

min/max: -0.5 ⇌ 105.5

stretch: [slider] 0.46

y axis

min/max: -0.5 ⇌ 245.5

stretch: [slider] 1.0

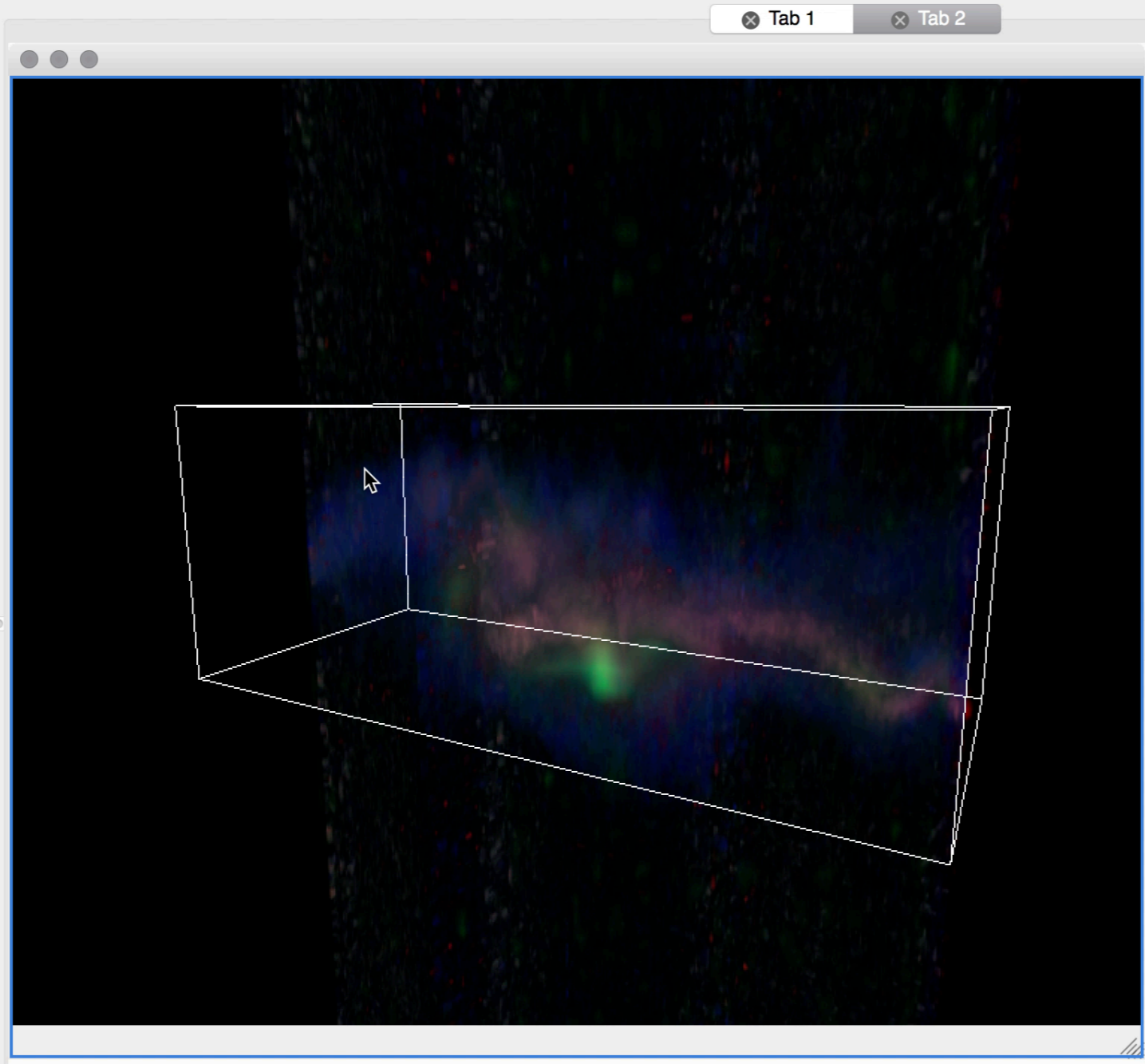
z axis

min/max: 170 ⇌ 220

stretch: [slider] 0.39

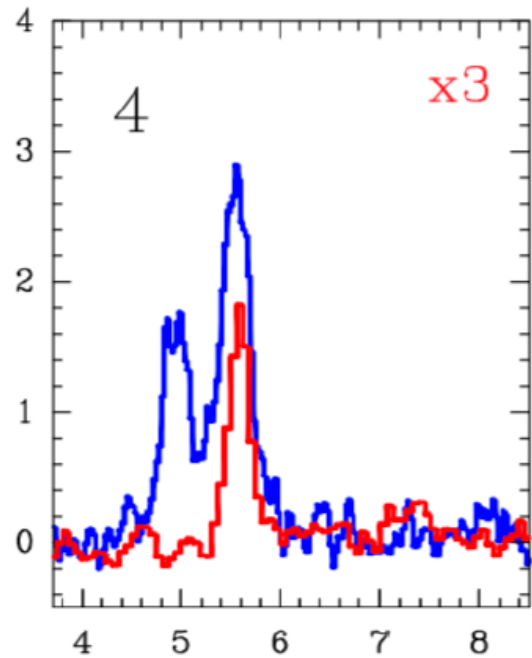
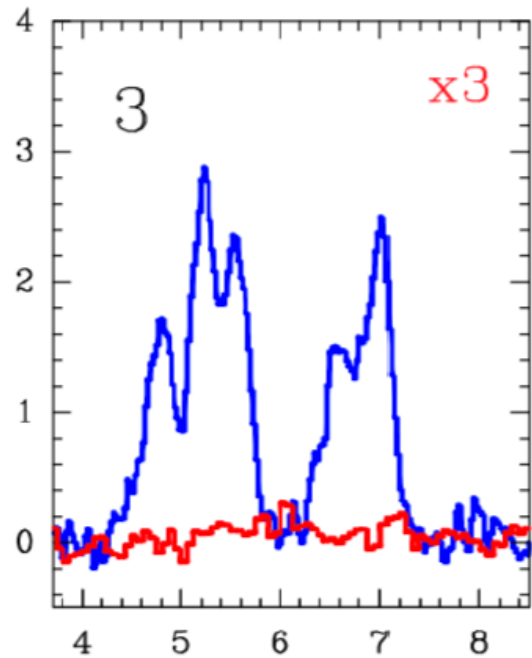
Coordinate axes

Reset View

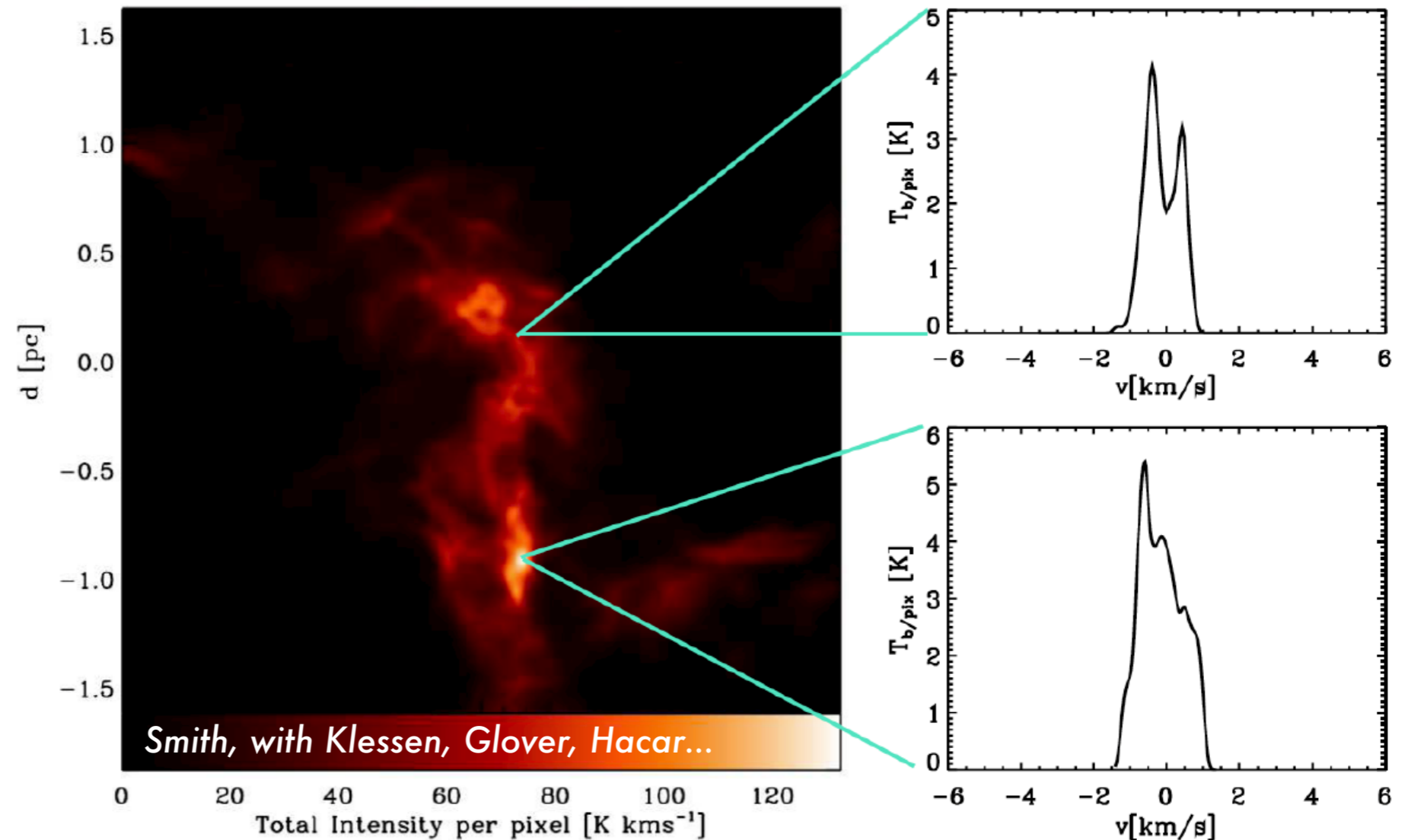


Simulators are almost observing enough lines...

Filaments in Filaments



Observed C¹⁸O emission in blue.



Synthetic observation of C¹⁸O emission from our time-dependent chemical model post-processed with radmc-3d

slide courtesy of Rowan Smith, from CfA-ITC talk, March 31, 2016
cf. Moeckl & Burkert 2015, work of Hacar et al...

SOME PLACES ARE SPECIAL



What are “special” places in ISM & how long do they last?

—galactic plane, **Bones**

—filaments’ influence may last into cores—how long, and when, simulators?

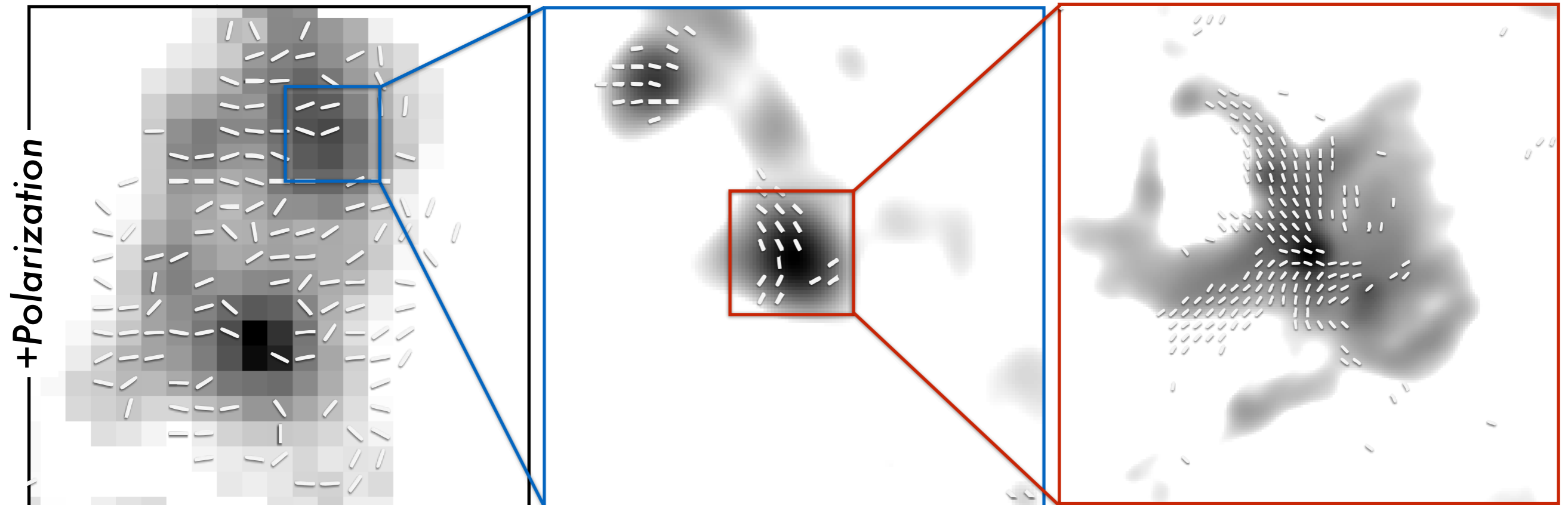
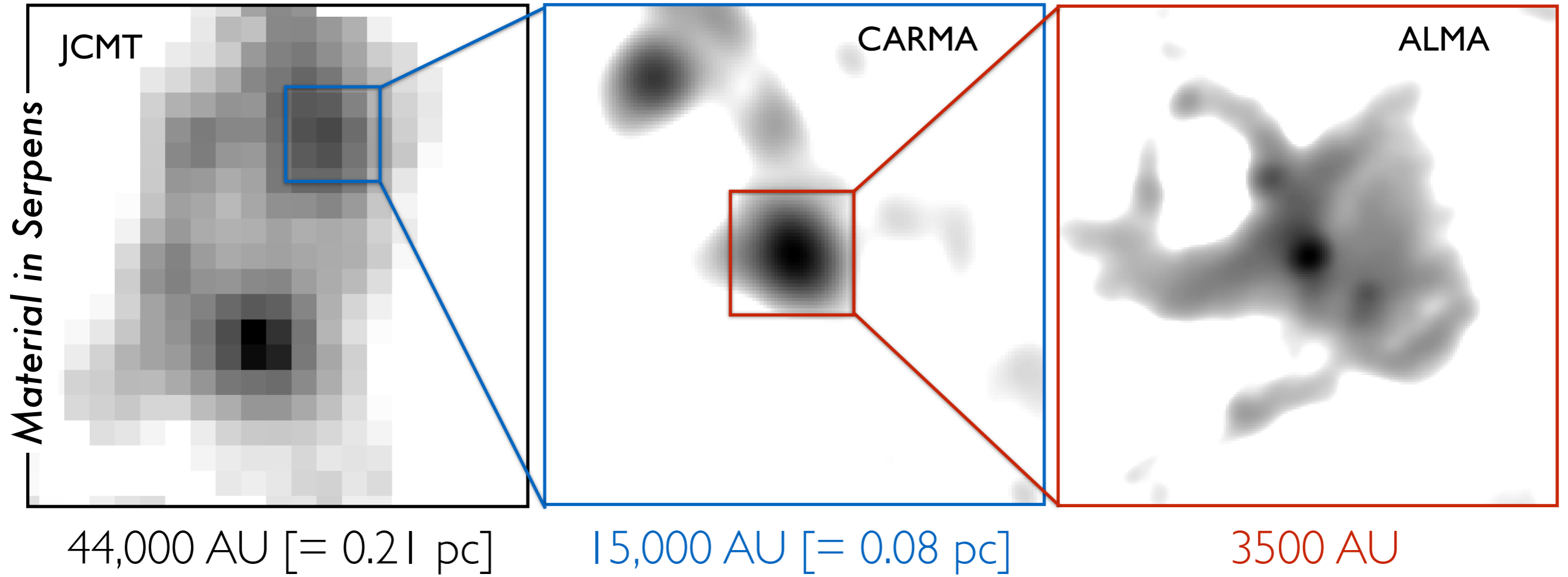
How do “influences” change what is special?

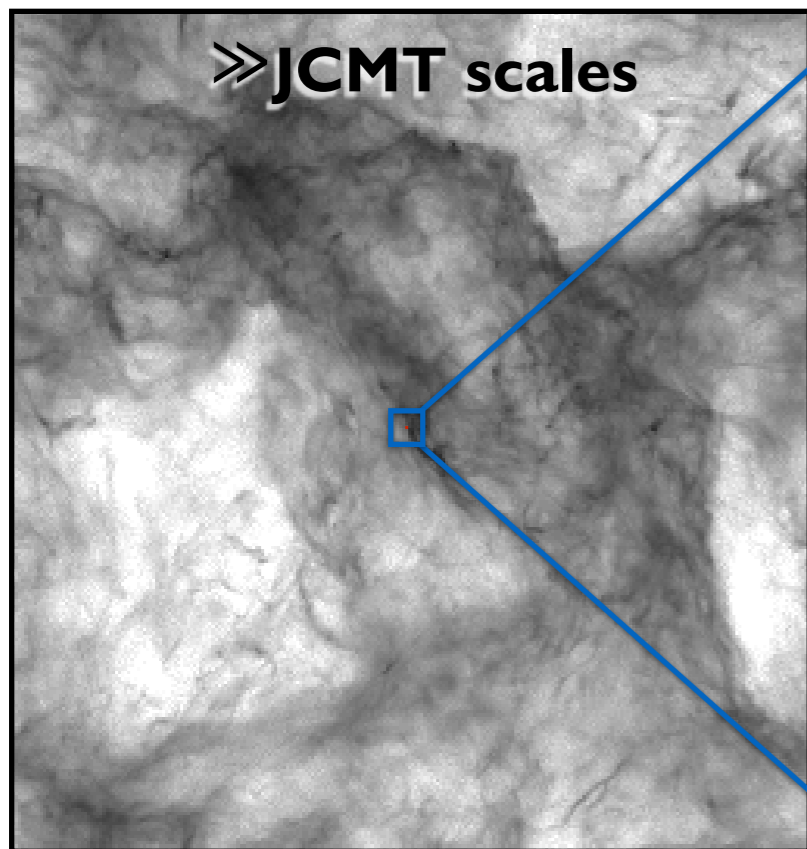
—magnetic fields, feedback, “collisions,” but when, how & where, simulators?



Sneak Preview of ALMA+AREPO B-field insights...

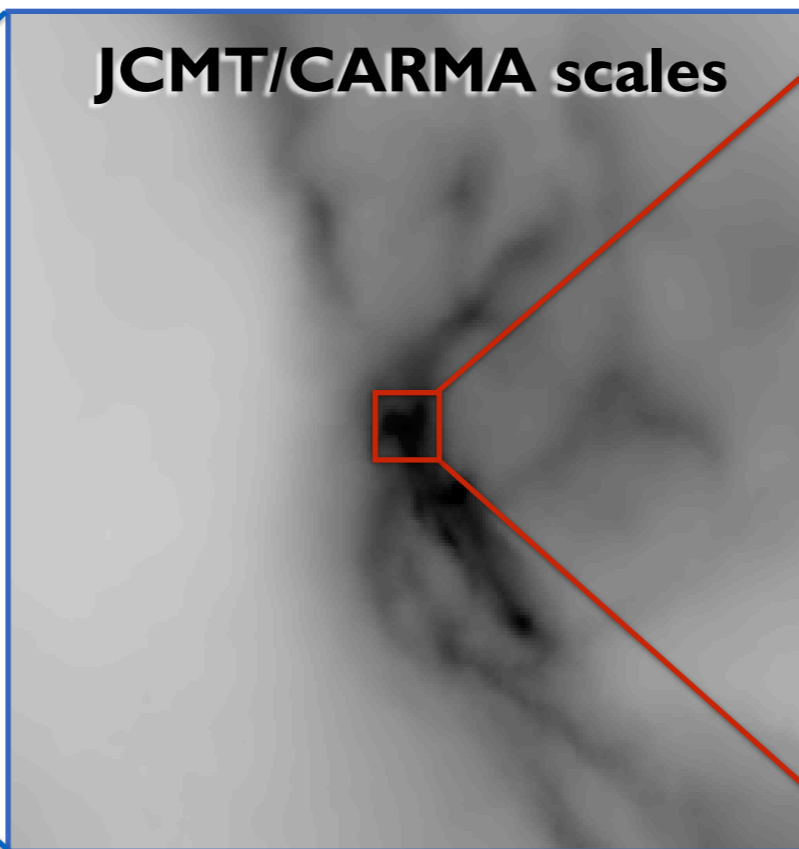
Hull, Mocz, Burkhart, Goodman, Girart, Cortes, Hernquist, Lai, Li, Springel 2016, *Nature*, under review.





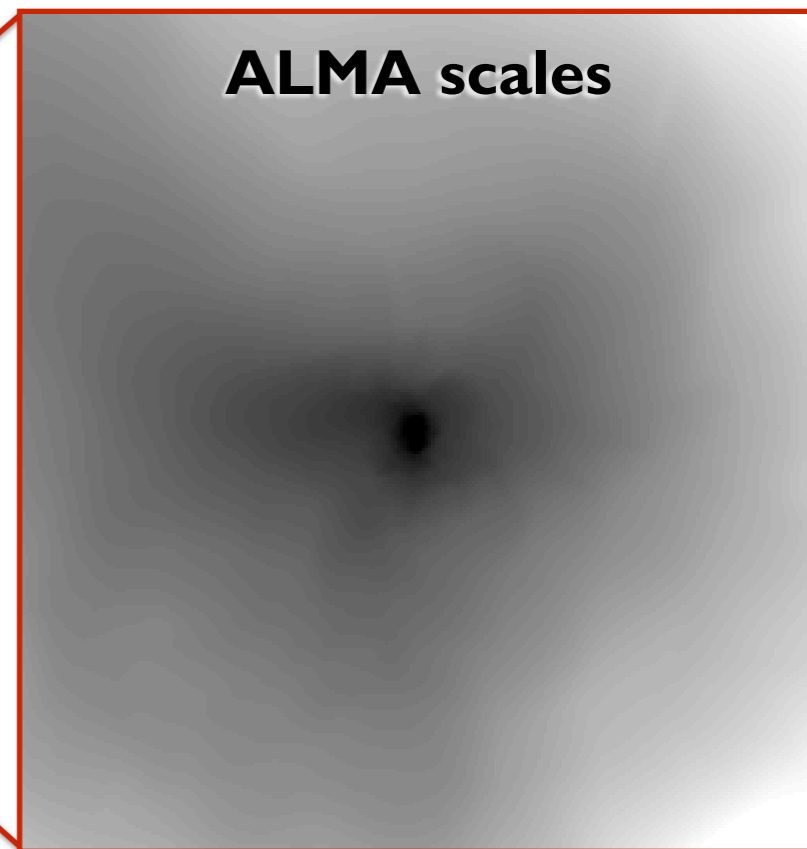
» JCMT scales

1 million AU [= 5 pc]



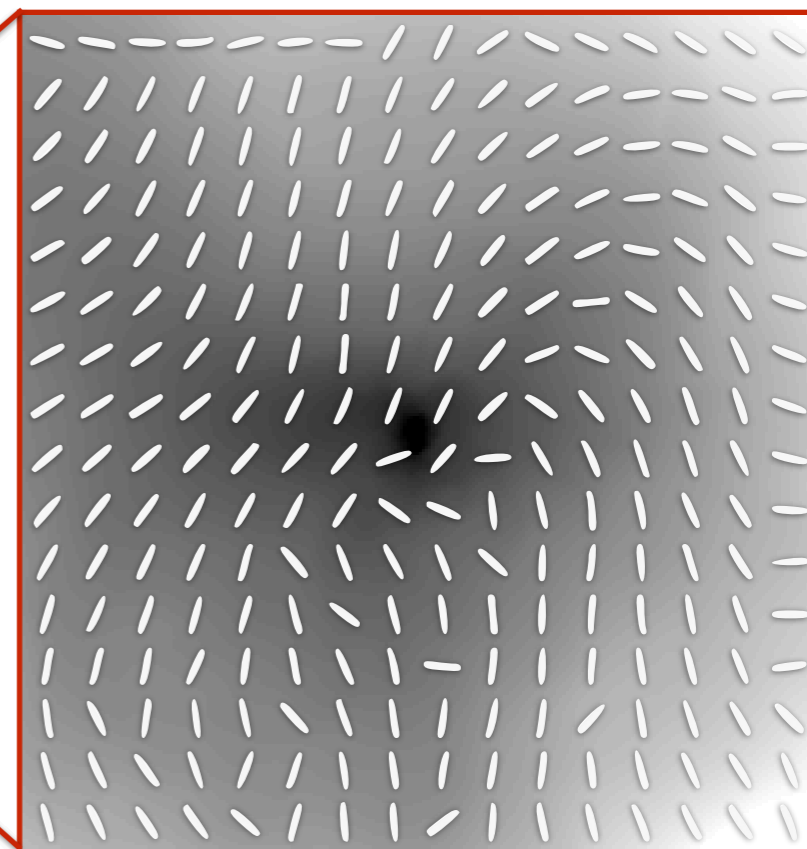
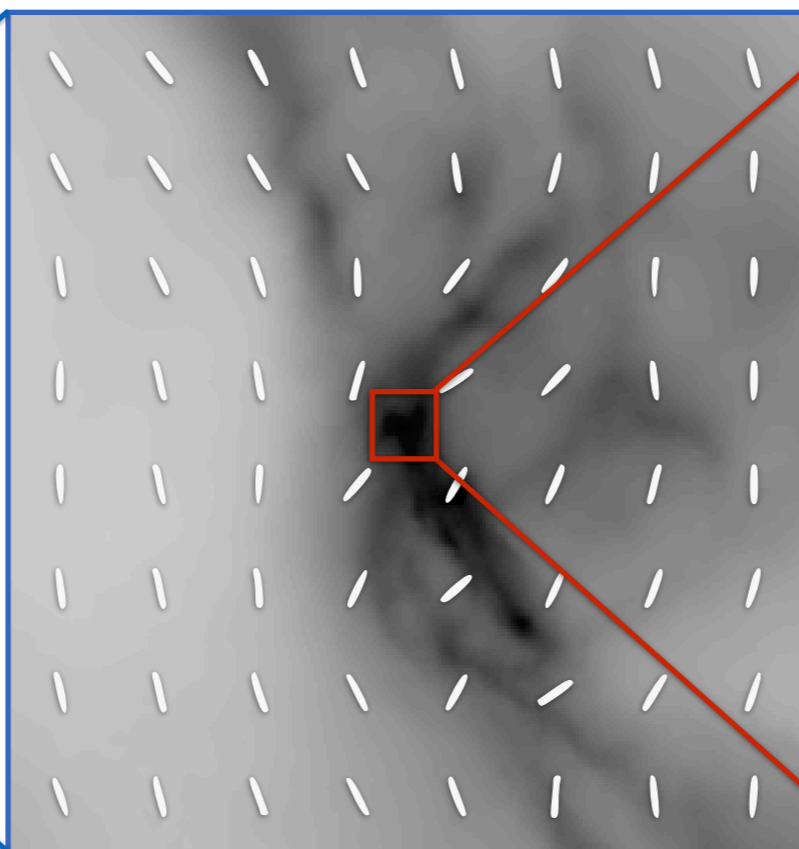
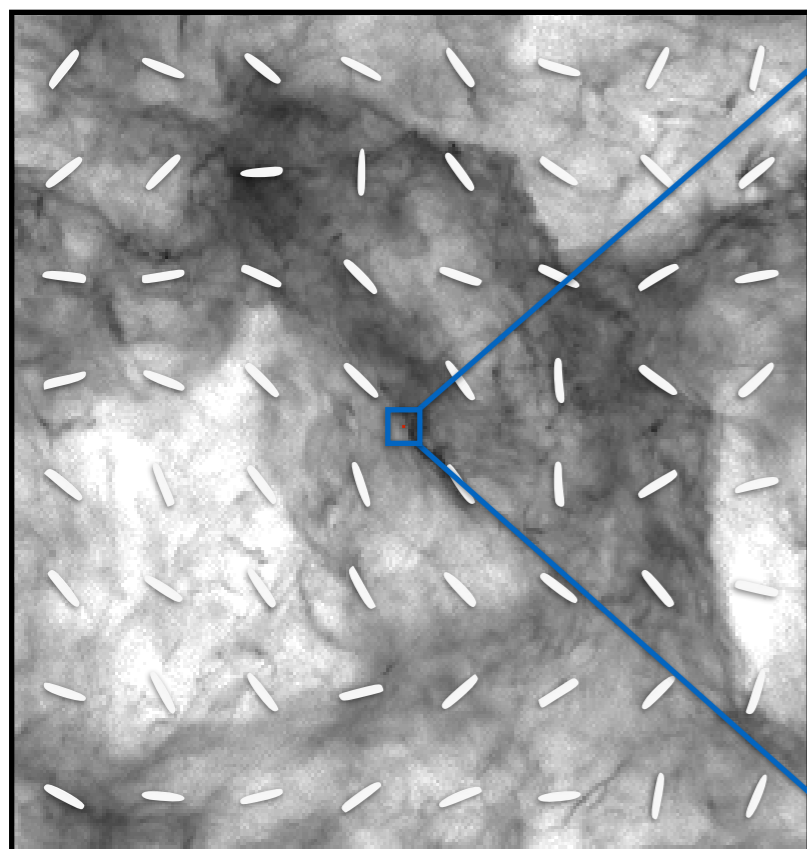
JCMT/CARMA scales

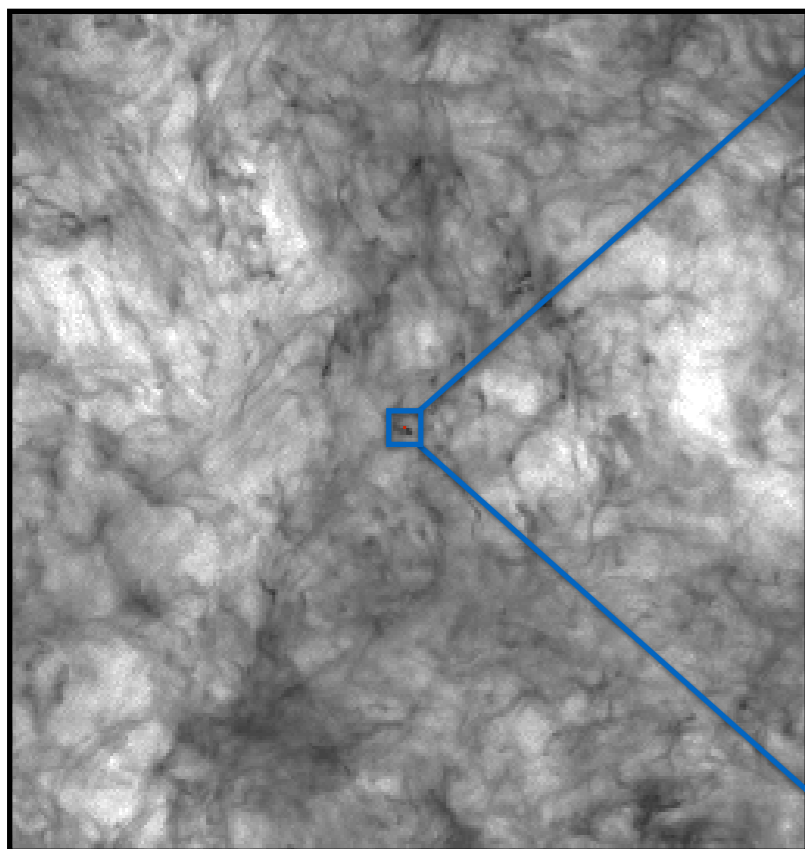
37350 AU [= 0.2 pc]



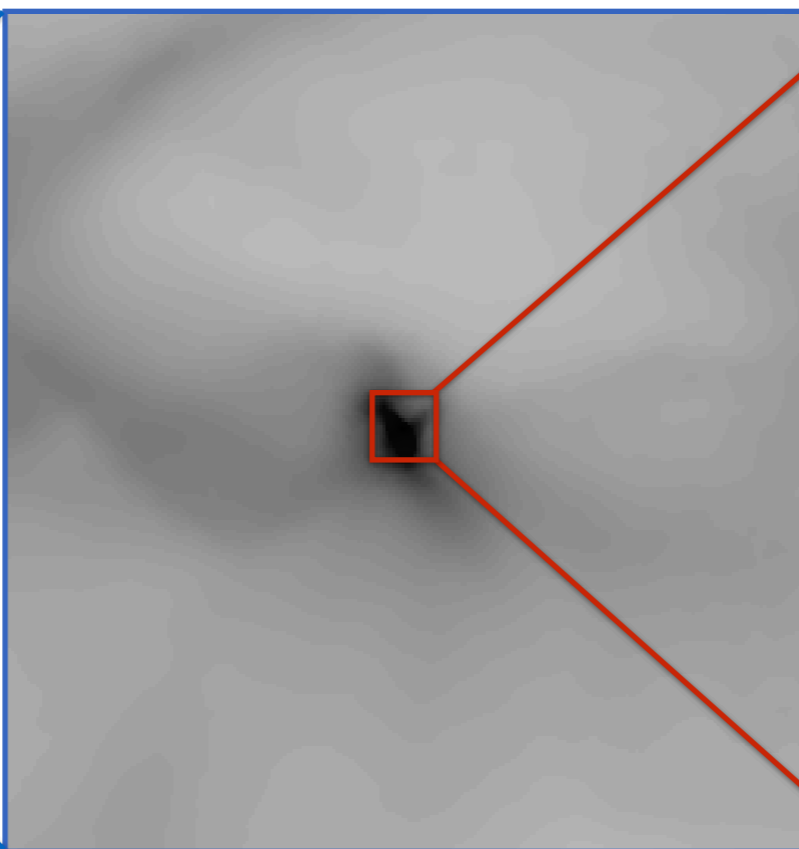
ALMA scales

3000 AU

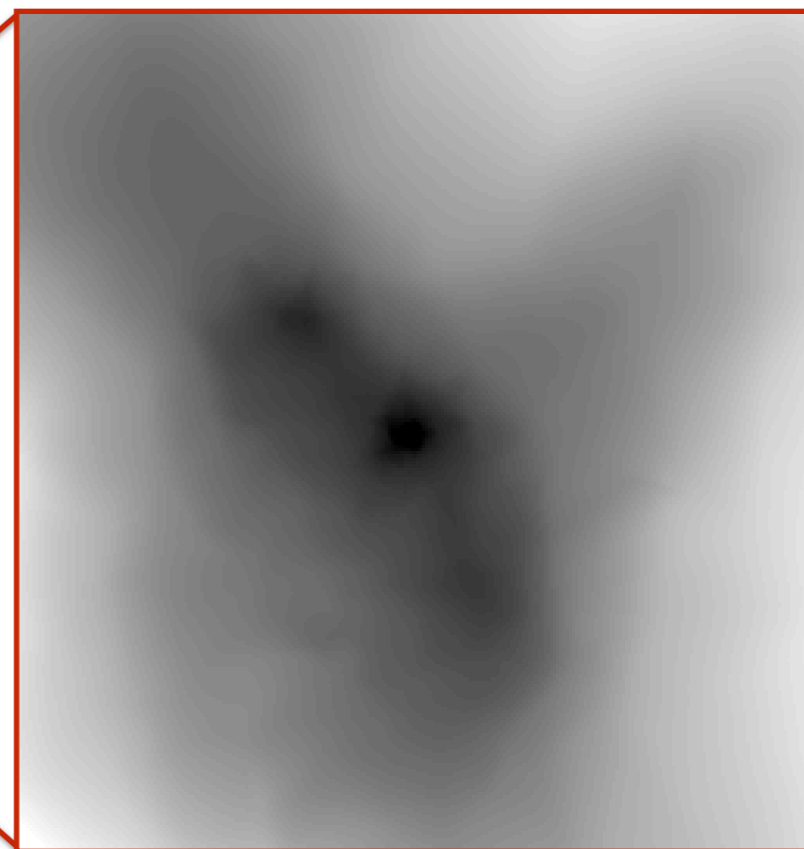




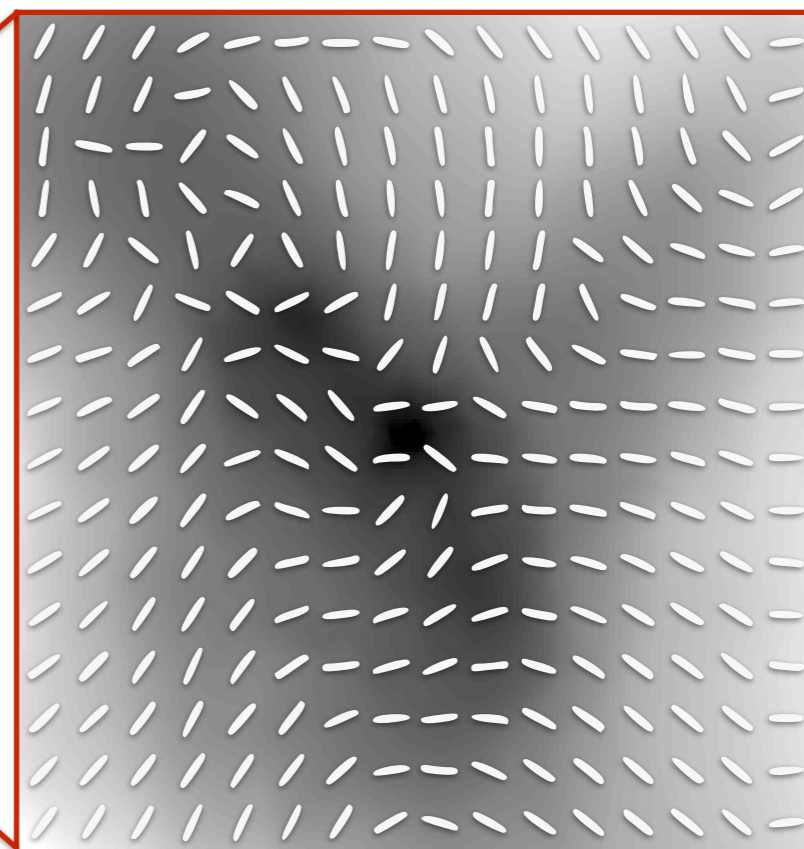
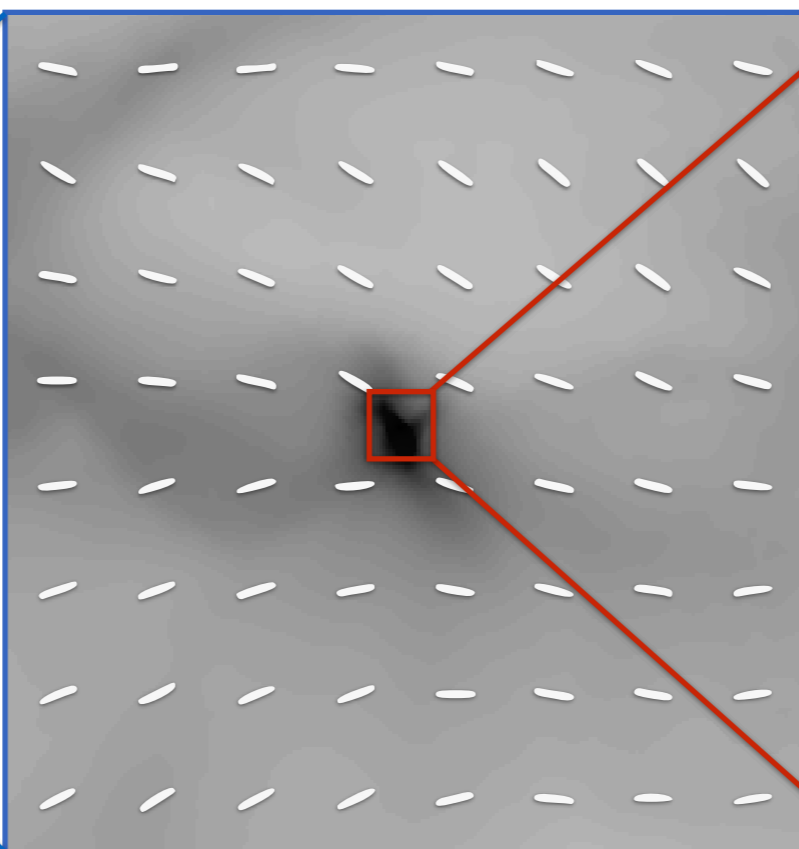
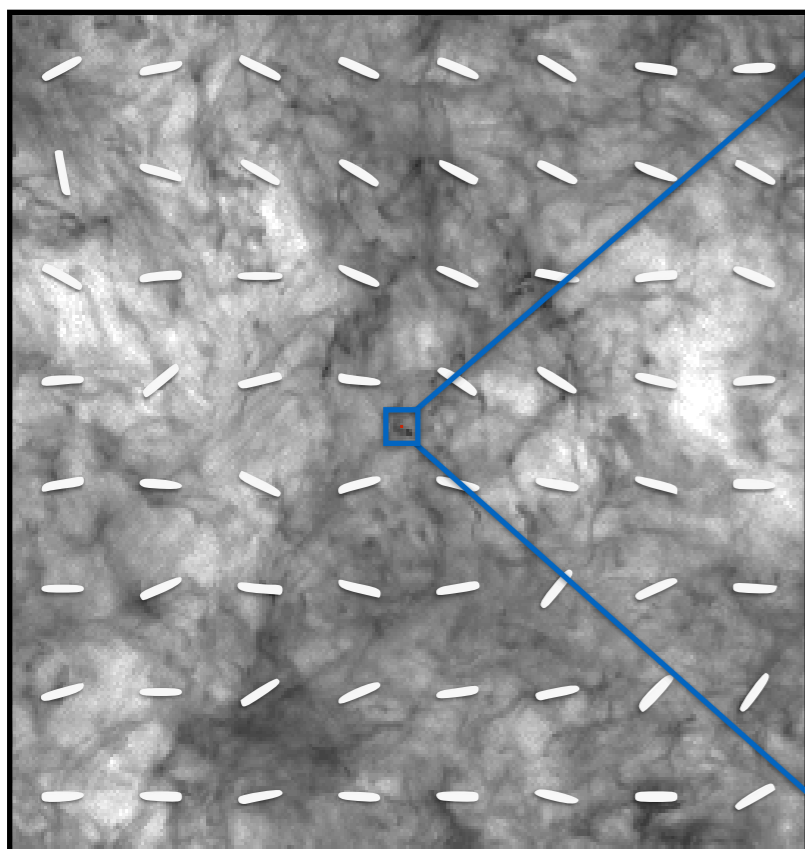
1 million AU [= 5 pc]

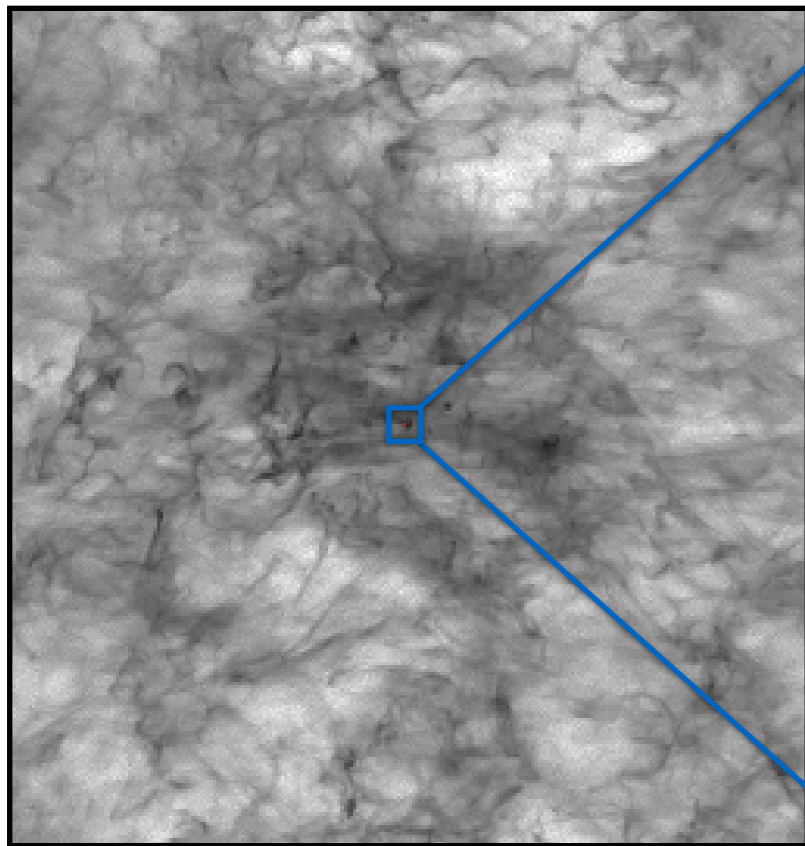


37350 AU [= 0.2 pc]

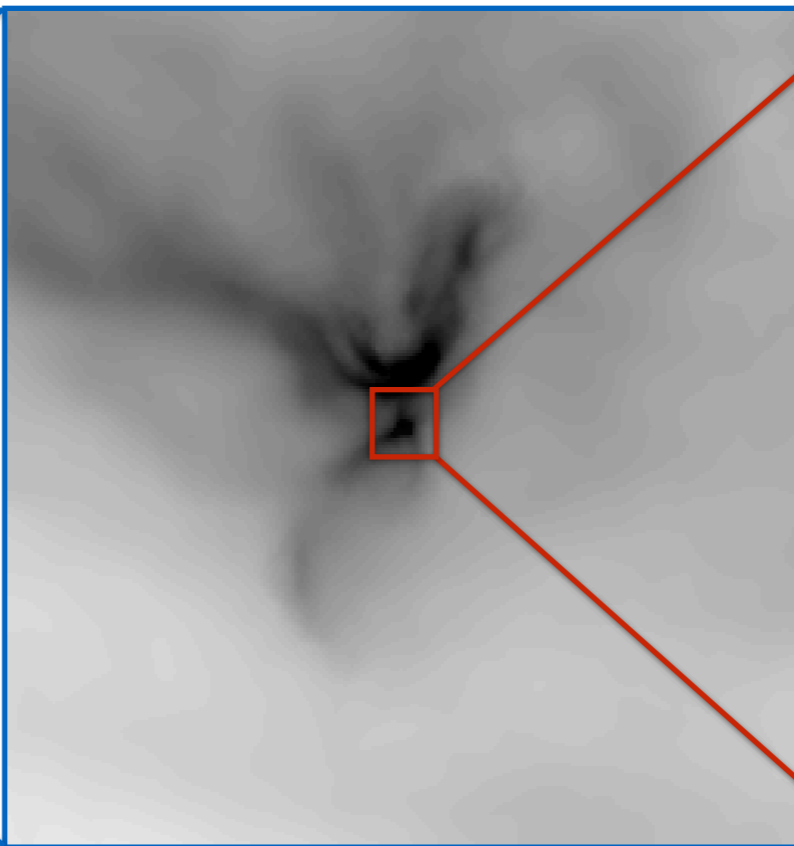


3000 AU

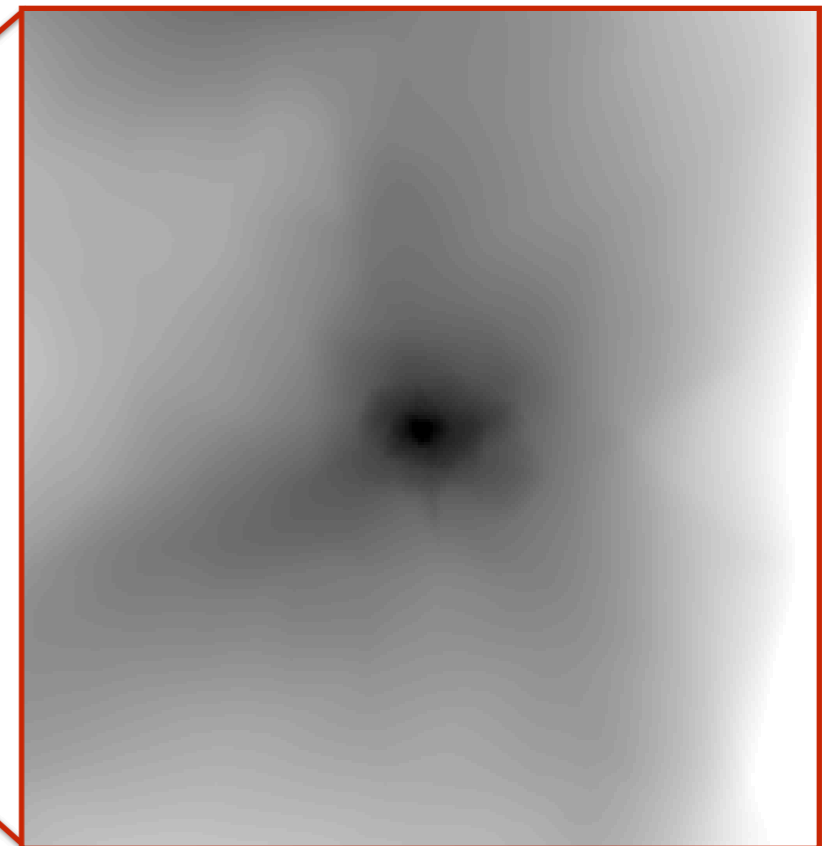




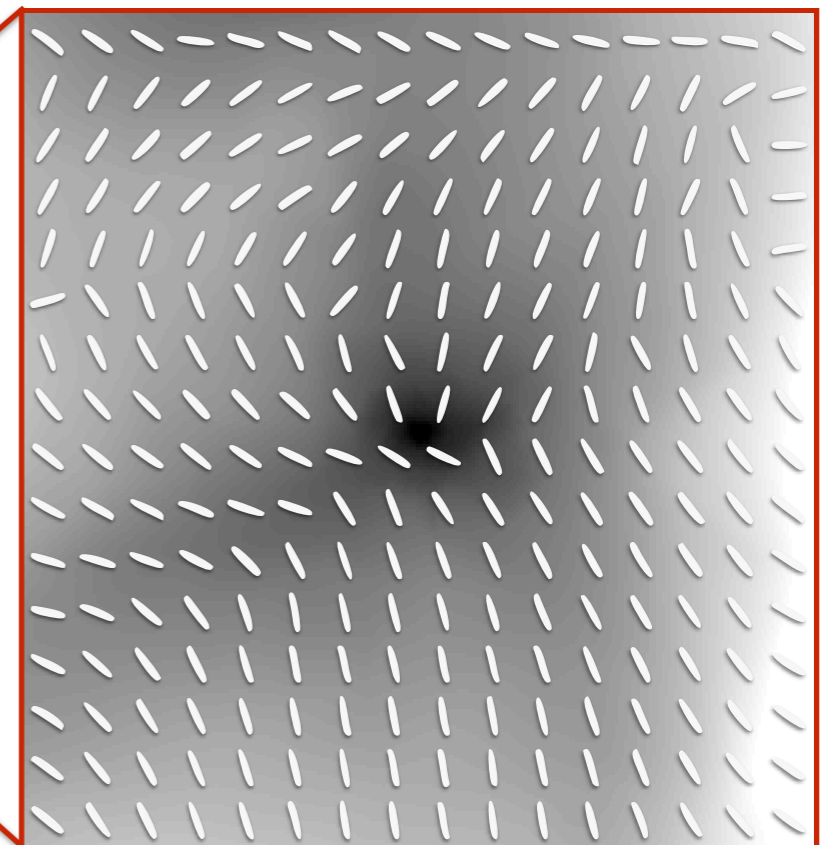
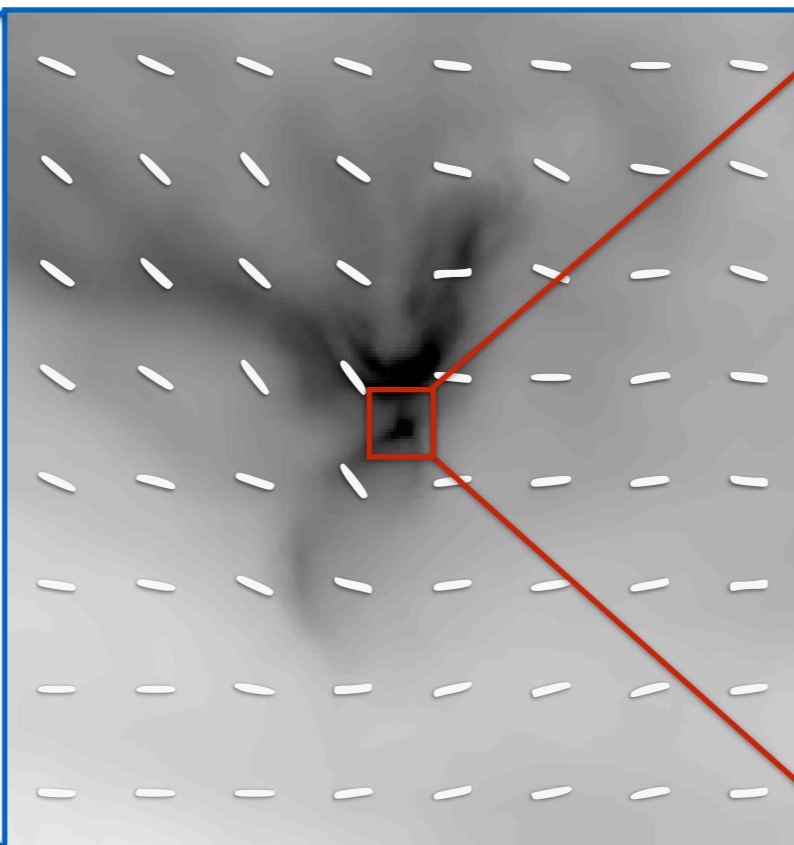
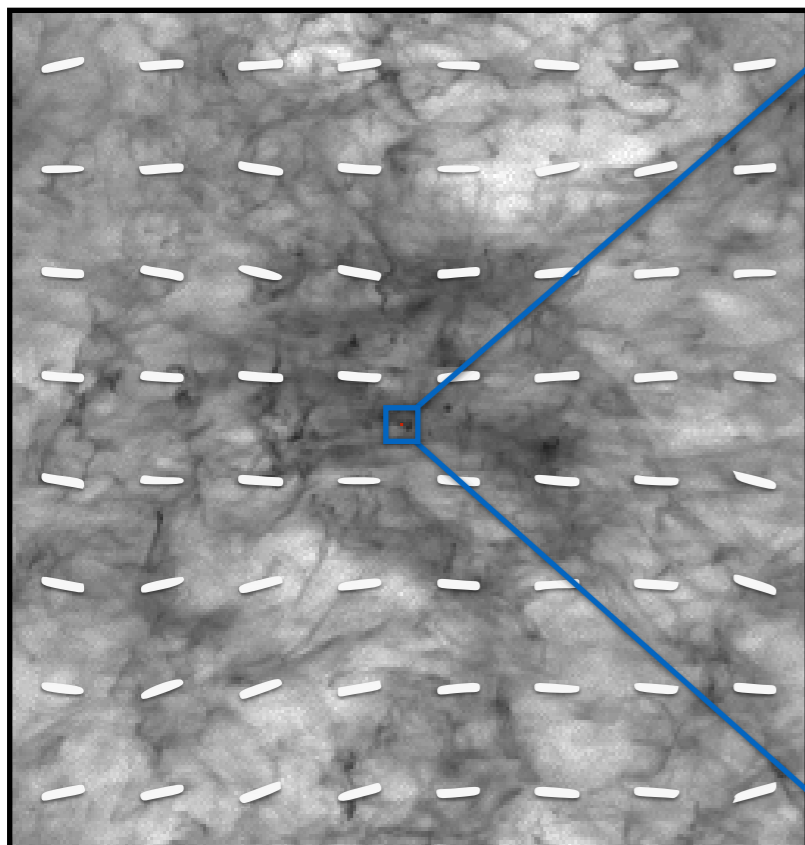
1 million AU [= 5 pc]

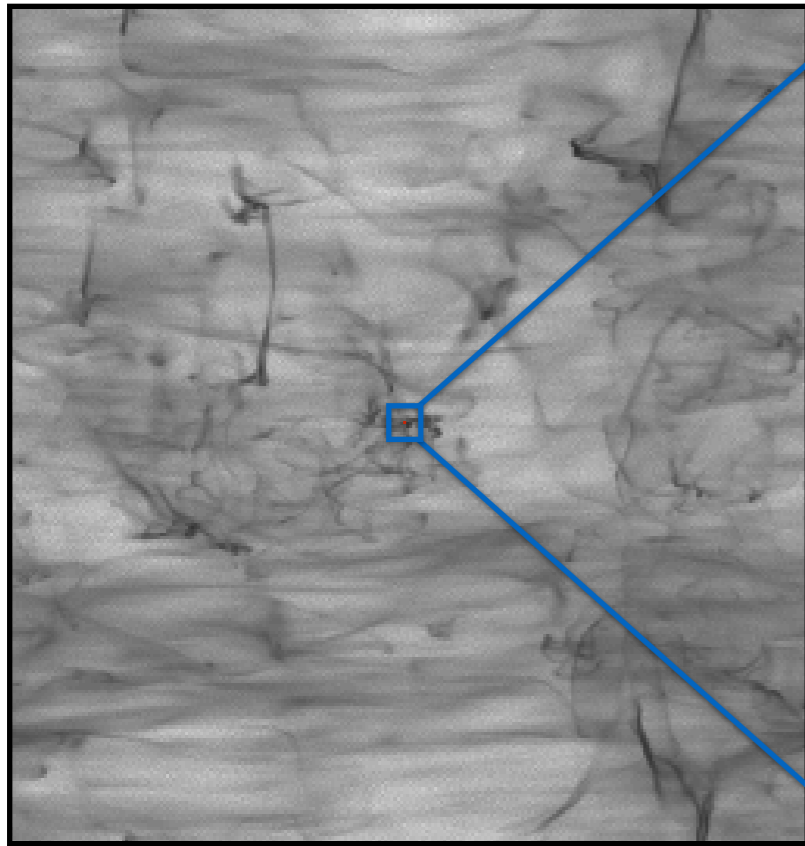


37350 AU [= 0.2 pc]

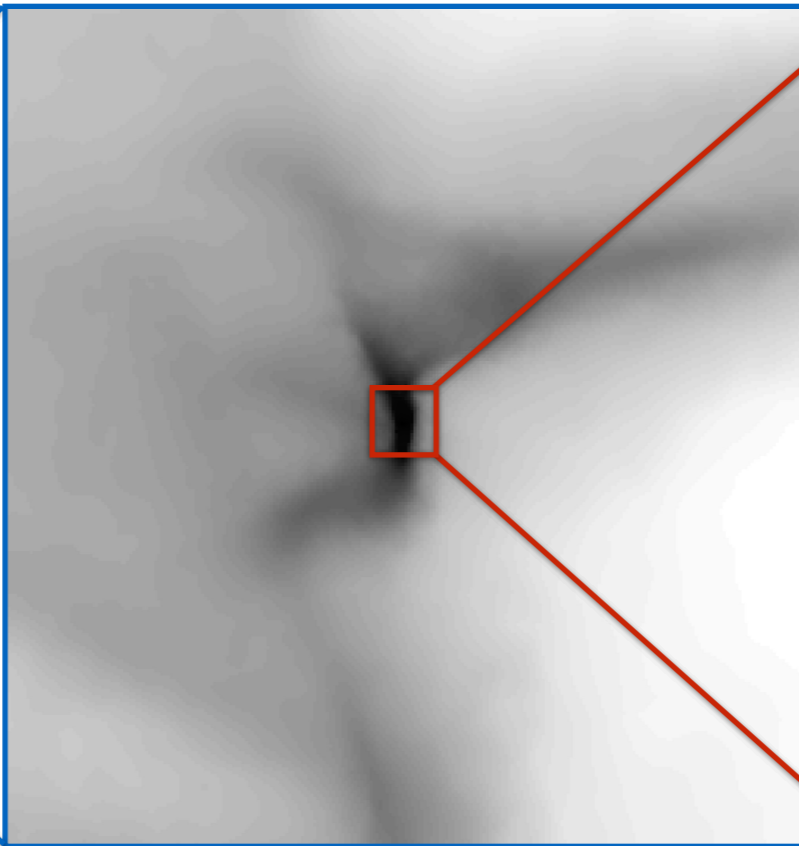


3000 AU

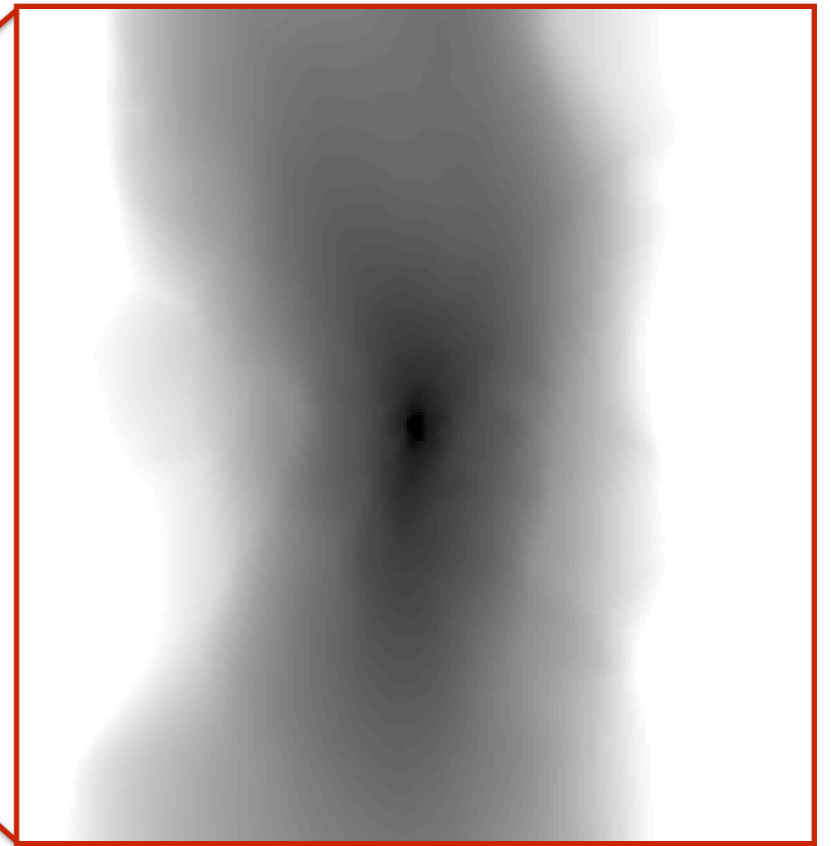




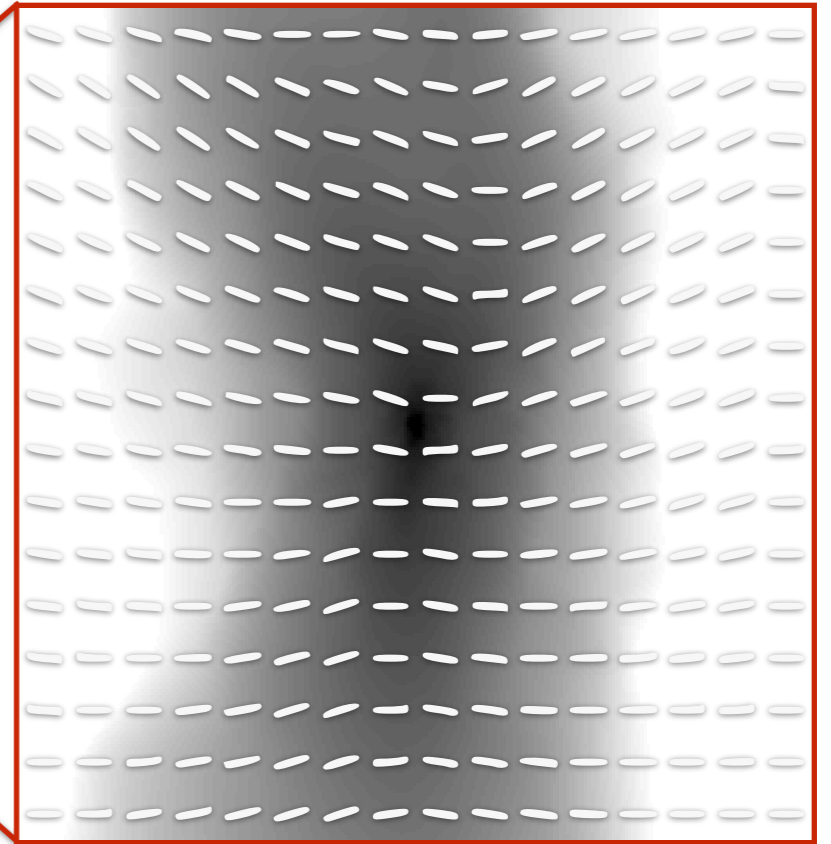
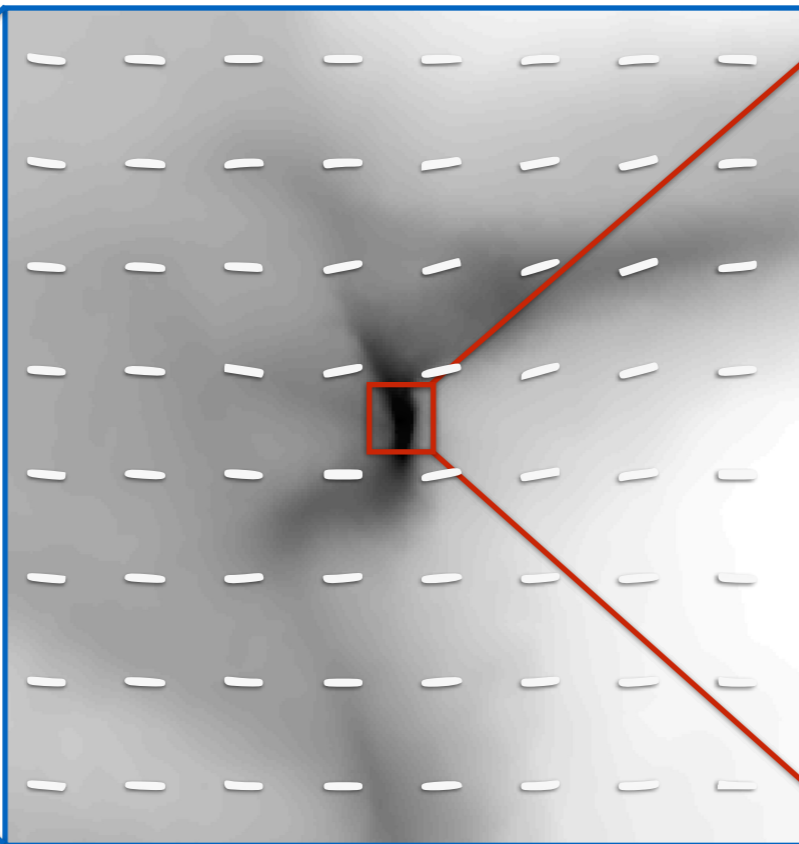
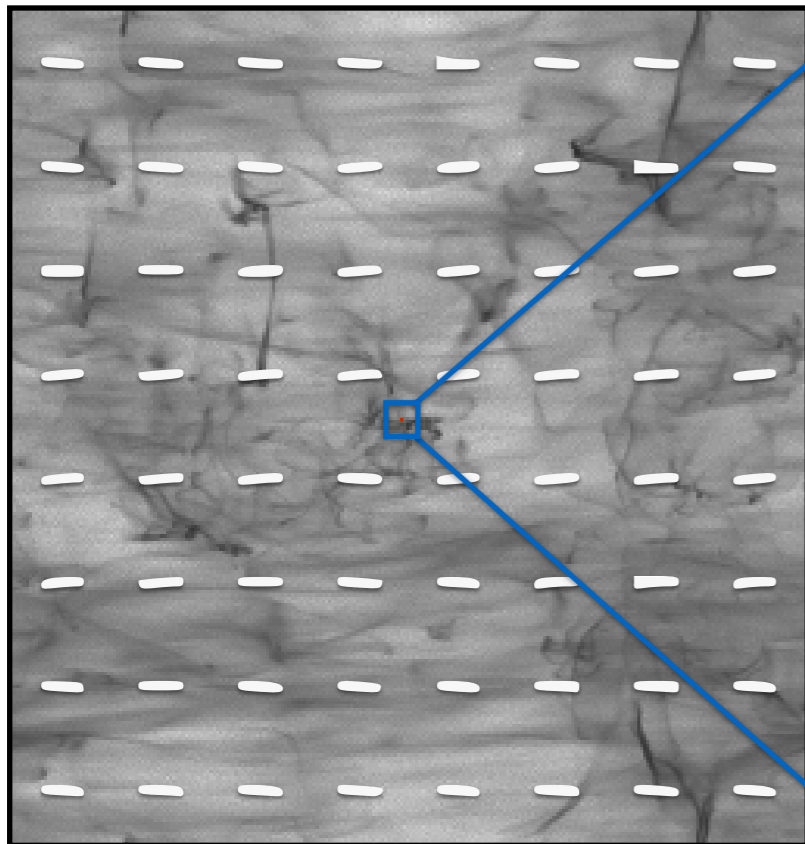
1 million AU [= 5 pc]

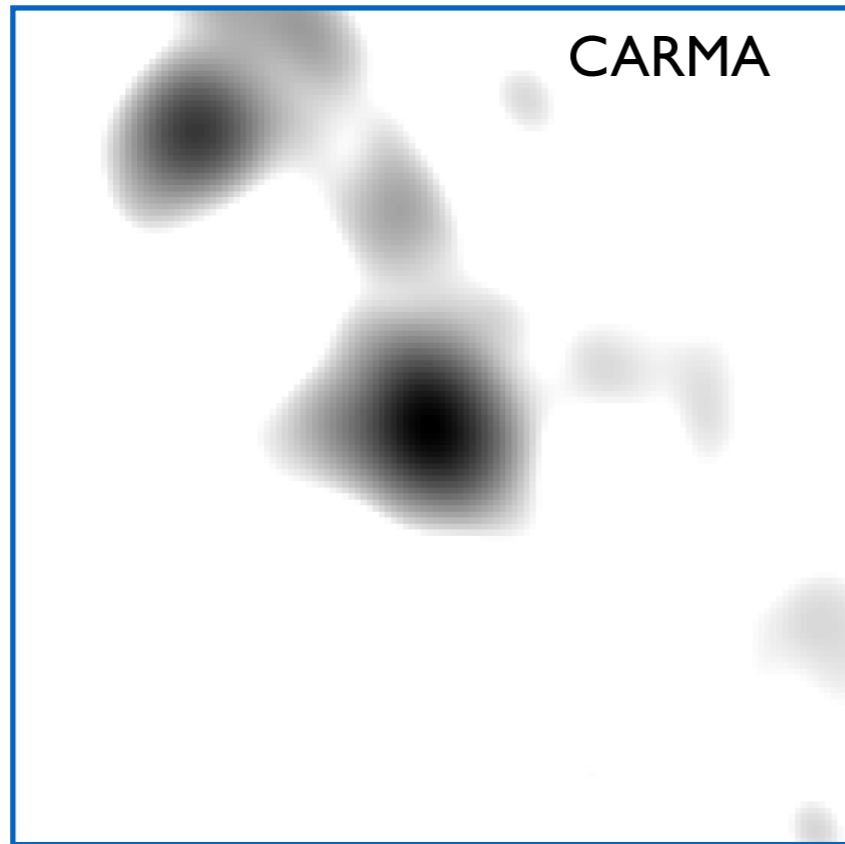


37350 AU [= 0.2 pc]

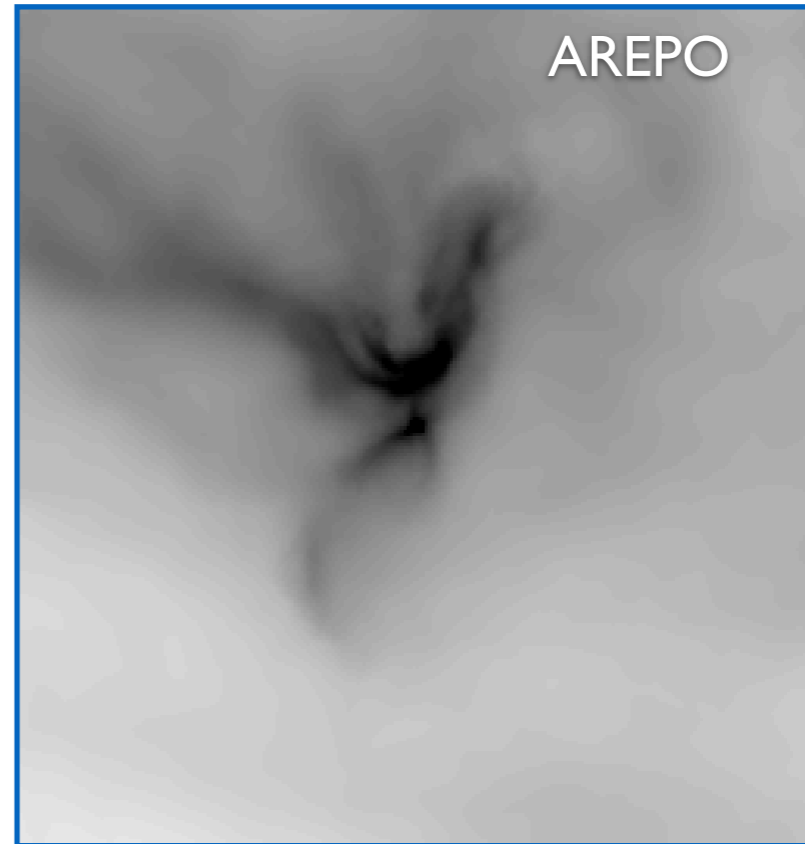


3000 AU

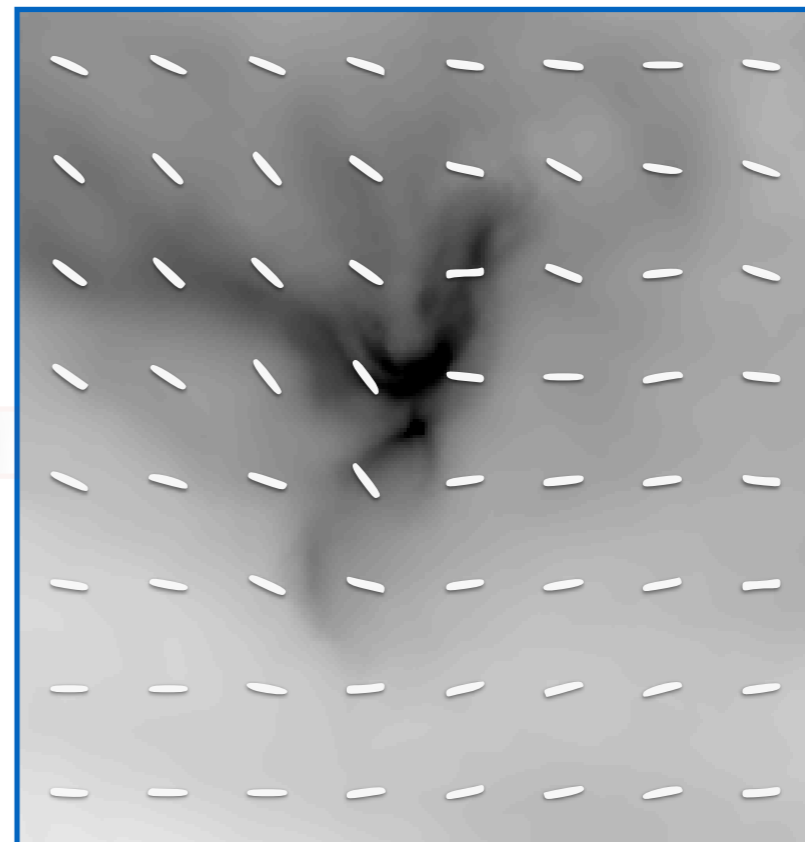
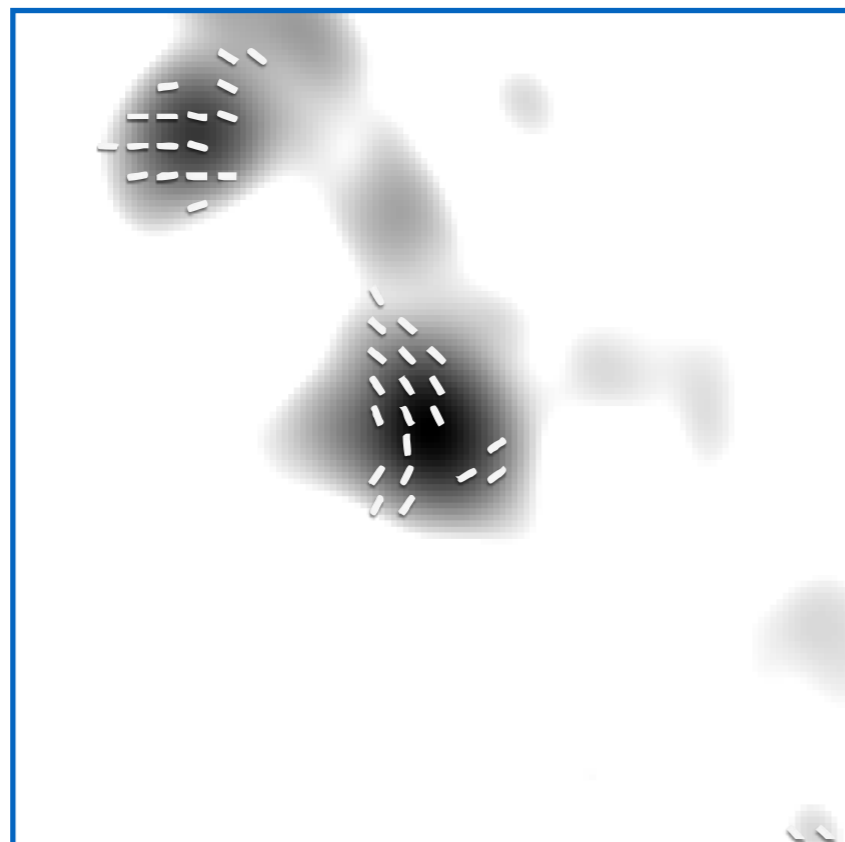


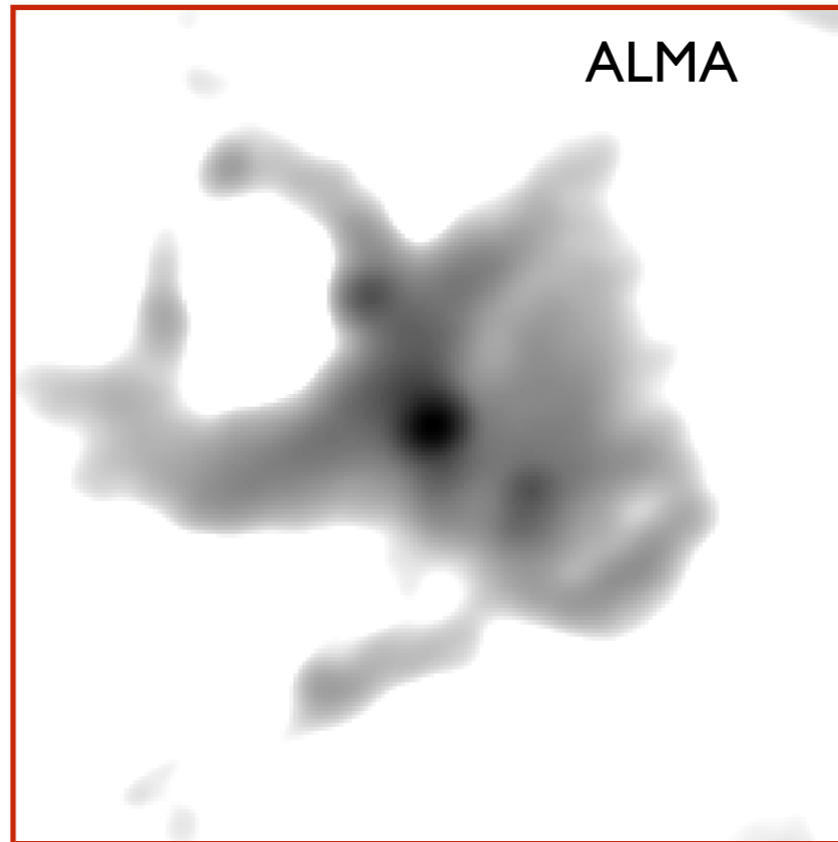


15,000 AU [= 0.08 pc]

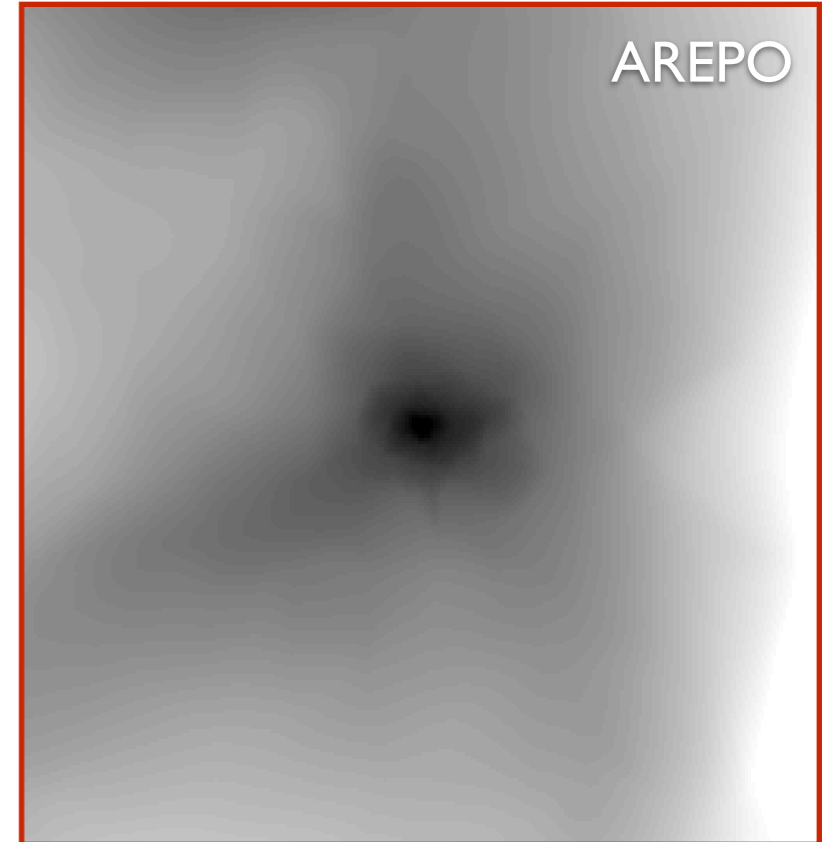


37350 AU [= 0.2 pc]

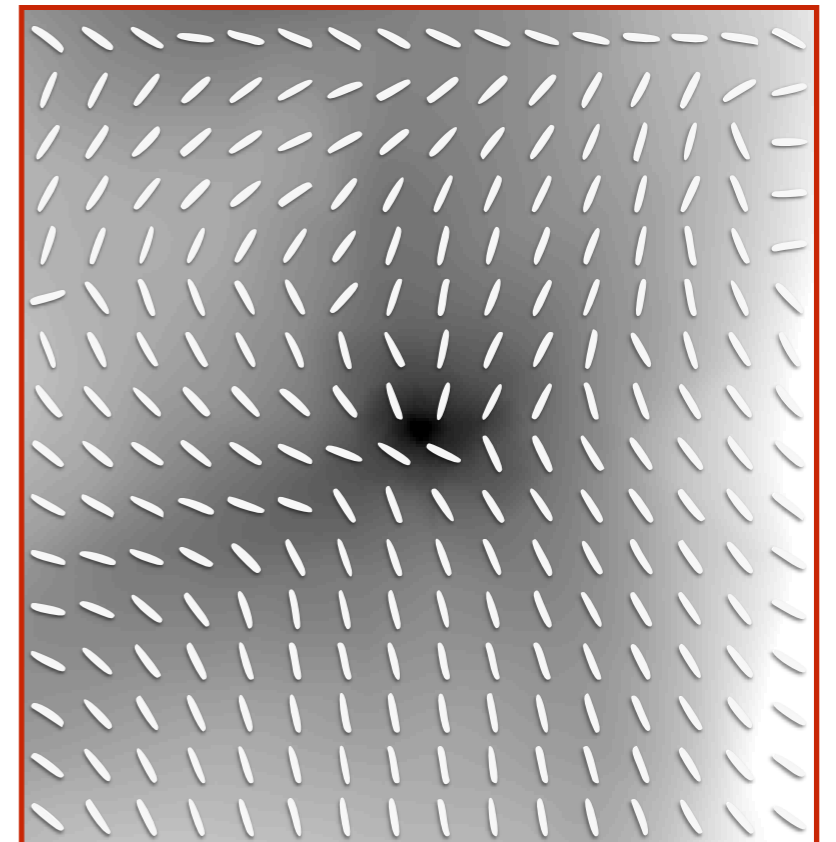
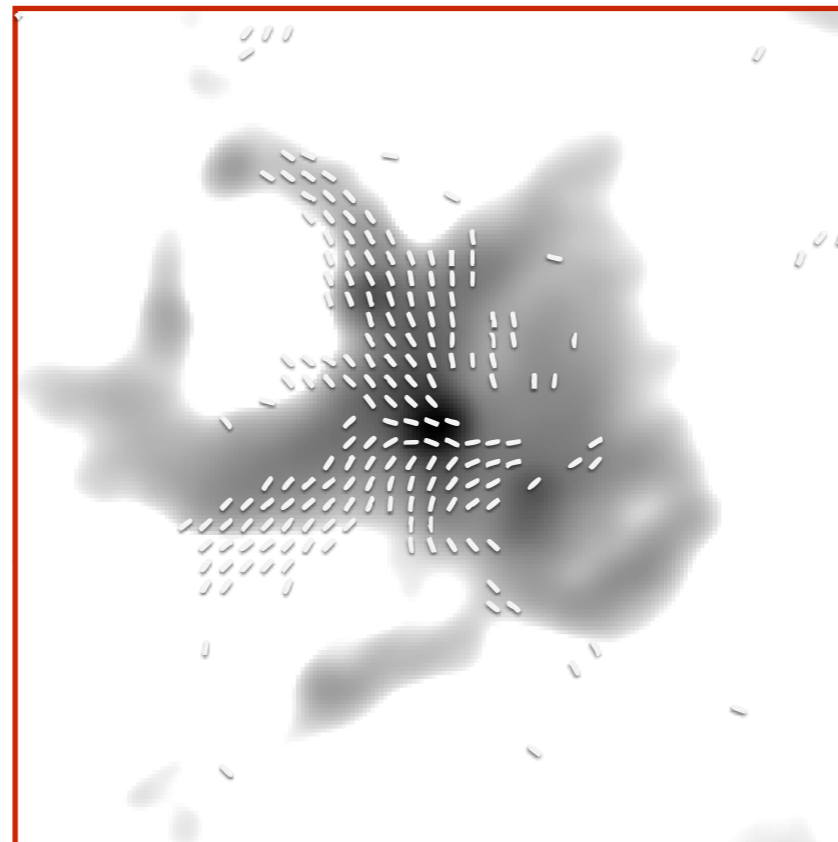


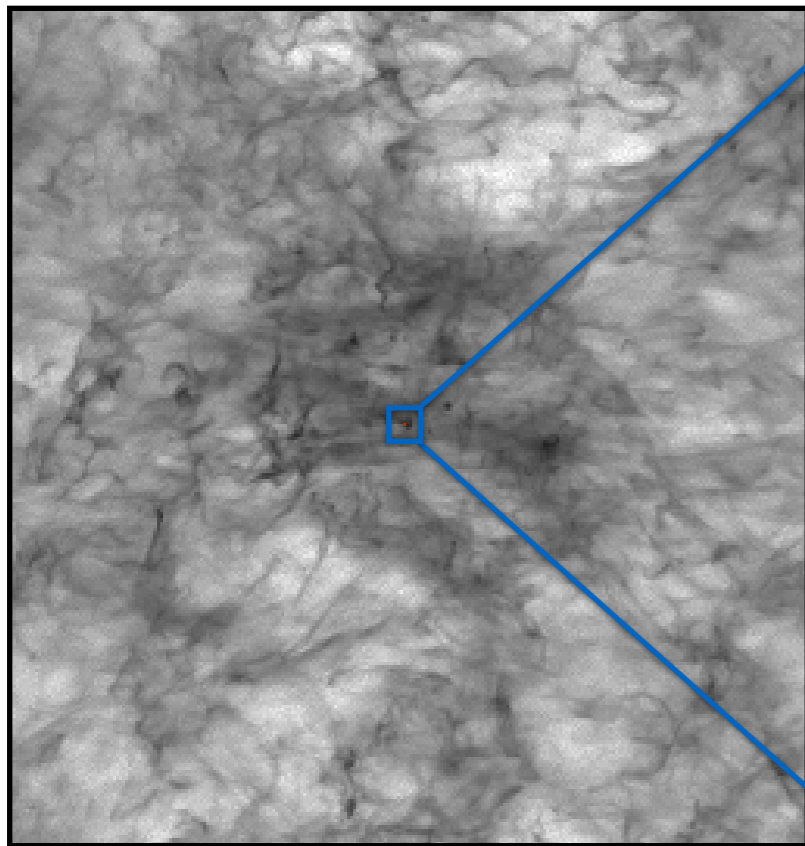


3500 AU

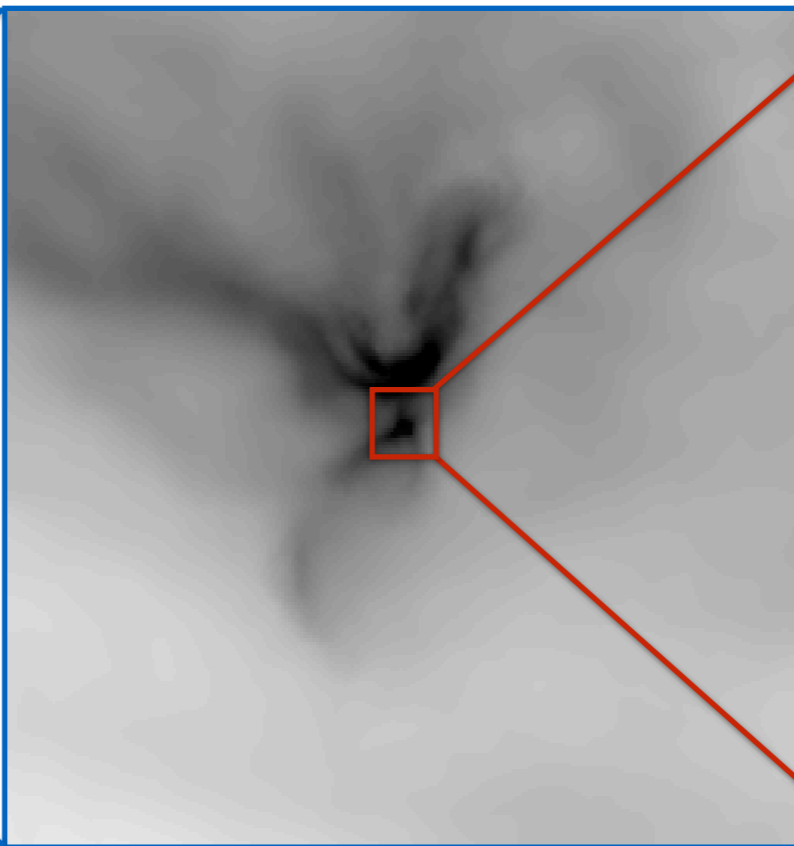


3000 AU

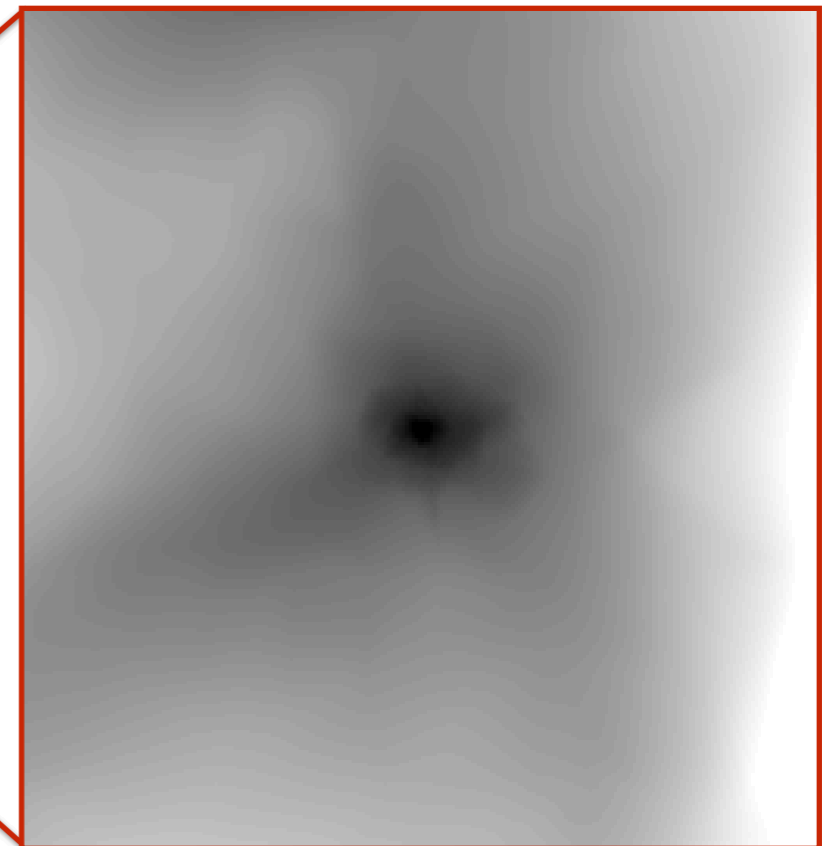




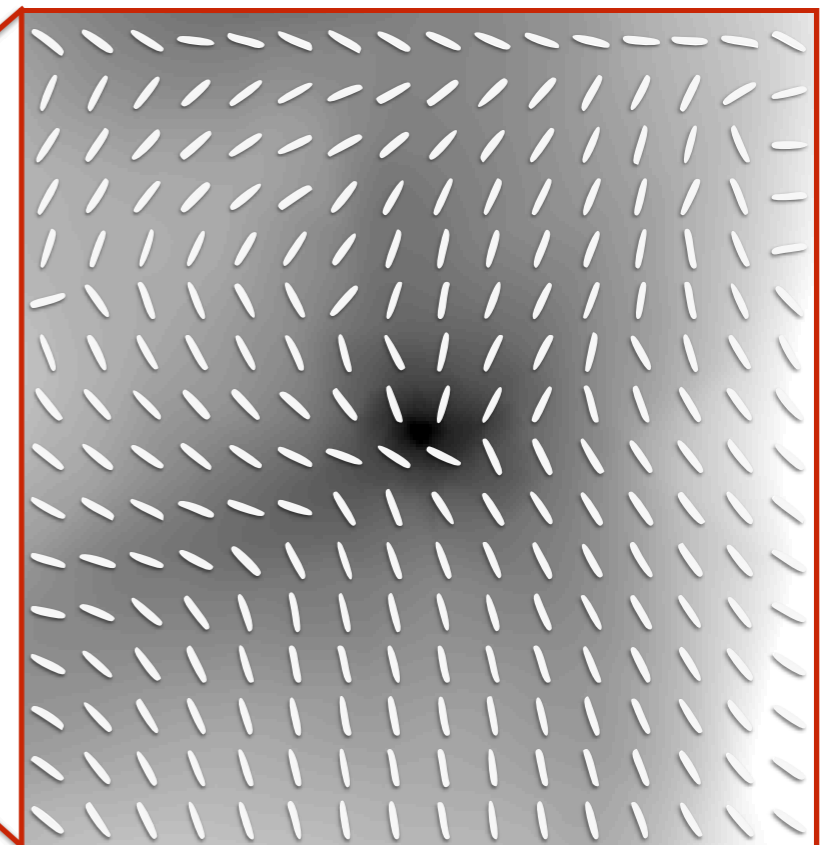
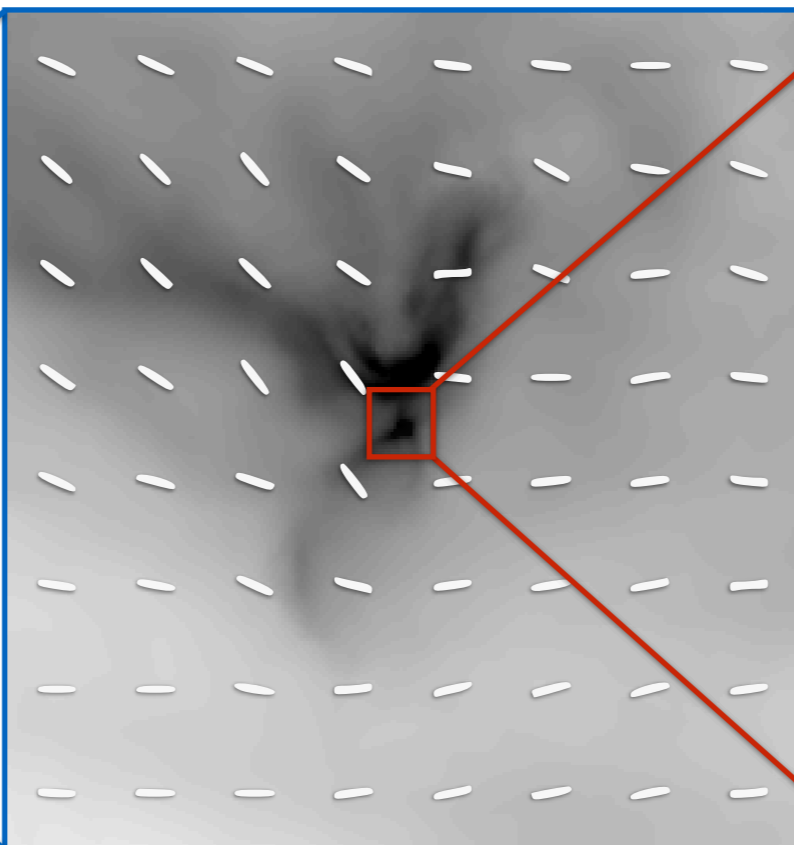
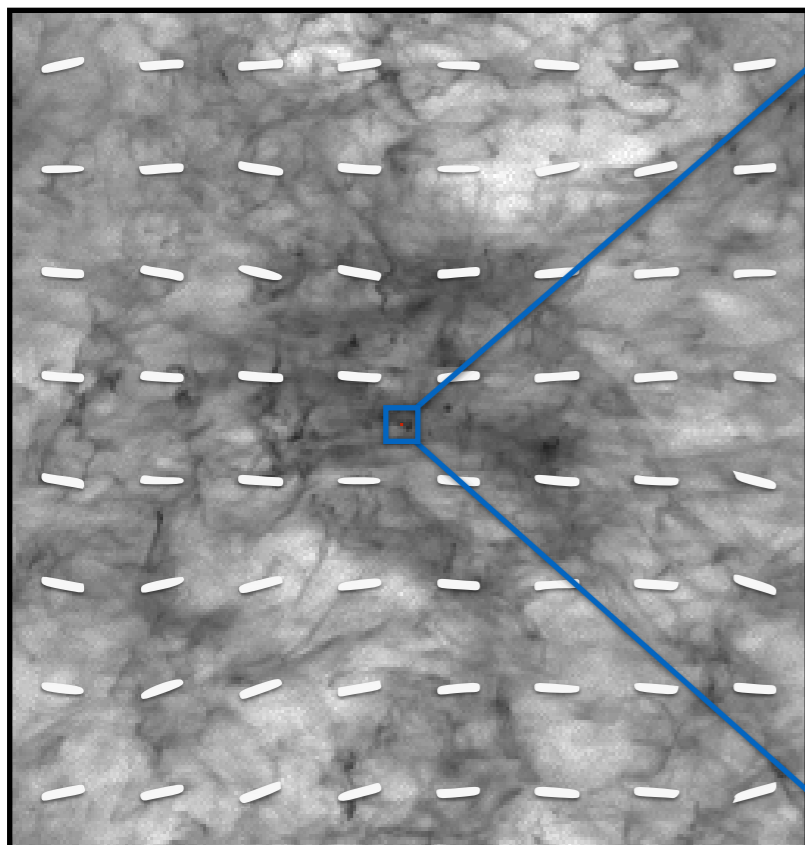
1 million AU [= 5 pc]



37350 AU [= 0.2 pc]



3000 AU

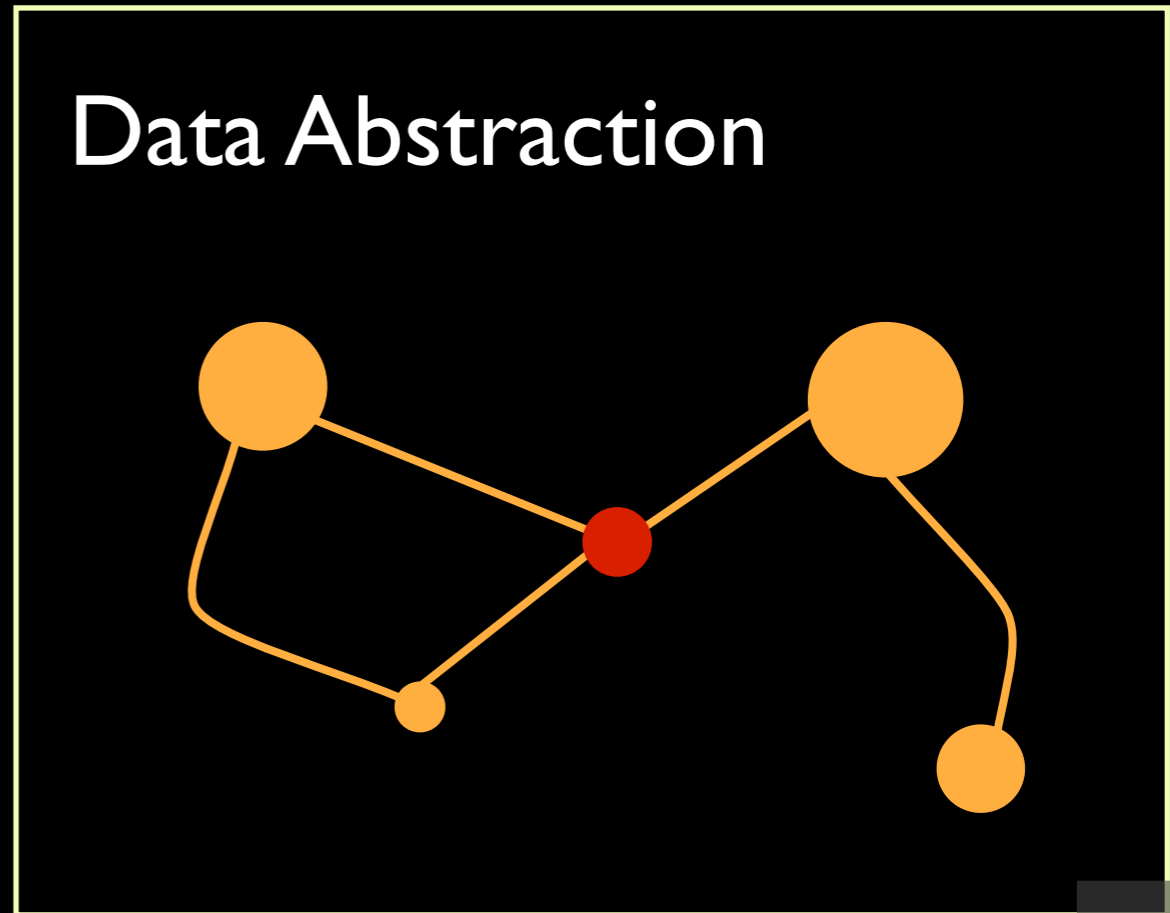
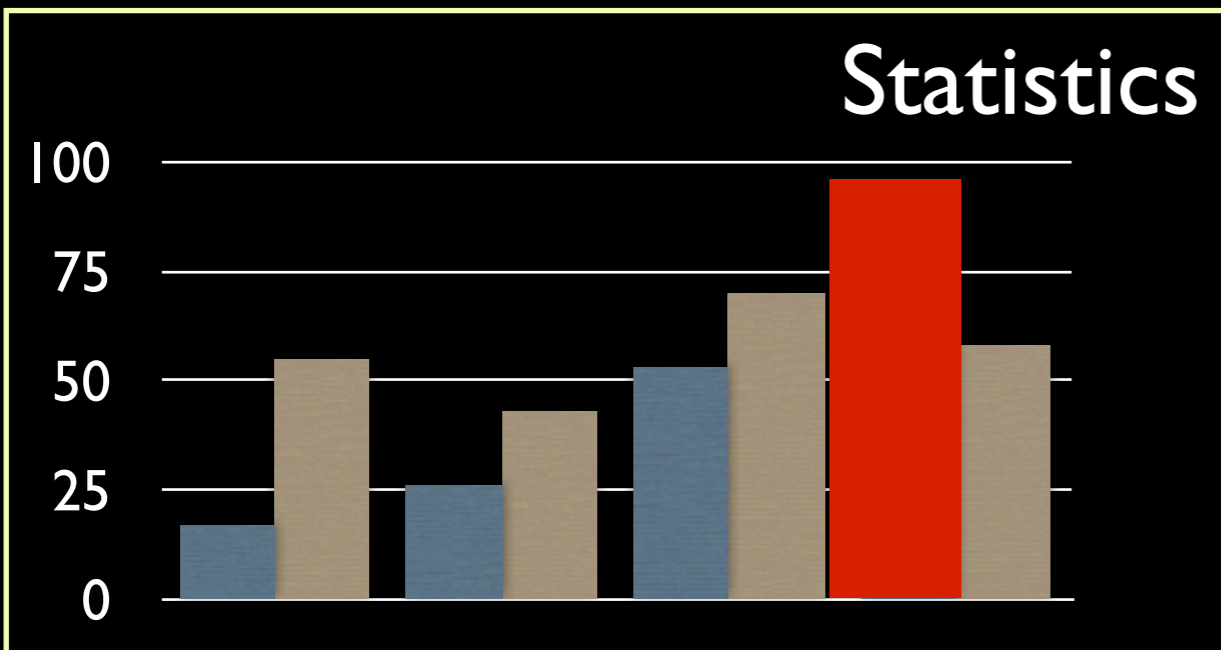
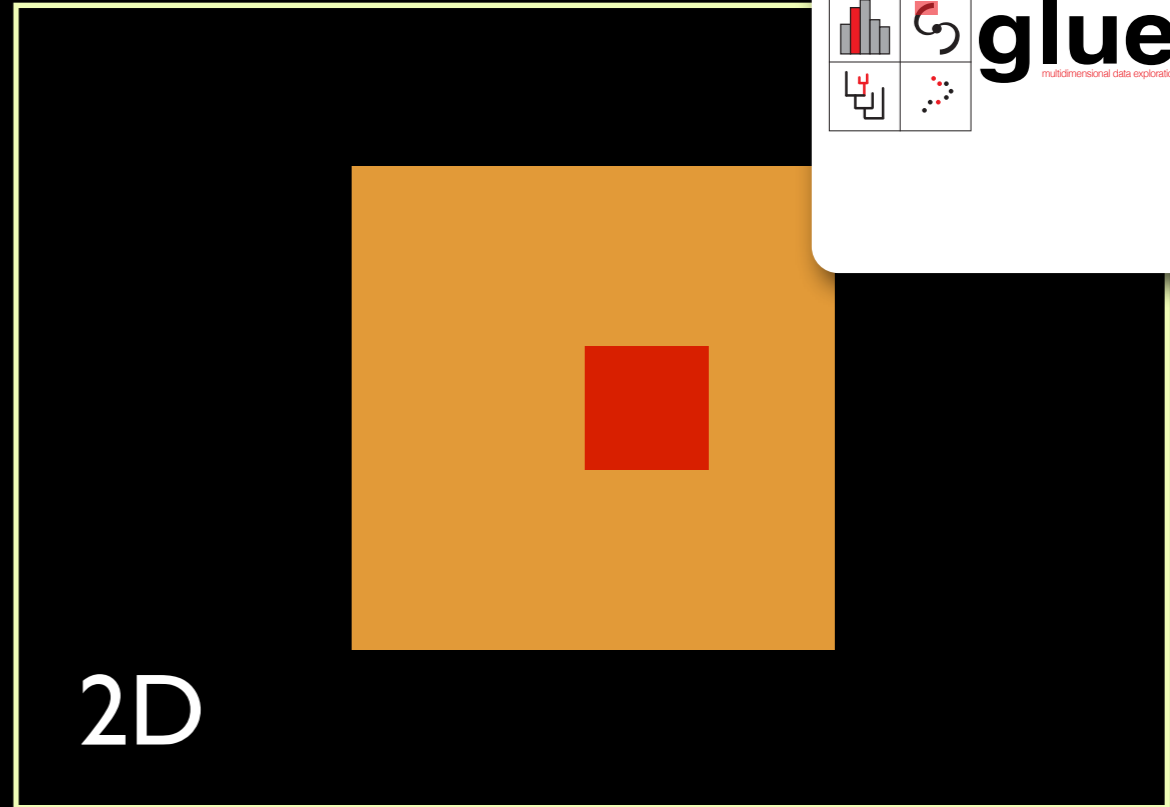
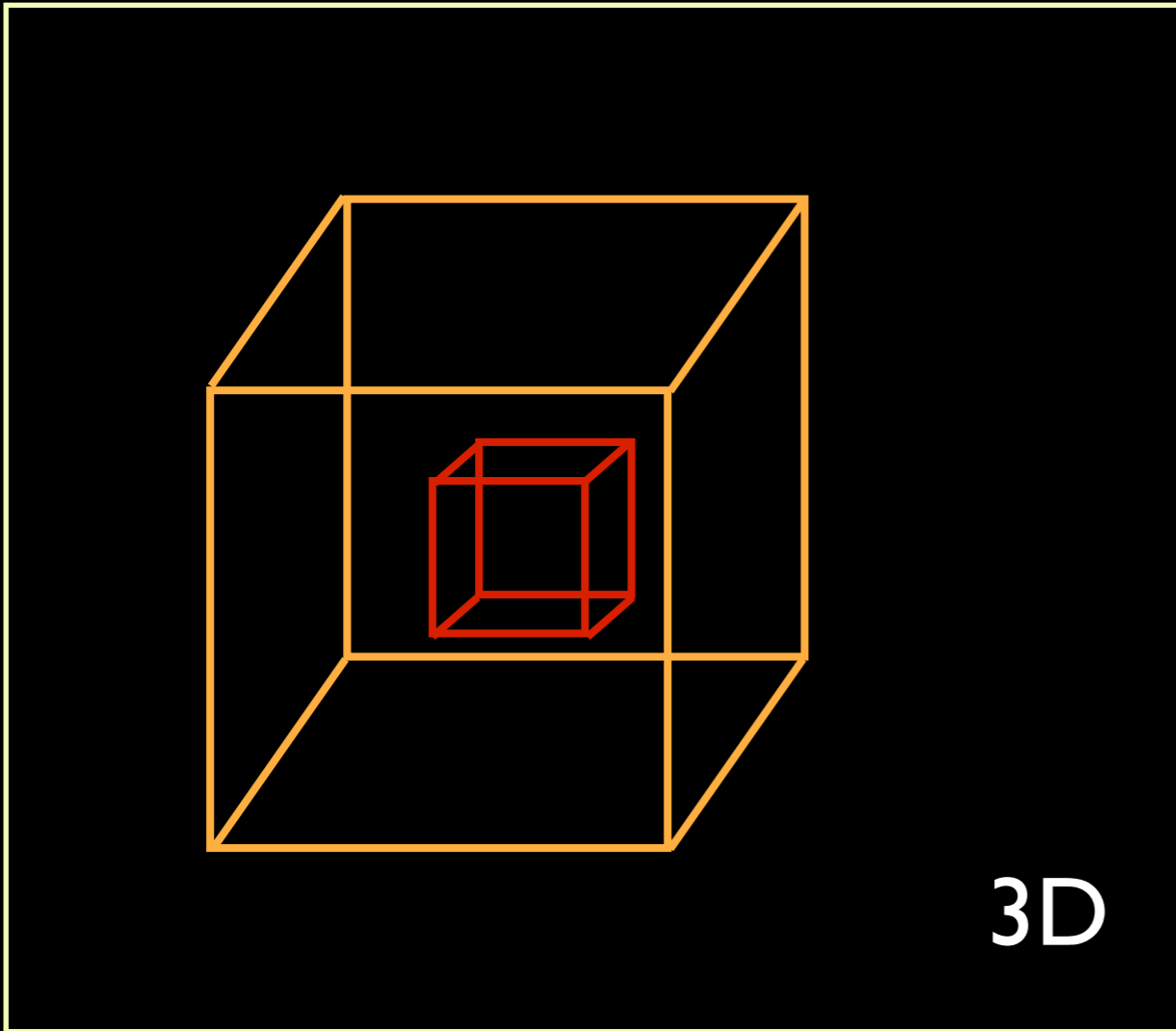
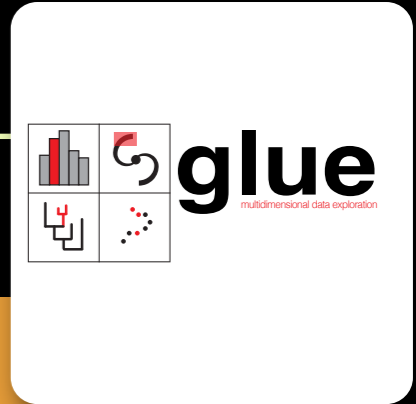


FILAMENTS: FAD OR FUNDAMENTAL?

Alyssa A. Goodman
Harvard-Smithsonian Center for Astrophysics
Radcliffe Institute for Advanced Study
[@aagie](#)

Ophiuchus, Barnard 1919

LINKED VIEWS OF HIGH-DIMENSIONAL DATA



figure, by M. Borkin, reproduced from *Goodman 2012, "Principles of High-Dimensional Data Visualization in Astronomy"*

JOHN TUKEY'S LEGACY



PRIM-9

PRIM-H

DataDesk®



XGobi

GGobi

RGGobi



1970

1980

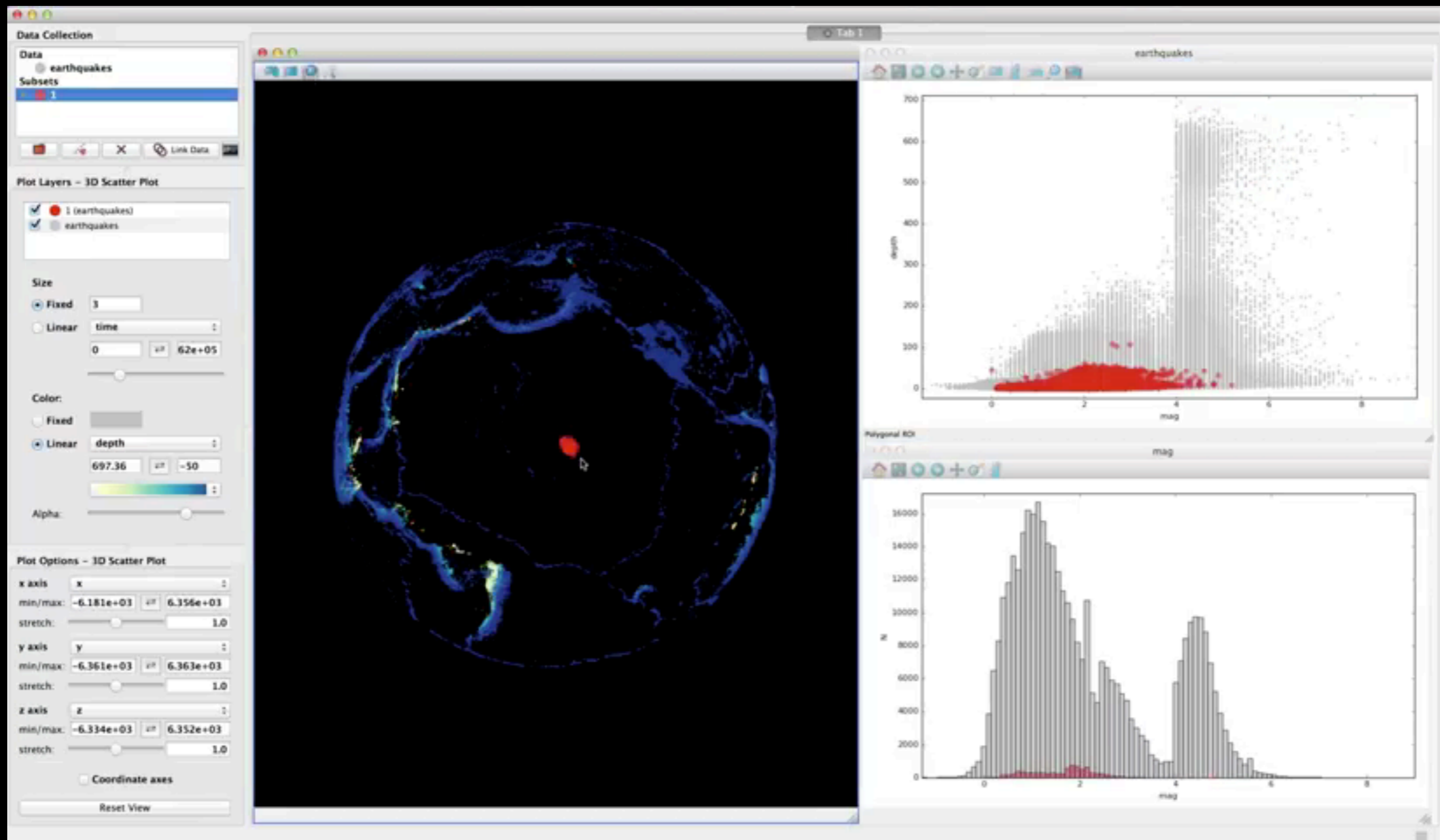
1990

2000

2010

LINKED VIEWS OF HIGH-DIMENSIONAL DATA (IN PYTHON)

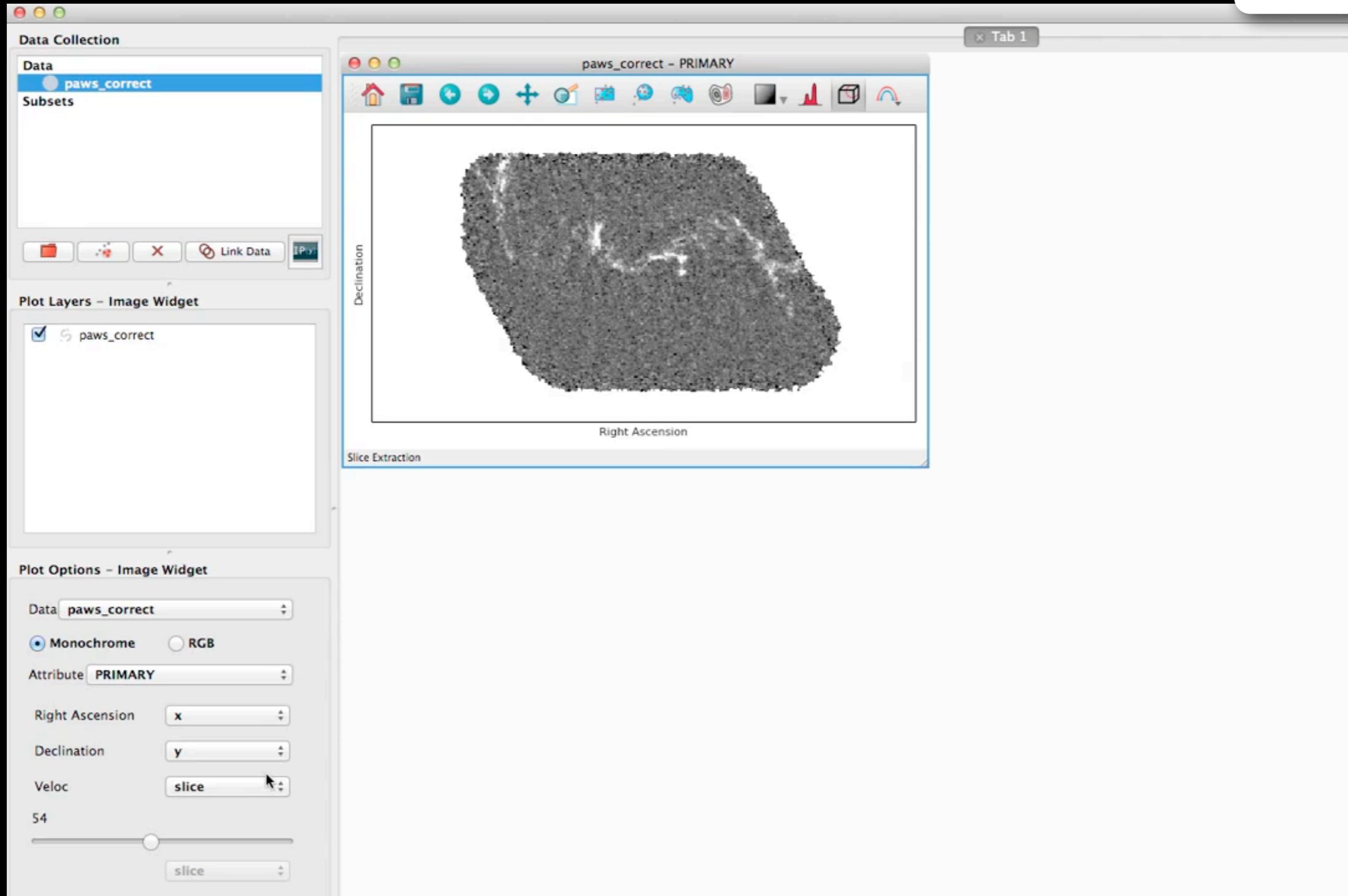
GLUE



video by Tom Robitaille, lead glue developer
glue created by: C. Beaumont, M. Borkin, P. Qian, T. Robitaille, and A. Goodman, PI

LINKED VIEWS OF HIGH-DIMENSIONAL DATA (IN PYTHON)

GLUE



*video by Chris Beaumont, glue developer
glue created by: C. Beaumont, M. Borkin, P. Qian, T. Robitaille, and A. Goodman, PI*

"BUT WAIT, THERE'S MORE..."



dollars logo - Google Search

Building Custom Data Viewers — Glue 0.9.0 documentation

balzer82.g

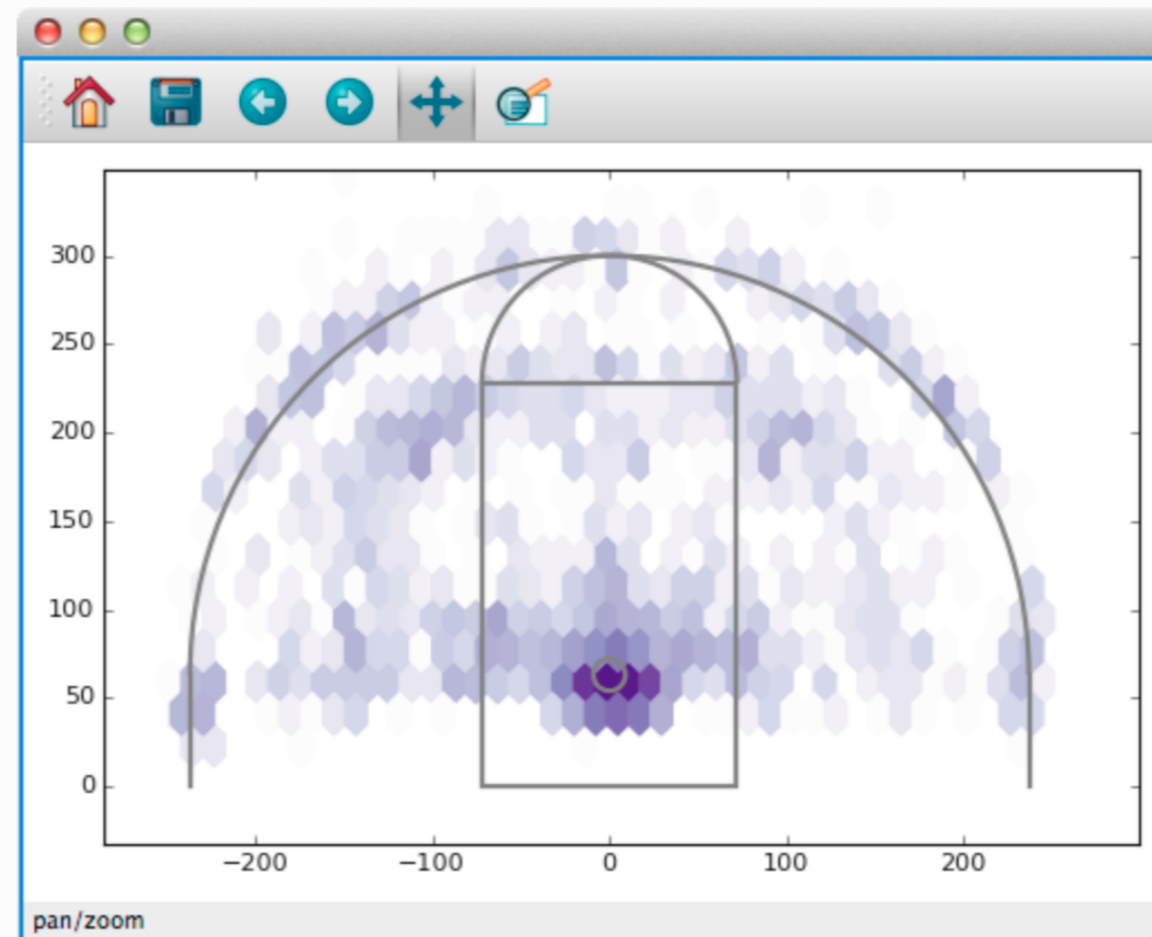
Glue

Search docs

[Docs](#) » Building Custom Data Viewers

[Edit on GitHub](#)

Building Custom Data Viewers



Glue's standard data viewers (scatter plots, images, histograms) are useful in a wide variety of data exploration settings. However, they represent a *tiny* fraction of the ways to view a particular dataset. For this reason, Glue provides a simple mechanism for creating custom visualizations using `matplotlib`.

Creating a `custom data viewer` requires writing a little bit of `Matplotlib` code but involves little to no GUI programming. The next several sections illustrate how to build a custom data viewer by

- Installing Glue
- Getting started
- User Interface Guide
- 3D viewers in Glue
 - Using the IPython terminal in Glue
- Working with Data objects
- Starting Glue from Python
- Configuring Glue via a startup file
- Customizing your Glue environment
- Programmatically configuring plots
- Building Custom Data Viewers**
 - The Goal: Basketball Shot Charts
 - Shot Chart Version 1: Heatmap and plot
 - Shot Chart Version 2: Court markings
 - Shot Chart Version 3: Widgets
 - Shot Chart Version 4: Selection
 - Viewer Subclasses
 - Valid Function Arguments
 - UI Elements
 - Other Guidelines

Watching data for changes

[Read the Docs](#)

v: stable

"BUT WAIT, THERE'S MORE..."



dollars logo - Google Search

Building Custom Data Viewers — Glue 0.9.0 documentation

balzer82.g

Glue

Search docs

Docs » Building Custom Data Viewers

Edit on GitHub

"cuts" along arbitrary paths

Building Custom Data Viewers

flood-fill selection (2D, 3D)

export to d3po, plotly

custom viewers (e.g. GIS, WorldWide Telescope, Super Mario)

plot manipulation/customization (via Matplotlib)

flexible import/export

saved sessions (.glu)

Anaconda Navigator install/upgrade

Glue's standard data viewers (scatter plots, images, histograms) are useful in a wide variety of data exploration settings. However, they represent a *tiny* fraction of the ways to view a particular dataset.

For this reason, Glue provides a simple mechanism for creating custom visualizations using

Yes, please do go start adding code now, at github.com/glue-viz.

Creating a `custom data viewer` requires writing a little bit of Matplotlib code but involves little to no GUI programming. The next several sections illustrate how to build a custom data viewer by

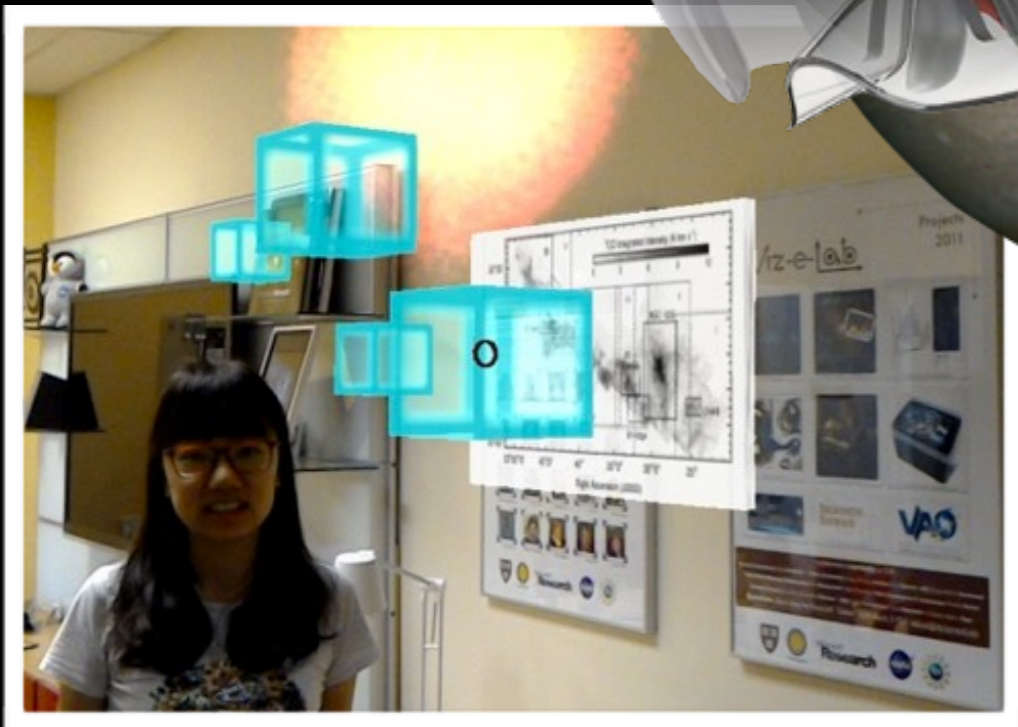


Watching data for changes

Read the Docs

v: stable

THE CHALLENGE OF 3D SELECTION



PUBLIC ROUGH DRAFT

Index Settings Fork Quickedit Word Count 42 Comments Export Unfollow

The "Paper" of the Future

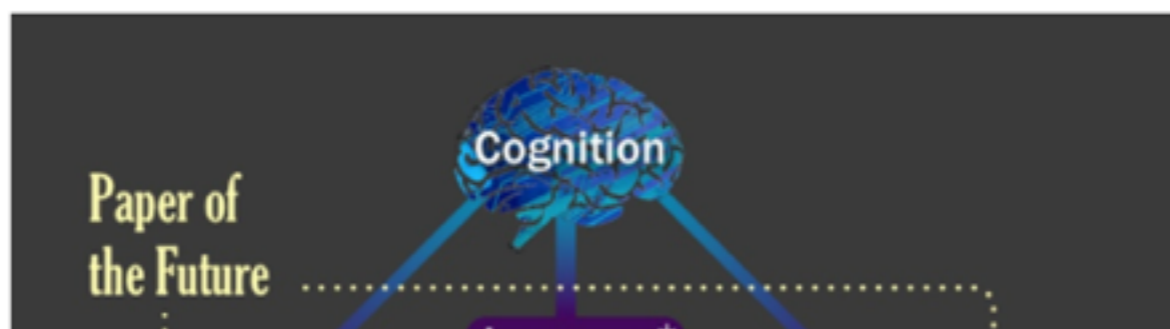
Alyssa Goodman, Josh Peek, Alberto Accomazzi, Chris Beaumont, Christine L. Borgman, How-Huan Hope Chen, Merce Crosas, Christopher Erdmann, August Muench, Alberto Pepe, Curtis Wong [+ Add author](#) [✕ Re-arrange authors](#)

A 5-minute video demonstration of this paper is available at [this YouTube link](#).

1 Preamble

A variety of research on human cognition demonstrates that humans learn and communicate best when more than one processing system (e.g. visual, auditory, touch) is used. And, related research also shows that, no matter how technical the material, most humans also retain and process information best when they can put a narrative "story" to it. So, when considering the future of scholarly communication, we should be careful not to do blithely away with the linear narrative format that articles and books have followed for centuries: instead, we should enrich it.

Much more than text is used to communicate in Science. Figures, which include images, diagrams, graphs, charts, and more, have enriched scholarly articles since the time of Galileo, and ever-growing volumes of data underpin most scientific papers. When scientists communicate face-to-face, as in talks or small discussions, these figures are often the focus of the conversation. In the best discussions, scientists have the ability to manipulate the figures, and to access underlying data, in real-time, so as to test out various what-if scenarios, and to explain findings more clearly. **This short article explains—and shows with demonstrations—how scholarly "papers" can morph into long-lasting rich records of scientific discourse, enriched with deep data and code linkages, interactive figures, audio, video, and commenting.**



3

Konrad Hinsien 3 days ago · Public
Many good suggestions, but if the goal is "long-lasting rich records of scientific discourse", a more careful and critical attitude towards electronic artifacts is appropriate. I do see it concerning videos, but not a word on the much more critical situation in software. Archiving source code is not sufficient: all the dependencies, plus the complete build environment, would have to be conserved as well to make things work a few years from now. An "executable figure" in the form of an IPython notebook will...
[more](#)

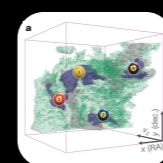
2

Merce Crosas 3 days ago · Public
Konrad, good points; this has been a concern for the community working on reproducibility. Regarding data repositories, Dataverse handles long-term preservation and access of data files in the following way: 1) for some data files that the repository recognizes (such as R Data, SPSS, STATA), which depend on a statistical package, the system converts them into a preservation format (such as a tab/CSV format). Even though the original format is also saved and can be accessed, the new preservation format gua...
[more](#)

0

Konrad Hinsien 1 day ago · Public
That sounds good. I hope more repositories will follow the example of Dataverse. Figshare in particular has a very different attitude, encouraging researchers to deposit as much as possible. That's perhaps a good strategy to change habits, but in the long run it could well backfire when people find out in a few years that 90% of those deposits have become useless.

Christine L. Borgman 4 months ago · Private
"publications"



THE GREEN BANK AMMONIA SURVEY (GAS): FIRST RESULTS OF NH₃ MAPPING THE GOULD BELT

RACHEL K. FRIESEN¹ AND JAIME E. PINEDA²

AND

ERIK ROSOLOWSKY³, FELIPE ALVES², ANA CHACÓN², HOW-HUAN CHEN⁴, MIKE CHEN⁵, JAMES DI FRANCESCO^{5,6},
 JARED KEOWN⁵, HELEN KIRK⁶, ANNA PUNANOVA², YOUNGMIN SEO⁷, YANCY SHIRLEY⁸, ADAM GINSBURG⁹,
 CHRISTINE HALL¹⁰, STELLA S. R. OFFNER¹¹, AYUSHI SINGH¹², HÉCTOR G. ARCE¹³, PAOLA CASELLI², ALYSSA A.
 GOODMAN⁴, PETER MARTIN¹⁴, CHRISTOPHER MATZNER¹², PHILIP C. MYERS⁴, ELENA REDAELLI²

¹Dunlap Institute for Astronomy & Astrophysics, University of Toronto, 50 St. George Street, Toronto, Ontario, Canada M5S 2H4

²Max-Planck-Institut für extraterrestrische Physik, Giessenbachstr

³Department of Physics, University of Alberta, Edmonton, AB, Ca

⁴Harvard-Smithsonian Center for Astrophysics, 60 Garden St., Ca

⁵Department of Physics and Astronomy, University of Victoria, 38

⁶Herzberg Astronomy and Astrophysics, National Research Counc

⁷Jet Propulsion Laboratory, NASA, 4800 Oak Grove Dr, Pasadena

⁸Steward Observatory, 933 North Cherry Avenue, Tucson, AZ 857

⁹National Radio Astronomy Observatory, Socorro, NM 87801, US

¹⁰Department of Physics, Engineering Physics & Astronomy, Queer

¹¹Department of Astronomy, University of Massachusetts, Amherst

¹²Department of Astronomy & Astrophysics, University of Toronto

¹³Department of Astronomy, Yale University, P.O. Box 208101, Nev

¹⁴Canadian Institute for Theoretical Astrophysics, University of To

A

We present an overview of the first data release of the Green Bank Ammonia Survey (GAS). GAS is an ambitious survey of all Gould Belt star-forming regions with $A_V \gtrsim 7$ mapped from NH₃ and other key molecular tracers. This paper presents the first results from the survey, showing the distribution of NH₃ in the Gould Belt clouds: B18 in Taurus, NGC 1333

GAS: FIRST RESULTS

7

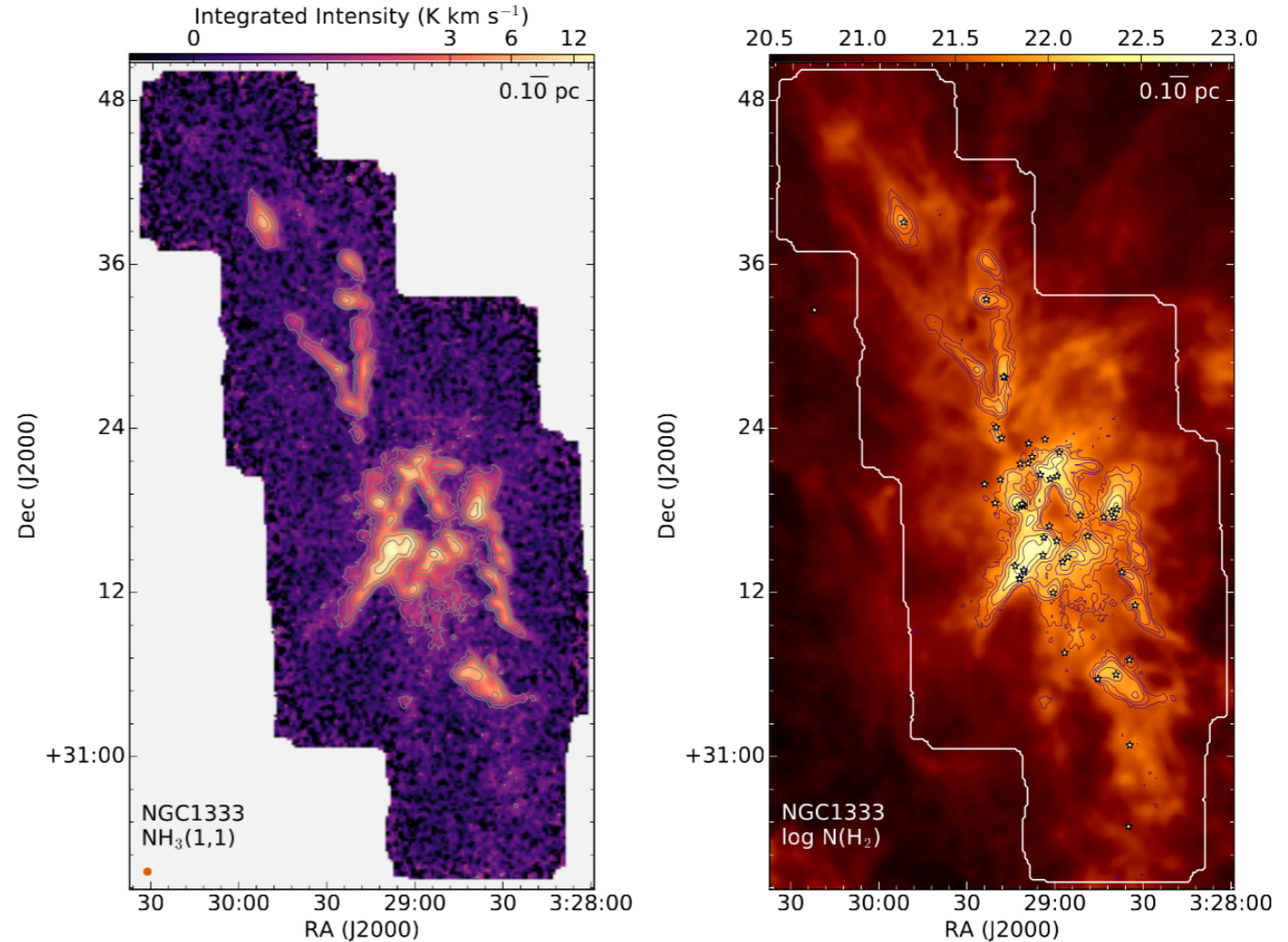


Figure 4. Left: Integrated intensity map of the NH₃ (1,1) line for the NGC 1333 region. Contours are drawn at [3,6,12,24,...]- σ , where σ is the rms estimated from emission-free pixels. Beam size and scale bar are shown in the bottom left and top right corners, respectively. Right: The H₂ column density, $\log N(\text{H}_2)$, derived from SED fitting of Herschel submillimeter continuum data (A. Singh et al., in preparation). Purple contours show NH₃(1,1) integrated intensity as in Figure 4. The white contour shows the GAS map extent. Stars show the locations of Class 0/I and flat spectrum protostars (Dunham et al. 2015).

Data Collection

Data

- ngc1333_hco+43_jcmt_reprojected
- ngc1333_c18o32_jcmt_reprojected
- ngc1333_13co32_jcmt_reprojected
- ngc1333_12co32_jcmt_reprojected
- NGC1333_singlecomp_reprojected
- ch1_mosaic_reprojected
- perseus_main_colden_500_res_m...

Link Data

perseus_main_colden_500_res_masked - image

NGC1333_singlecomp

Plot Layers - Image Widget

- 3 (NGC1333_singlecomp_reprojected)
- live (NGC1333_singlecomp_reprojected)
- everything (NGC1333_singlecomp_reprojected)
- NGC1333_singlecomp_reprojected

Plot Options - Image Widget

Data: NGC1333_singlecomp_reproj

Attribute: PRIMARY

Aspect: Square Pixels

Monochrome RGB

Right Ascension: x

Declination: y

Vrad: slice

8065.61398 m/s

Show real coordinates for slices

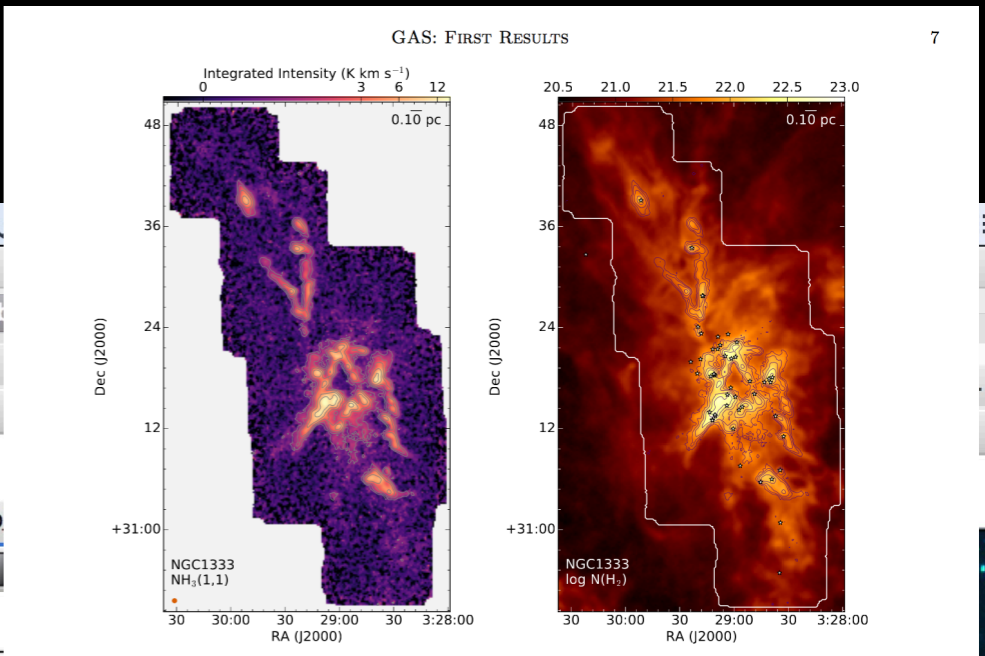
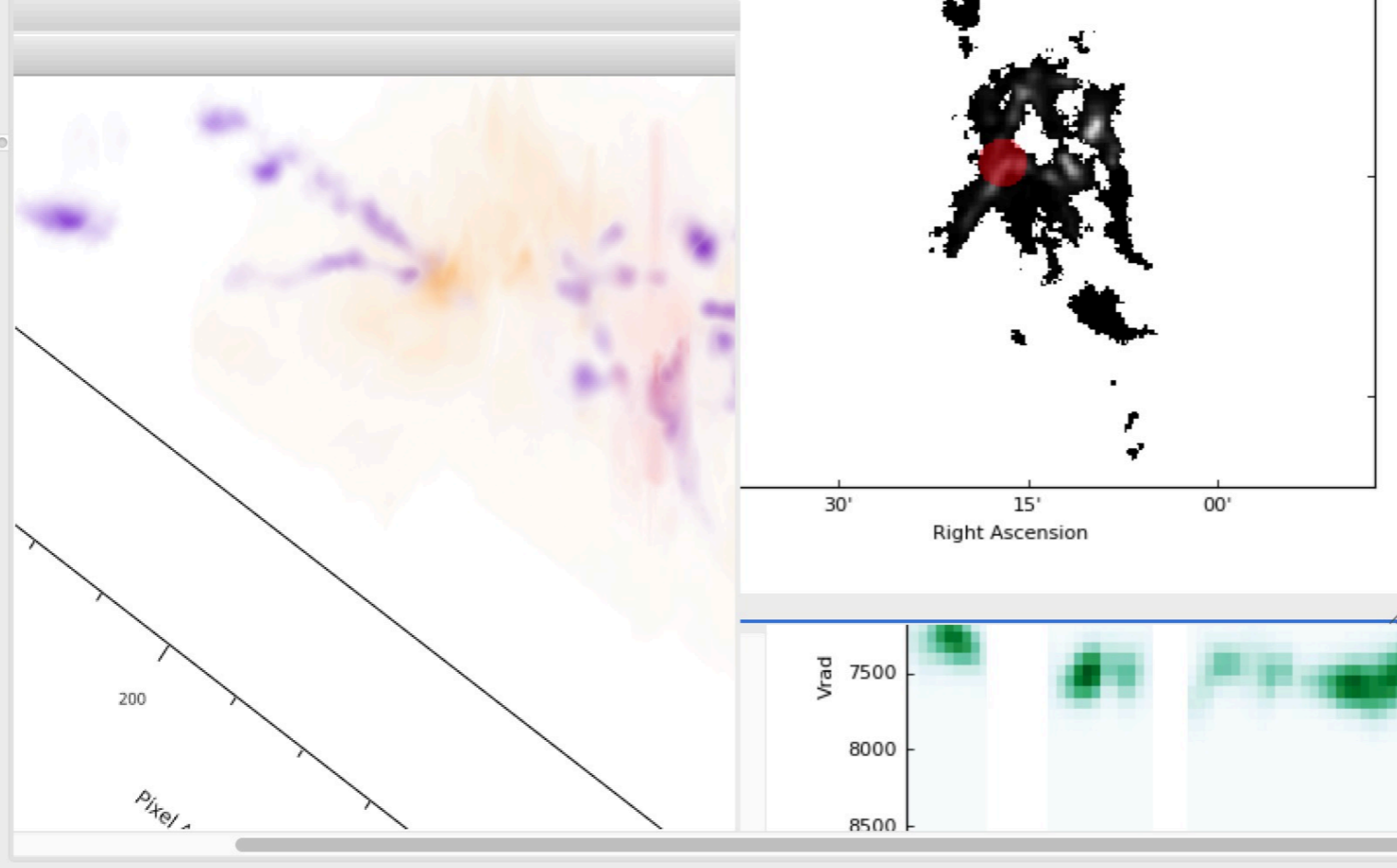
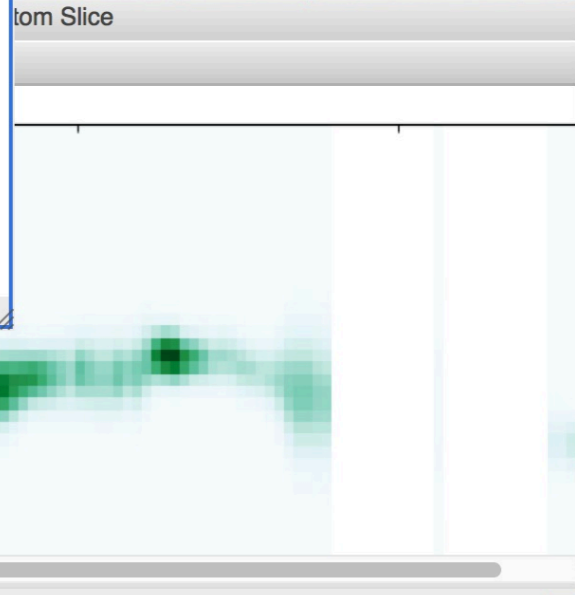
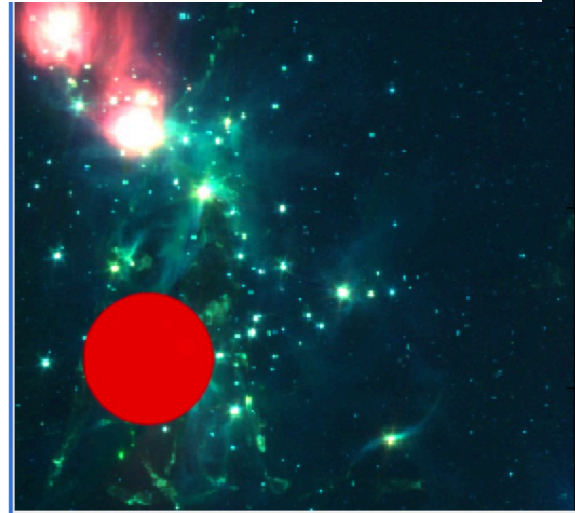


Figure 4. Left: Integrated intensity map of the $\text{NH}_3(1,1)$ line for the NGC 1333 region. Contours are drawn at $[3, 6, 12, 24, \dots] \cdot \sigma$, where σ is the rms estimated from emission-free pixels. Beam size and scale bar are shown in the bottom left and top right corners, respectively. Right: The H_2 column density, $\log N(\text{H}_2)$, derived from SED fitting of Herschel submillimeter continuum data (A. Singh et al., in preparation). Purple contours show $\text{NH}_3(1,1)$ integrated intensity as in Figure 4. The white contour shows the GAS map extent. Stars show the locations of Class 0/I and flat spectrum protostars (Dunham et al. 2015).



Principles of high-dimensional data visualization in astronomy

A.A. Goodman*

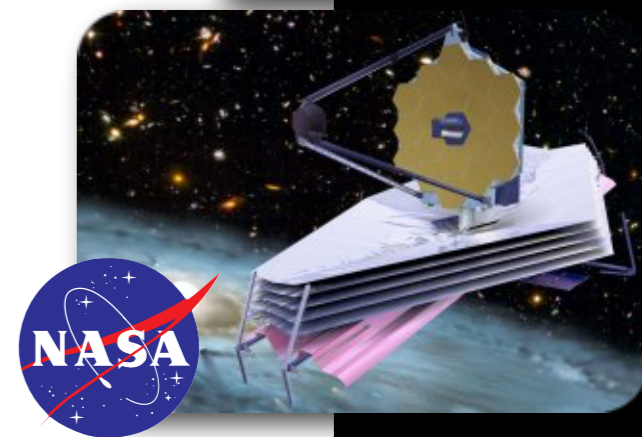
Harvard-Smithsonian Center for Astrophysics, Cambridge, MA, USA

Received 2012 May 3, accepted 2012 May 4

Published online 2012 Jun 15

Key words cosmology: large-scale structure – ISM: clouds – methods: data analysis – techniques: image processing – techniques: radial velocities

Astronomical researchers often think of analysis and visualization as separate tasks. In the case of high-dimensional data sets, though, interactive *exploratory data visualization* can give far more insight than an approach where data processing and statistical analysis are followed, rather than accompanied, by visualization. This paper attempts to chart a course toward “linked view” systems, where multiple views of high-dimensional data sets update live as a researcher selects, highlights, or otherwise manipulates, one of several open views. For example, imagine a researcher looking at a 3D volume visualization of simulated or observed data, and simultaneously viewing statistical displays of the data set’s properties (such as an x - y plot of temperature vs. velocity, or a histogram of vorticities). Then, imagine that when the researcher selects an interesting group of points in any one of these displays, that the same points become a highlighted subset in all other open displays. Selections can be graphical or algorithmic, and they can be combined, and saved. For tabular (ASCII) data, this kind of analysis has long been possible, even though it has been under-used in astronomy. The bigger issue for astronomy and other “high-dimensional” fields, though, is that no extant system allows for full integration of images and data cubes within a linked-view environment. The paper concludes its history and analysis of the present situation with suggestions that look toward cooperatively-developed open-source modular software as a way to create an evolving, flexible, high-dimensional, linked-view visualization environment useful in astrophysical research.



FILAMENTS: FAD OR FUNDAMENTAL?

Alyssa A. Goodman
Harvard-Smithsonian Center for Astrophysics
Radcliffe Institute for Advanced Study
[@aagie](#)

Ophiuchus, Barnard 1919

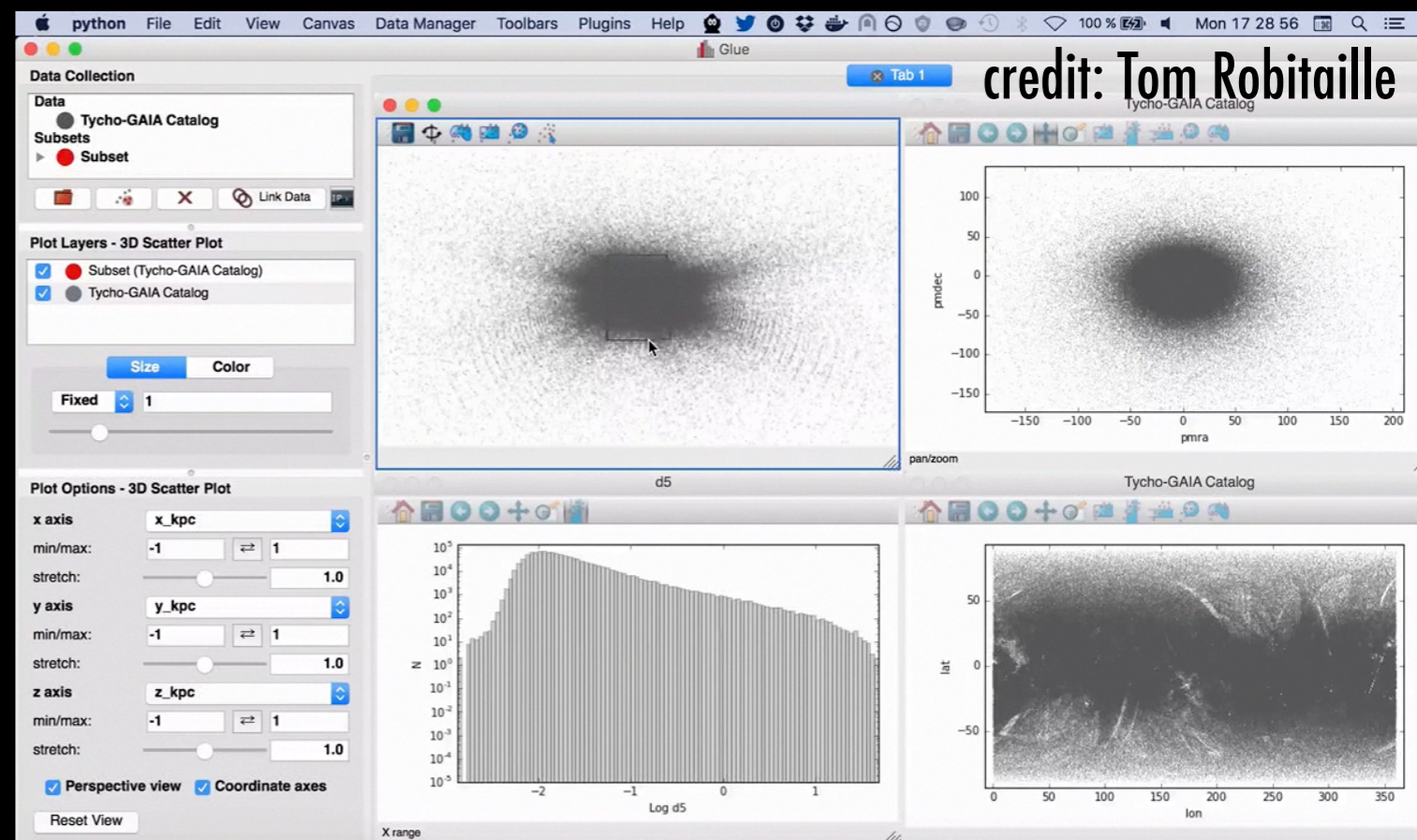
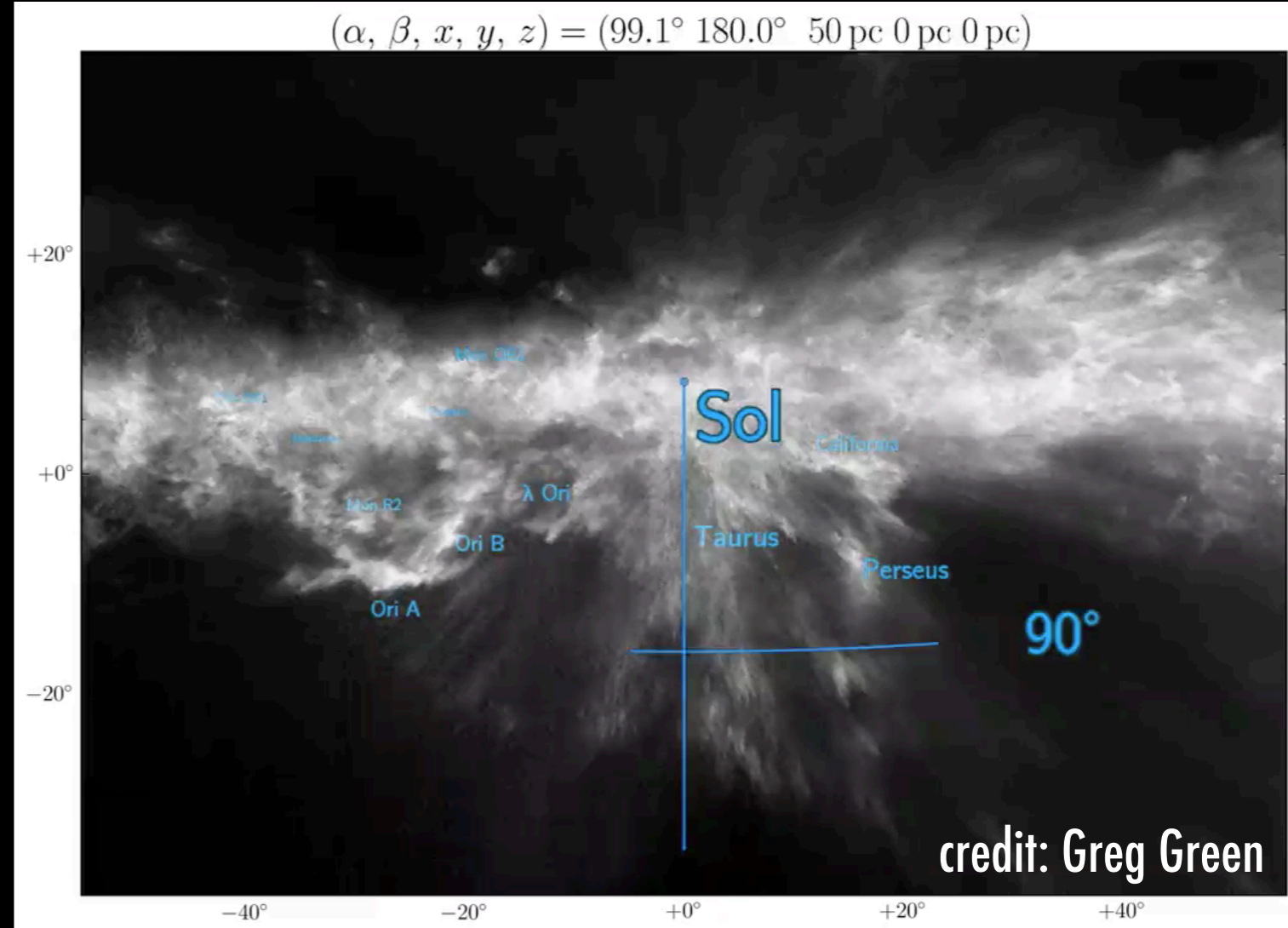
extra slides

3D dust: <http://argonaut.skymaps.info>

Gaia 3D dust & glue



glue: <http://glueviz.org>



Data Collection

Data

- Tycho-GAIA Catalog

Subsets

- Subset

Link Data

Plot Layers - 3D Scatter Plot

- Subset (Tycho-GAIA Catalog)
- Tycho-GAIA Catalog

Size **Color**

Fixed 1

Plot Options - 3D Scatter Plot

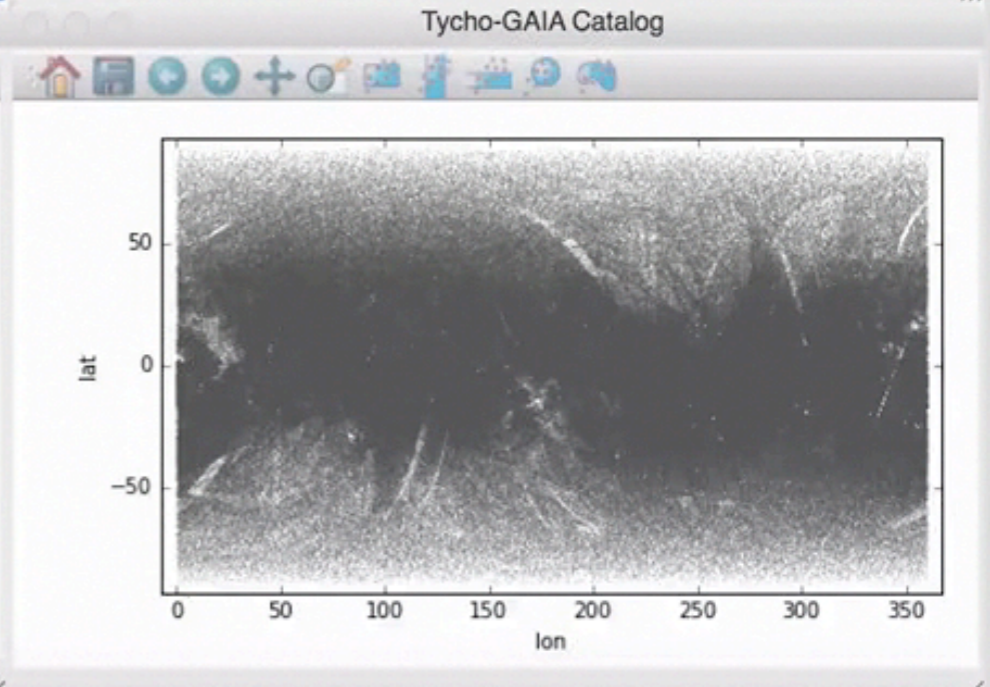
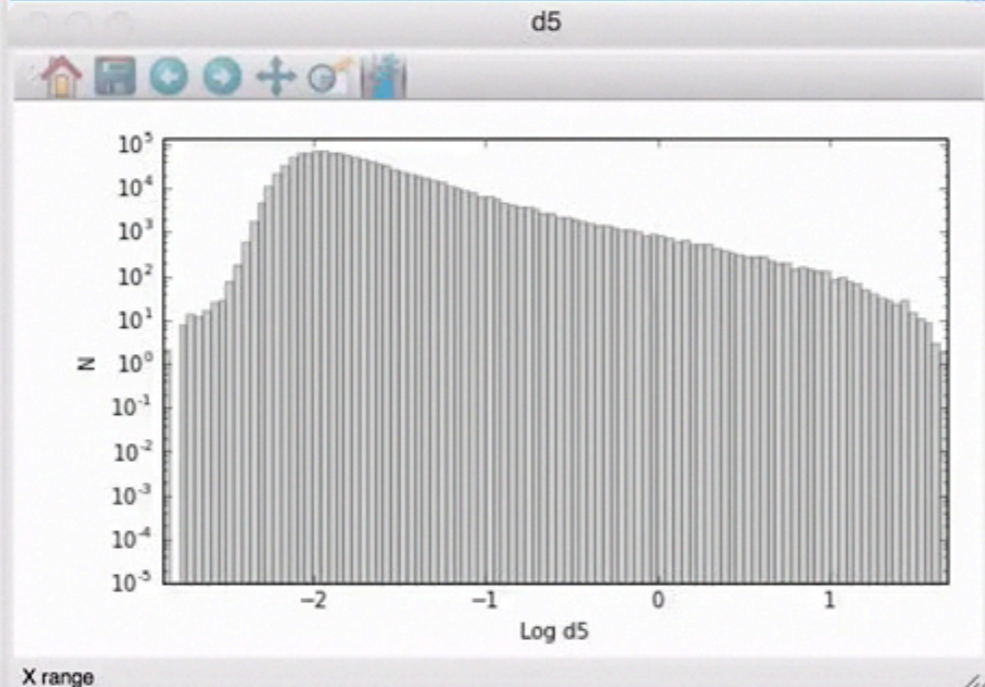
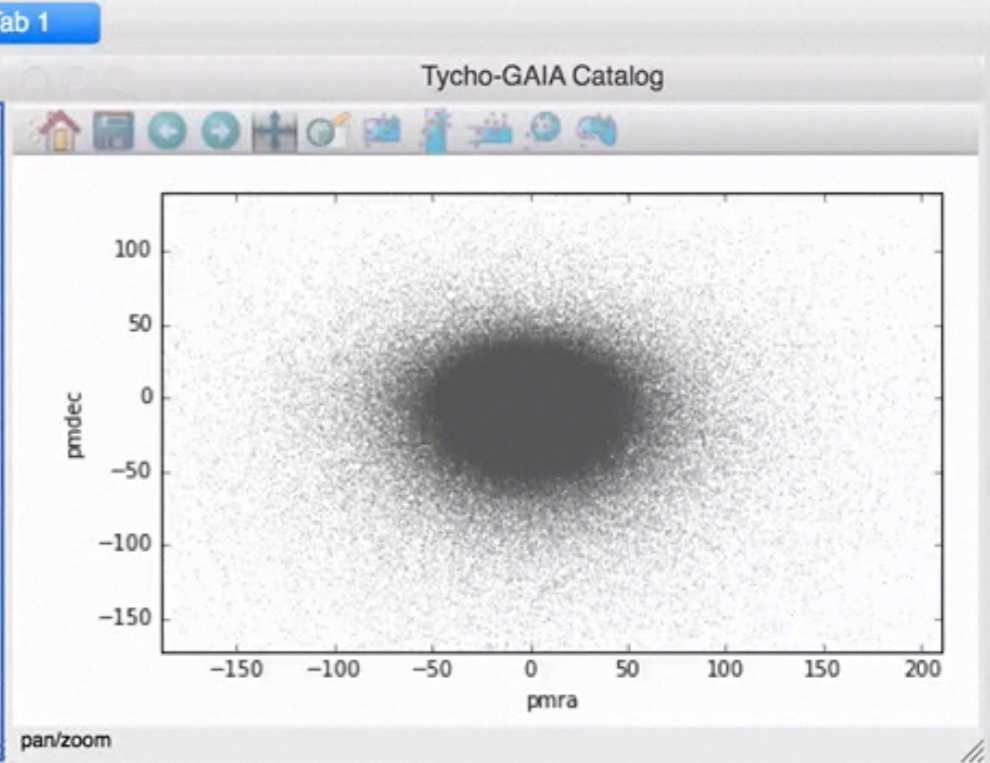
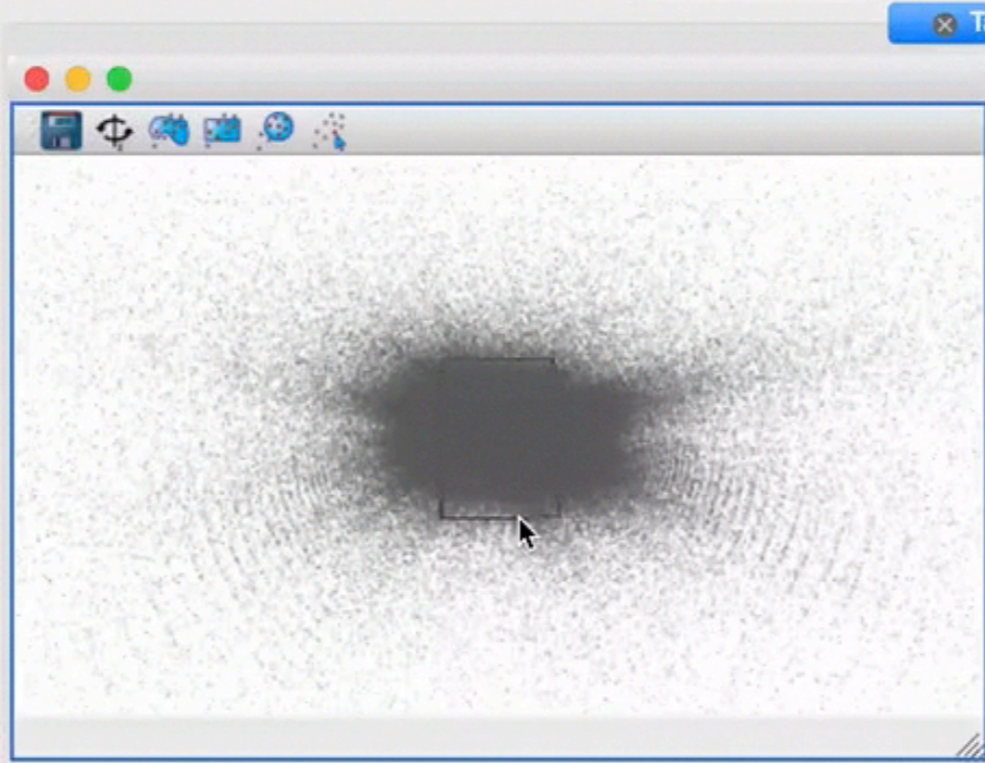
x axis: x_kpc, min/max: -1 to 1, stretch: 1.0

y axis: y_kpc, min/max: -1 to 1, stretch: 1.0

z axis: z_kpc, min/max: -1 to 1, stretch: 1.0

Perspective view Coordinate axes

Reset View



Principles of high-dimensional data visualization in astronomy

A.A. Goodman*

Harvard-Smithsonian Center for Astrophysics, Cambridge, MA, USA

Received 2012 May 3, accepted 2012 May 4

Published online 2012 Jun 15

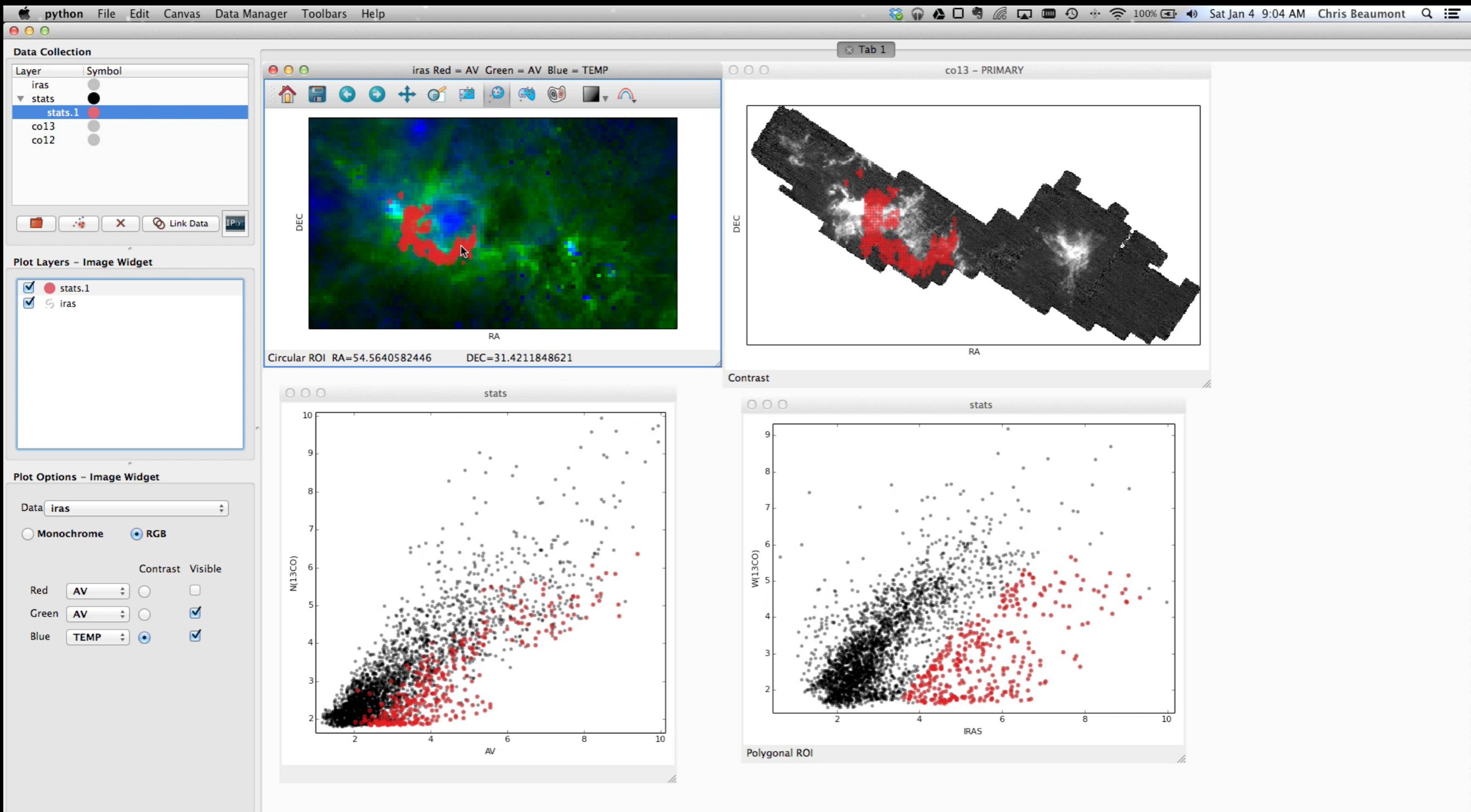
Key words cosmology: large-scale structure – ISM: clouds – methods: data analysis – techniques: image processing – techniques: radial velocities

Astronomical researchers often think of analysis and visualization as separate tasks. In the case of high-dimensional data sets, though, interactive *exploratory data visualization* can give far more insight. In this paper, analysis and statistical analysis are followed, rather than accompanied, by visualization. We move toward “linked view” systems, where multiple views of high-dimensional data are shown simultaneously. One view highlights, or otherwise manipulates, one of several open views. For example, one view shows visualization of simulated or observed data, and simultaneously viewing statistical data (such as an x - y plot of temperature vs. velocity, or a histogram of vorticity). Another view selects an interesting group of points in any one of these displays, that the same group is shown in the other open displays. Selections can be graphical or algorithmic, and they can be applied to the data, this kind of analysis has long been possible, even though it has been difficult to do for astronomy and other “high-dimensional” fields, though, is that no extant software exists for displaying and data cubes within a linked-view environment. The paper concludes with suggestions that look toward cooperatively-developed open-source modeling environments for flexible, high-dimensional, linked-view visualization environment useful in a

#	Bibcode Authors	Cites Title	Date	List of Links Access Control Help
1	2016A&C....15...50N Naiman, J. P.	1.000 AstroBlend: An astrophysical visualization package for Blender	04/2016	A Z E L X R C U
2	2015A&A...584A..26B Bouy, H.; Alves, J.	1.000 Cosmography of OB stars in the solar neighbourhood	12/2015	A Z E F L D R C S O U
3	2015ASPC..495..121R Rosolowsky, E.; Kern, J.; Federl, P.; Jacobs, J.; Loveland, S.; Taylor, J.; Sivakoff, G.; Taylor, R.	1.000 The Cube Analysis and Rendering Tool for Astronomy	09/2015	A Z E L T R U
4	2015ASPC..495..101B Beaumont, C.; Goodman, A.; Greenfield, P.	1.000 Hackable User Interfaces In Astronomy with Glue	09/2015	A Z E L T R U
5	2015A&C....12...86P Punzo, D.; van der Hulst, J. M.; Roerdink, J. B. T. M.; Oosterloo, T. A.; Ramatsoku, M.; Verheijen, M. A. W.	1.000 The role of 3-D interactive visualization in blind surveys of HI in galaxies	09/2015	A Z E L X R C U
6	2015arXiv150604621T Taylor, Rhys	1.000 Comment on 'The role of 3-D interactive visualization in blind surveys of HI in galaxies'	06/2015	A Z X R C U
7	2013arXiv1307.0712B Burton, Michael; Crocker, Roland; Dickey, John; Filipovic, Miroslav; Purcell, Cormac; Rathborne, Jill; Rowell, Gavin; Tohill, Nick; Walsh, Andrew	1.000 The Interstellar Medium White Paper	07/2013	A Z X R U
8	2013PASP..125..731K Kent, Brian R.	1.000 Visualizing Astronomical Data with Blender	06/2013	A Z E F L X R C S U
9	2013arXiv1304.6615C Cavuoti, Stefano	1.000 Data-rich astronomy: mining synoptic sky surveys	04/2013	A Z X R U

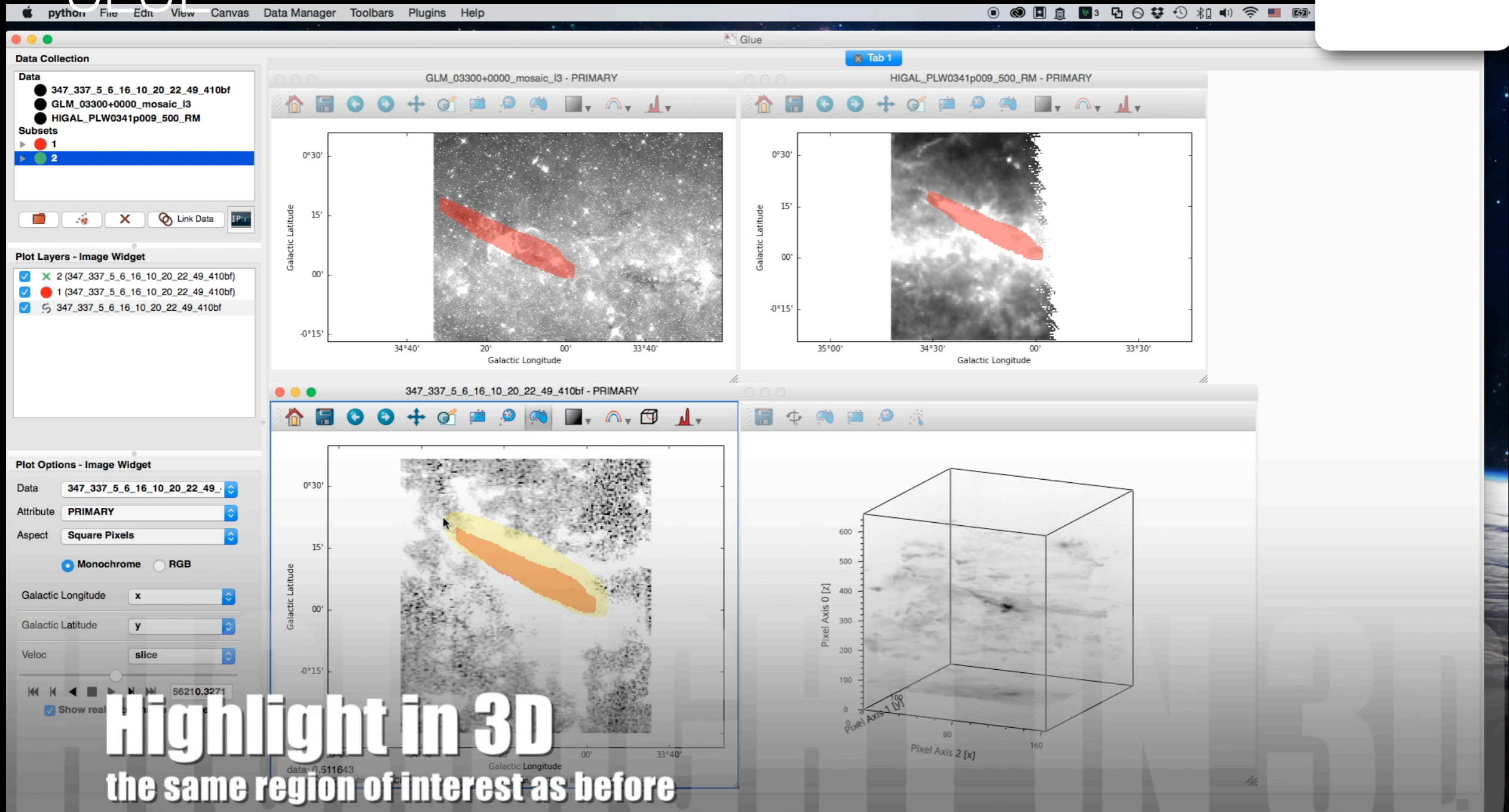
LINKED VIEWS OF HIGH-DIMENSIONAL DATA (IN PYTHON)

GLUE

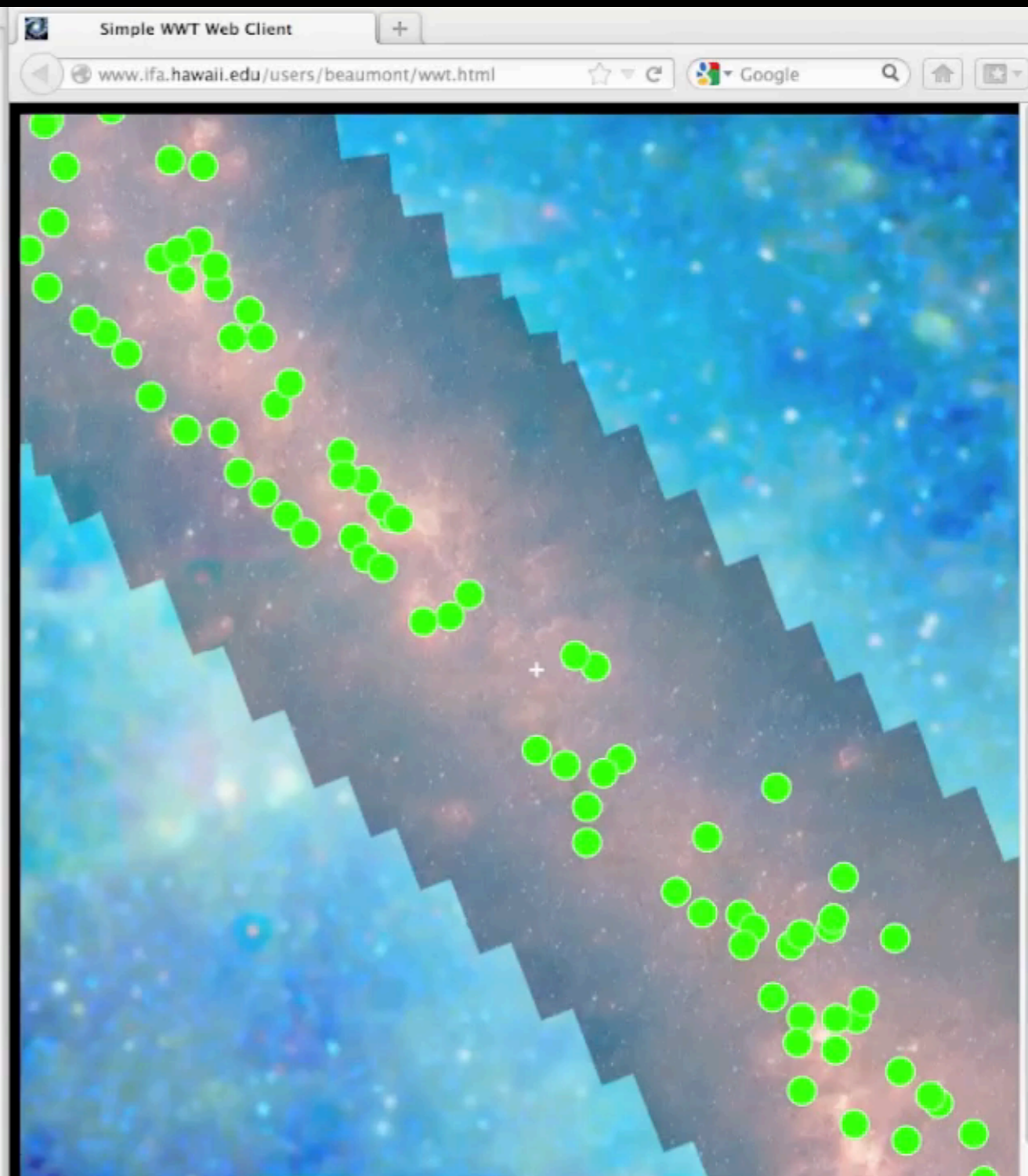
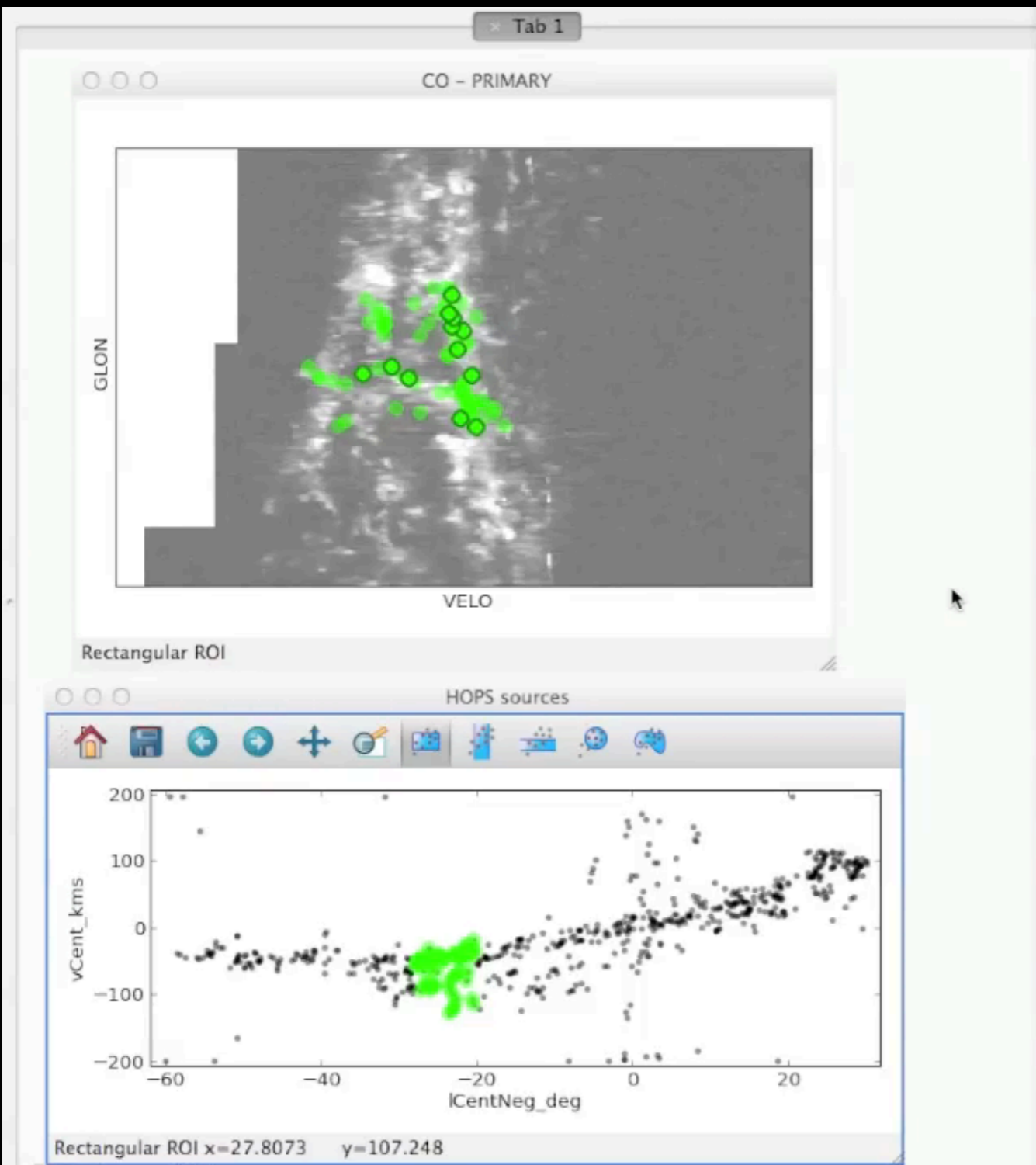


LINKED VIEWS OF HIGH-DIMENSIONAL DATA (IN PYTHON)

GLUE



video by Penny Qian, with Catherine Zucker, graduate students
glue created by: C. Beaumont, M. Borkin, P. Qian, T. Robitaille, and A. Goodman, PI



Video courtesy of Chris Beaumont

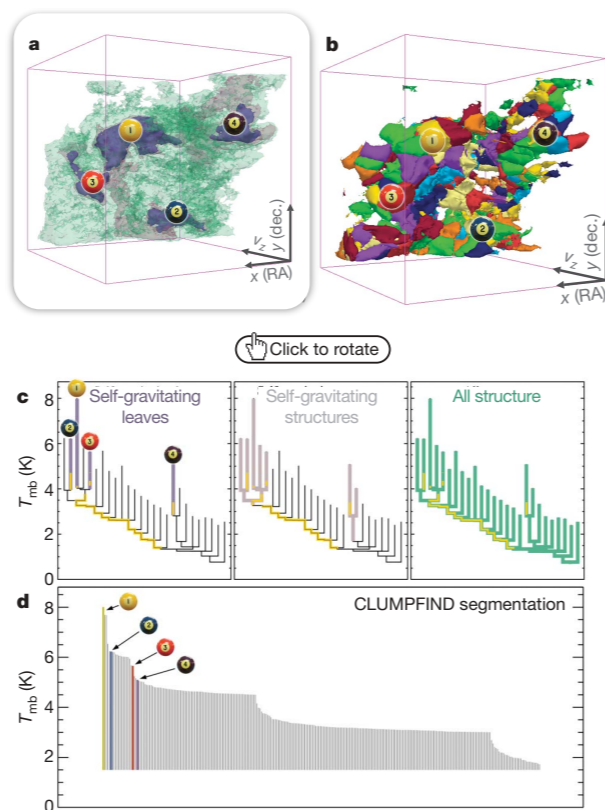


Figure 2 | Comparison of the 'dendrogram' and 'CLUMPFIND' feature-identification algorithms as applied to ^{13}CO emission from the L1448 region of Perseus. **a**, 3D visualization of the surfaces indicated by colours in the dendrogram shown in **c**. Purple illustrates the smallest scale self-gravitating structures in the region corresponding to the leaves of the dendrogram; pink shows the smallest surfaces that contain distinct self-gravitating leaves within them; and green corresponds to the surface in the data cube containing all the significant emission. Dendrogram branches corresponding to self-gravitating objects have been highlighted in yellow over the range of T_{mb} (main-beam temperature) test-level values for which the virial parameter is less than 2. The x - y locations of the four 'self-gravitating' leaves labelled with billiard balls are the same as those shown in Fig. 1. The 3D visualizations show position-position-velocity (p - p - v) space. RA, right ascension; dec., declination. For comparison with the ability of dendrograms (**c**) to track hierarchical structure, **d** shows a pseudo-dendrogram of the CLUMPFIND segmentation (**b**), with the same four labels used in Fig. 1 and in **a**. As 'clumps' are not allowed to belong to larger structures, each pseudo-branch in **d** is simply a series of lines connecting the maximum emission value in each clump to the threshold value. A very large number of clumps appears in **b** because of the sensitivity of CLUMPFIND to noise and small-scale structure in the data. In the online PDF version, the 3D cubes (**a** and **b**) can be rotated to any orientation, and surfaces can be turned on and off (interaction requires Adobe Acrobat version 7.0.8 or higher). In the printed version, the front face of each 3D cube (the 'home' view in the interactive online version) corresponds exactly to the patch of sky shown in Fig. 1, and velocity with respect to the Local Standard of Rest increases from front (-0.5 km s^{-1}) to back (8 km s^{-1}).

data, CLUMPFIND typically finds features on a limited range of scales, above but close to the physical resolution of the data, and its results can be overly dependent on input parameters. By tuning CLUMPFIND's two free parameters, the same molecular-line data set⁸ can be used to show either that the frequency distribution of clump mass is the same as the initial mass function of stars or that it follows the much shallower mass function associated with large-scale molecular clouds (Supplementary Fig. 1).

Four years before the advent of CLUMPFIND, 'structure trees'⁹ were proposed as a way to characterize clouds' hierarchical structure

using 2D maps of column density. With the help of 2D work as inspiration, we have developed a structure-identification algorithm that abstracts the hierarchical structure of a data cube into an easily visualized representation called a dendrogram, a technique well developed in other data-intensive applications. Dendrograms find application of tree methodologies so far as they go, and almost exclusively within the astrophysics community. 'merger trees' are being used with increasing frequency.

Figure 3 and its legend explain the dendrogram process schematically. The dendrogram of a data cube is determined almost entirely by the choice of a test level, the sensitivity to algorithm parameters, and the choice of what is possible on paper and 2D screen. The dendrogram of a data cube (see Fig. 3 and its legend) is a cross, which eliminates dimensions, preserving all information. Numbered 'billiard ball' labels are used to track features between a 2D map (online) and a sorted dendrogram.

A dendrogram of a spectrum shows the hierarchy of key physical properties. The dendrogram of a surface, such as radius (K), velocity dispersion (km s^{-1}), or luminosity (L). The volumes can have any shape, and the dendrogram shows the significance of the especially elongated features (Fig. 2a). The luminosity is an approximate proxy for mass, such that $M_{\text{lum}} = X_{13\text{CO}} L_{13\text{CO}}$, where $X_{13\text{CO}} = 8.0 \times 10^{20} \text{ cm}^{-2} \text{ K}^{-1} \text{ s}$ (ref. 15; see Supplementary Methods and Supplementary Fig. 2). The derived values for size, mass and velocity dispersion can then be used to estimate the role of self-gravity at each point in the hierarchy, via calculation of an 'observed' virial parameter, $\alpha_{\text{obs}} = 5\sigma_v^2 R / GM_{\text{lum}}$. In principle, extended portions of the tree (Fig. 2, yellow highlighting) where $\alpha_{\text{obs}} < 2$ (where gravitational energy is comparable to or larger than kinetic energy) correspond to regions of p - p - v space where self-gravity is significant. As α_{obs} only represents the ratio of kinetic energy to gravitational energy at one point in time, and does not explicitly capture external over-pressure and/or magnetic fields¹⁶, its measured value should only be used as a guide to the longevity (boundedness) of any particular feature.

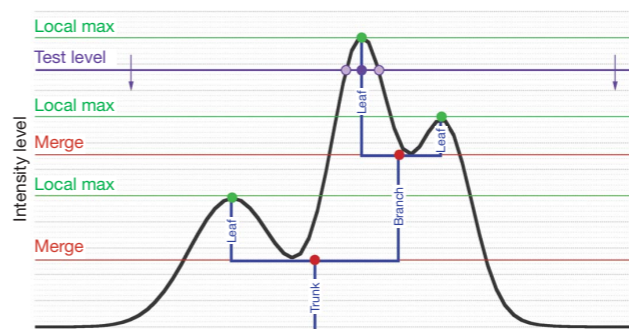
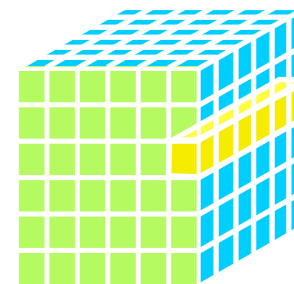
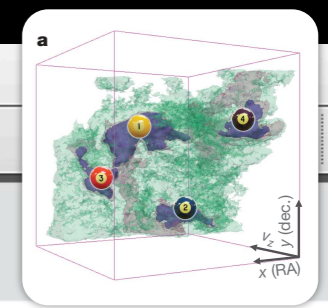


Figure 3 | Schematic illustration of the dendrogram process. Shown is the construction of a dendrogram from a hypothetical one-dimensional emission profile (black). The dendrogram (blue) can be constructed by 'dropping' a test constant emission level (purple) from above in tiny steps (exaggerated in size here, light lines) until all the local maxima and mergers are found, and connected as shown. The intersection of a test level with the emission is a set of points (for example the light purple dots) in one dimension, a planar curve in two dimensions, and an isosurface in three dimensions. The dendrogram of 3D data shown in Fig. 2c is the direct analogue of the tree shown here, only constructed from 'isosurface' rather than 'point' intersections. It has been sorted and flattened for representation on a flat page, as fully representing dendrograms for 3D data cubes would require four dimensions.

Goodman et al. 2009, Nature,
cf. Fluke et al. 2009

2009
3D PDF
HIGH-DIMENSIONAL
DATA IN A
"PAPER"





LETTERS

A role for self-gravity at multiple length scales in the process of star formation

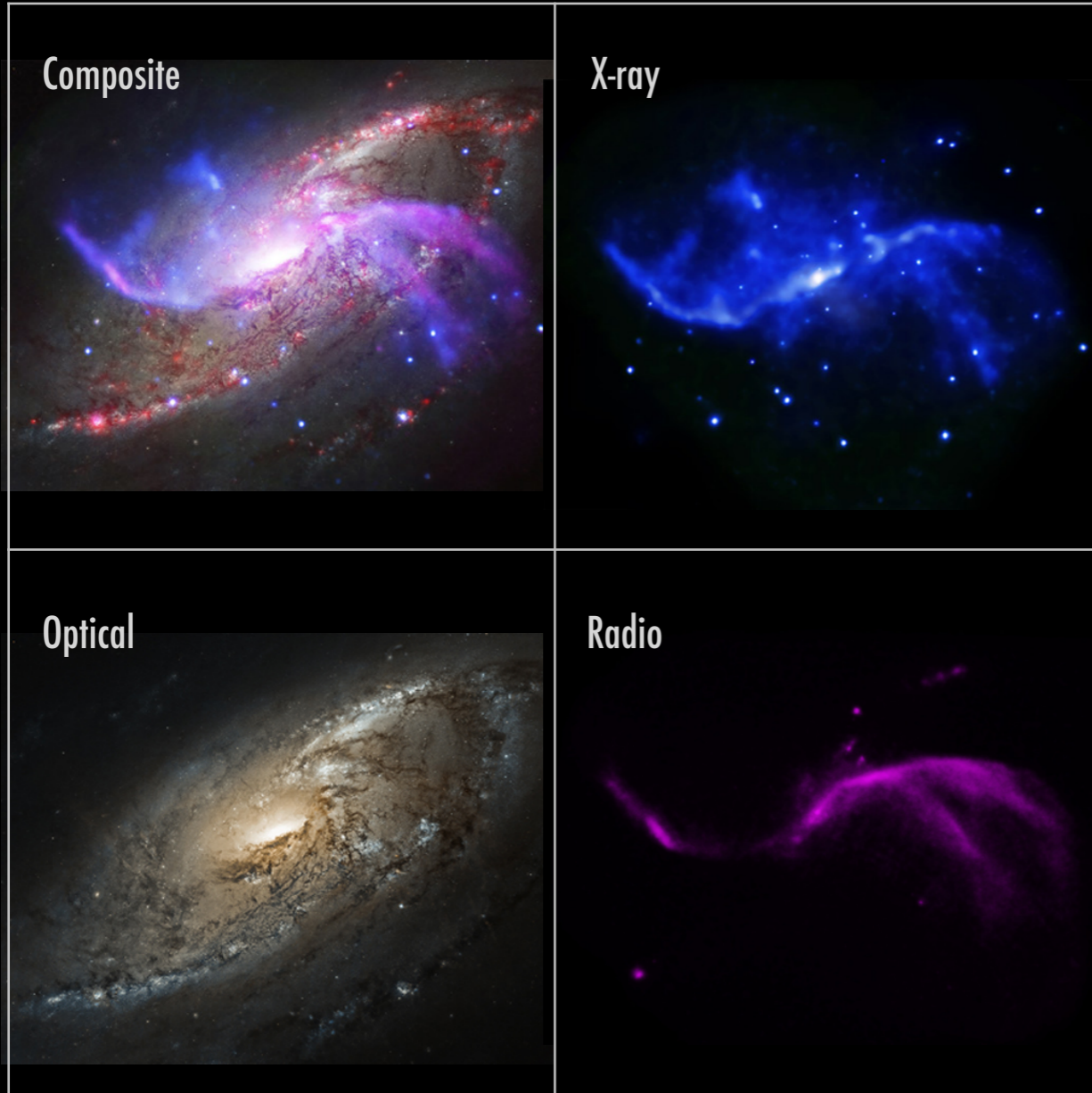
Alyssa A. Goodman^{1,2}, Erik W. Rosolowsky^{2,3}, Michelle A. Borkin^{1†}, Jonathan B. Foster², Michael Halle^{1,4}, Jens Kauffmann^{1,2} & Jaime E. Pineda²

Self-gravity plays a decisive role in the final stages of star formation, where dense cores (size ~ 0.1 parsecs) inside molecular clouds collapse to form star-plus-disk systems¹. But self-gravity's role at earlier times (and on larger length scales, such as ~ 1 parsec) is unclear; some molecular cloud simulations that do not include self-gravity suggest that 'turbulent fragmentation' alone is sufficient to create a mass distribution of dense cores that resembles, and sets, the stellar initial mass function². Here we report a 'dendrogram' (hierarchical tree-diagram) analysis that reveals that self-gravity plays a significant role over the full range of possible scales traced by ¹³CO observations in the L1448 molecular cloud, but not everywhere in the observed region. In particular, more than 90 per cent of the compact 'pre-stellar cores' traced by peaks of dust emission³ are projected on the sky within one of the dendrogram's self-gravitating 'leaves'. As these peaks mark the locations of already-forming stars, or of those probably about to form, a self-gravitating cocoon seems a critical condition for their exist-

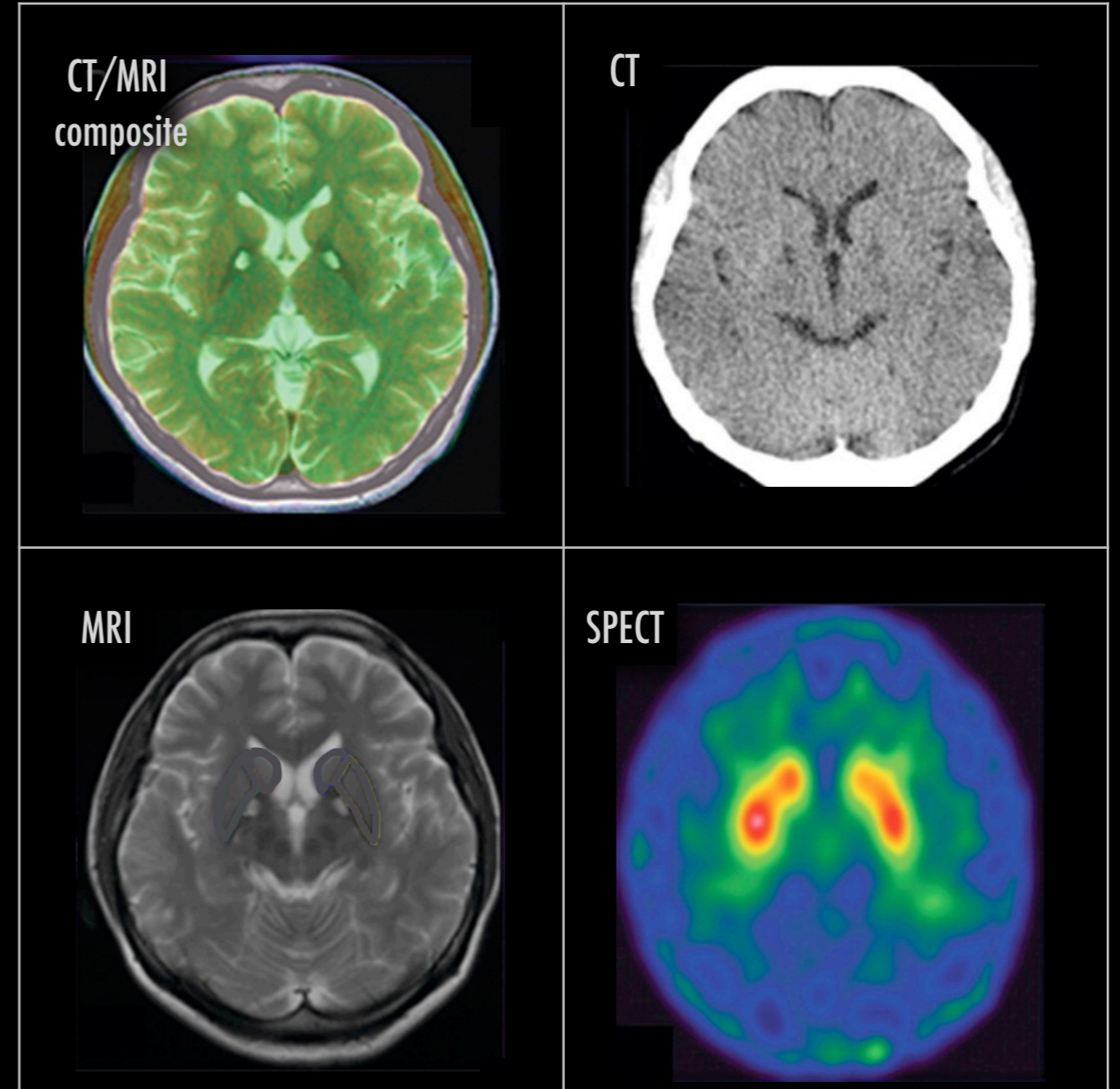
overlapping features as an option, significant emission found between prominent clumps is typically either appended to the nearest clump or turned into a small, usually 'pathological', feature needed to encompass all the emission being modelled. When applied to molecular-line



ASTRONOMICAL MEDICINE



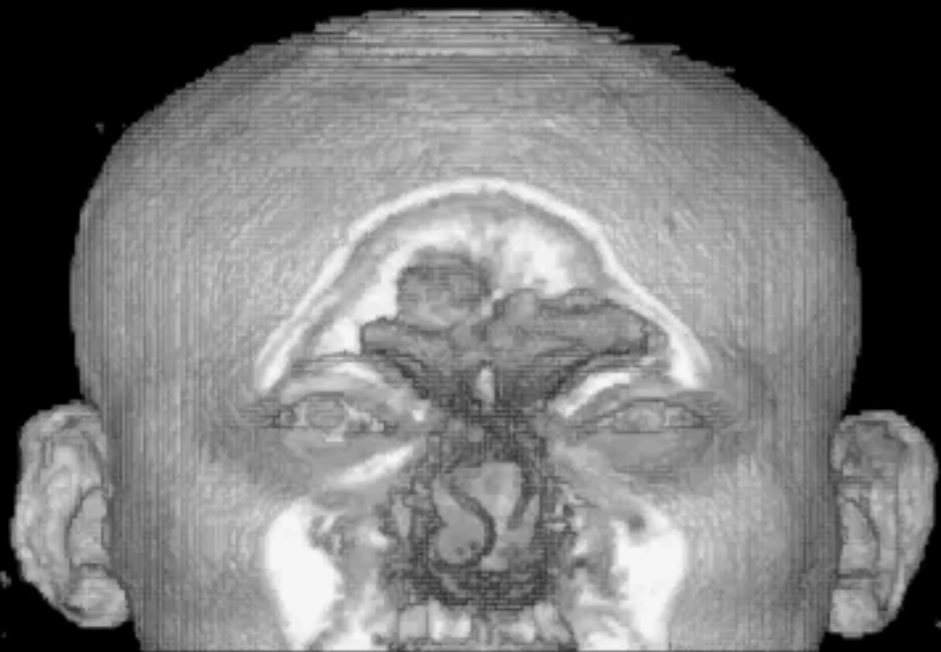
chandra.harvard.edu/photo/2014/m106/



Chang, et al. 2011, brain.oxfordjournals.org/content/134/12/3632

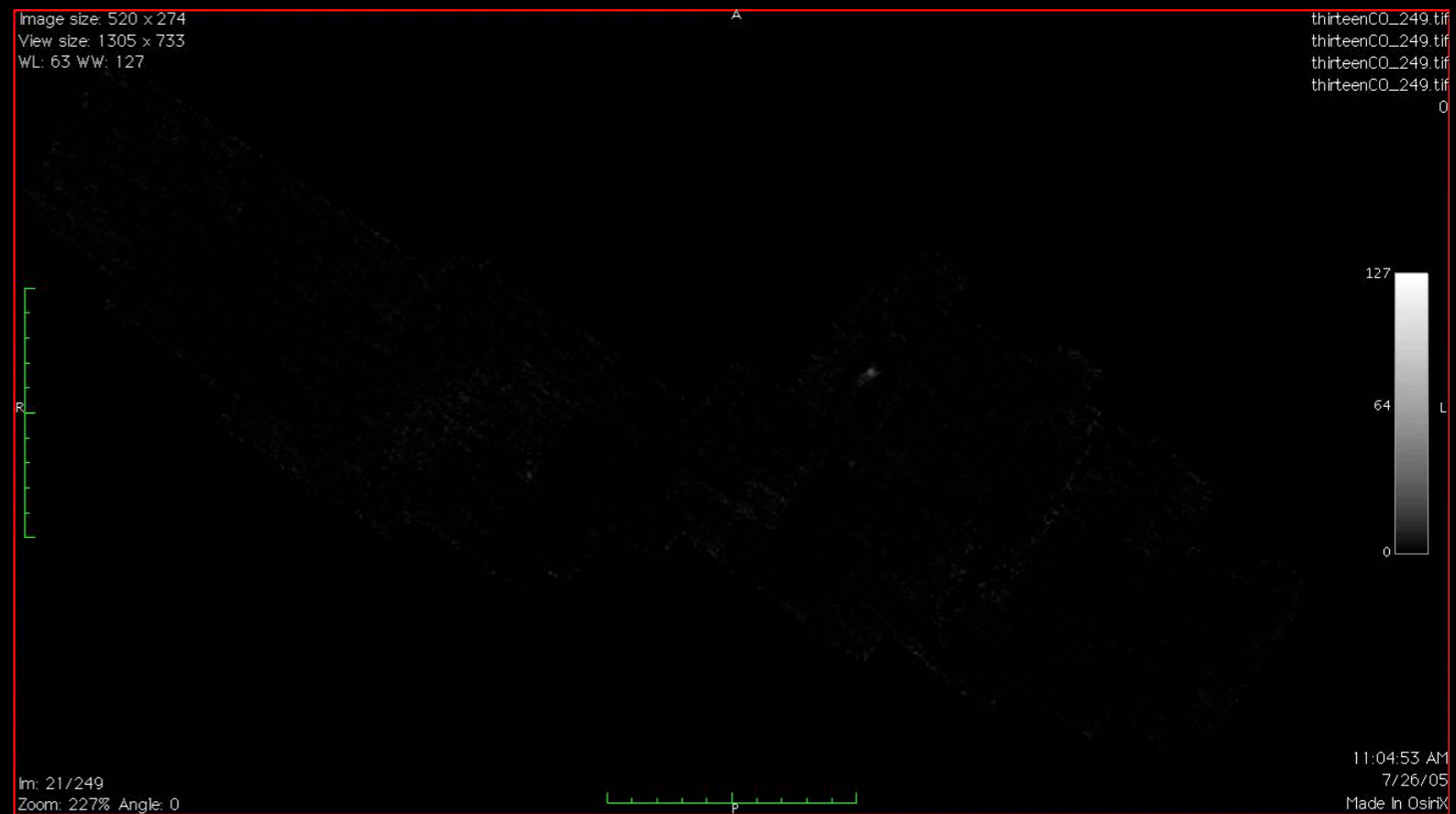
ASTRONOMICAL MEDICINE

"KEITH"



"z" is depth into head




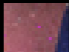

"PERSEUS"

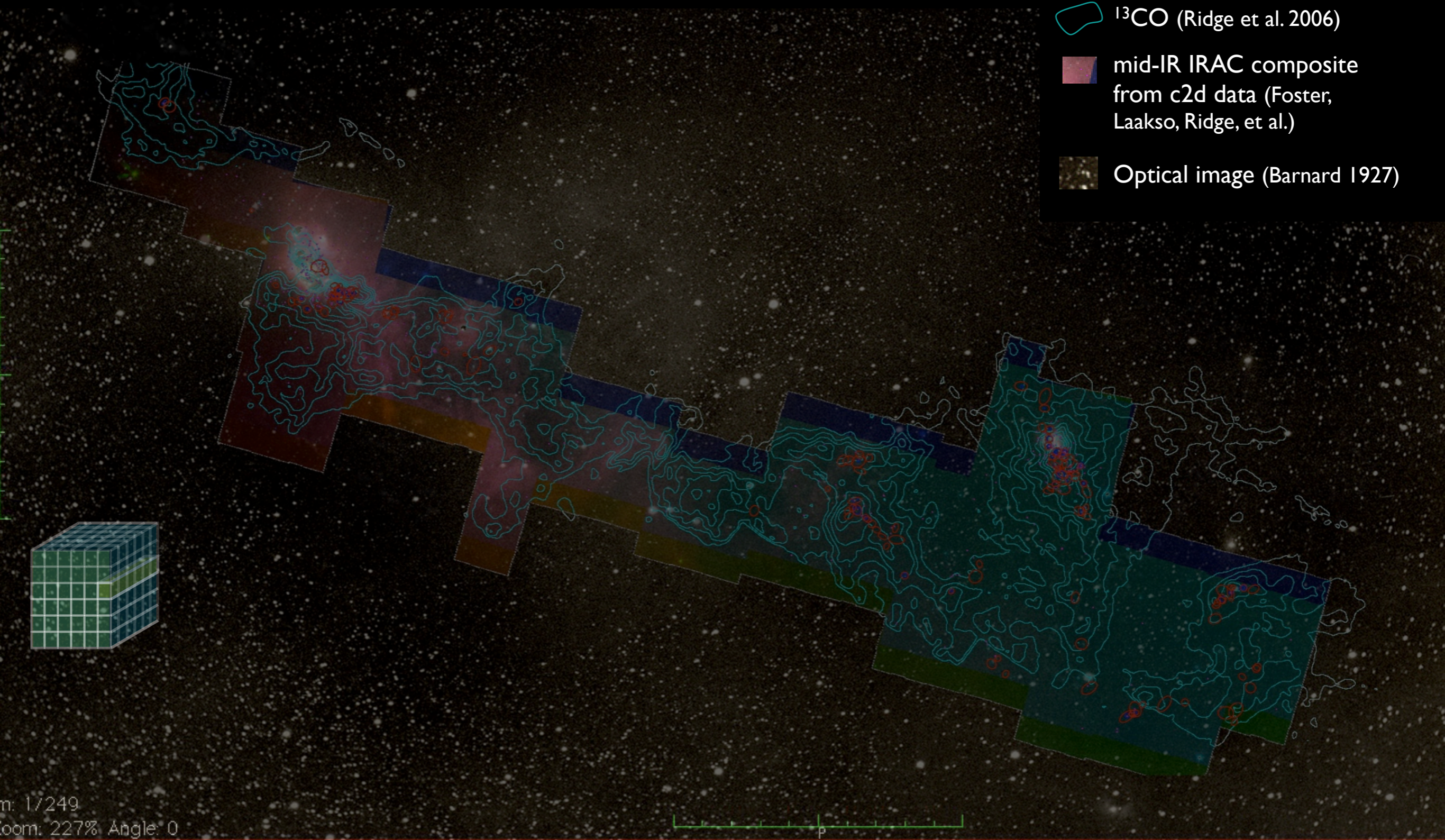


"z" is line-of-sight velocity

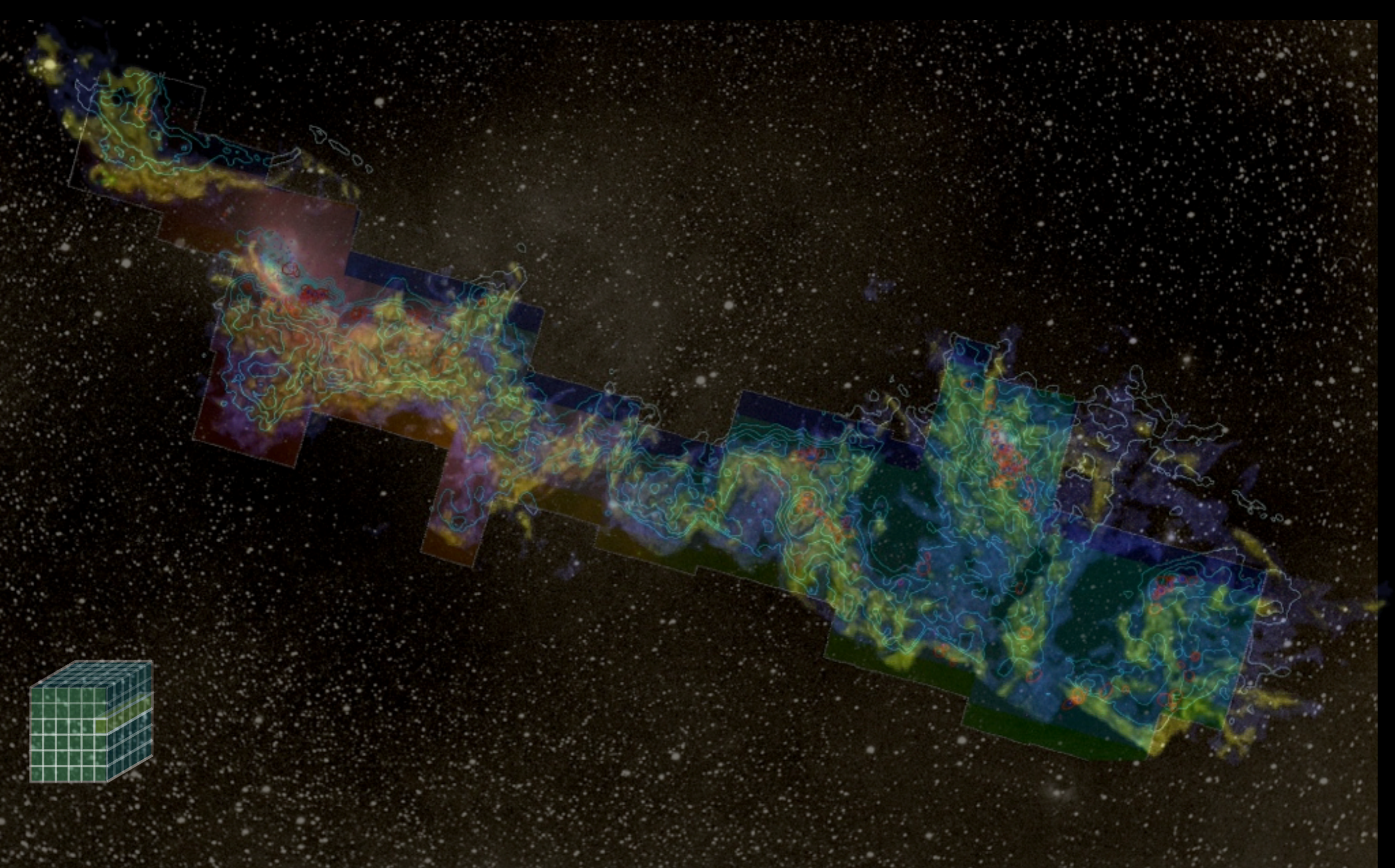
Image size: 520 x 274
View size: 1305 x 733
W/L: 63 WW: 127

ASTRONOMICAL MEDICINE

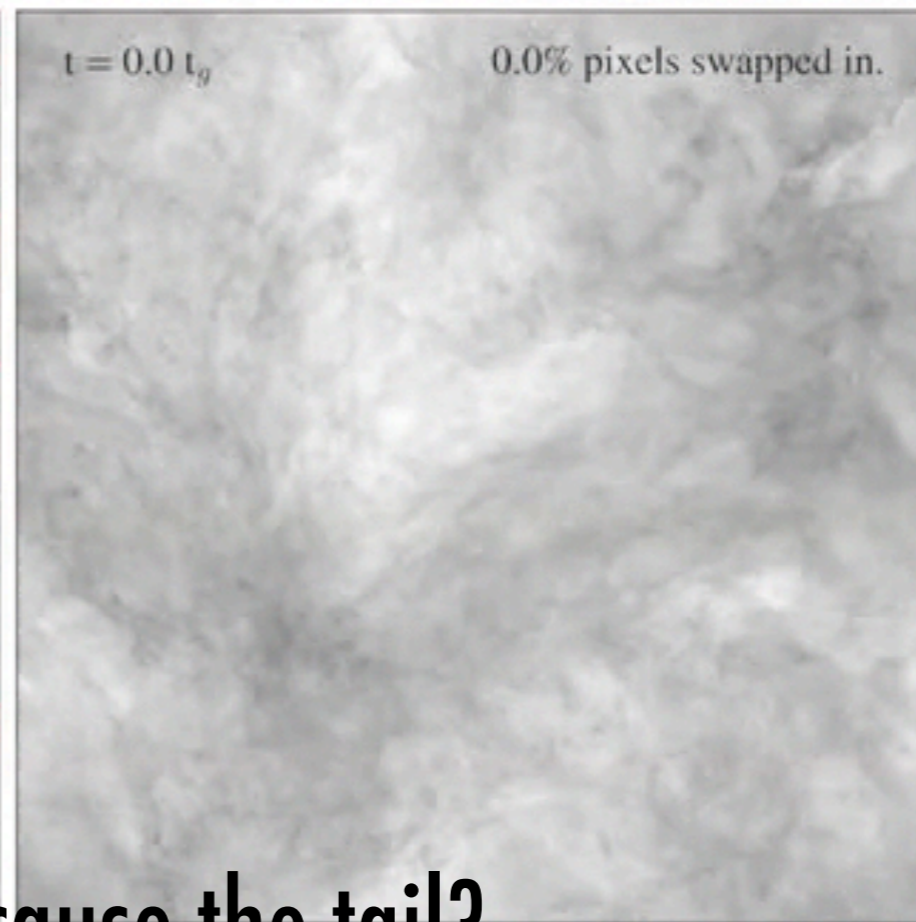
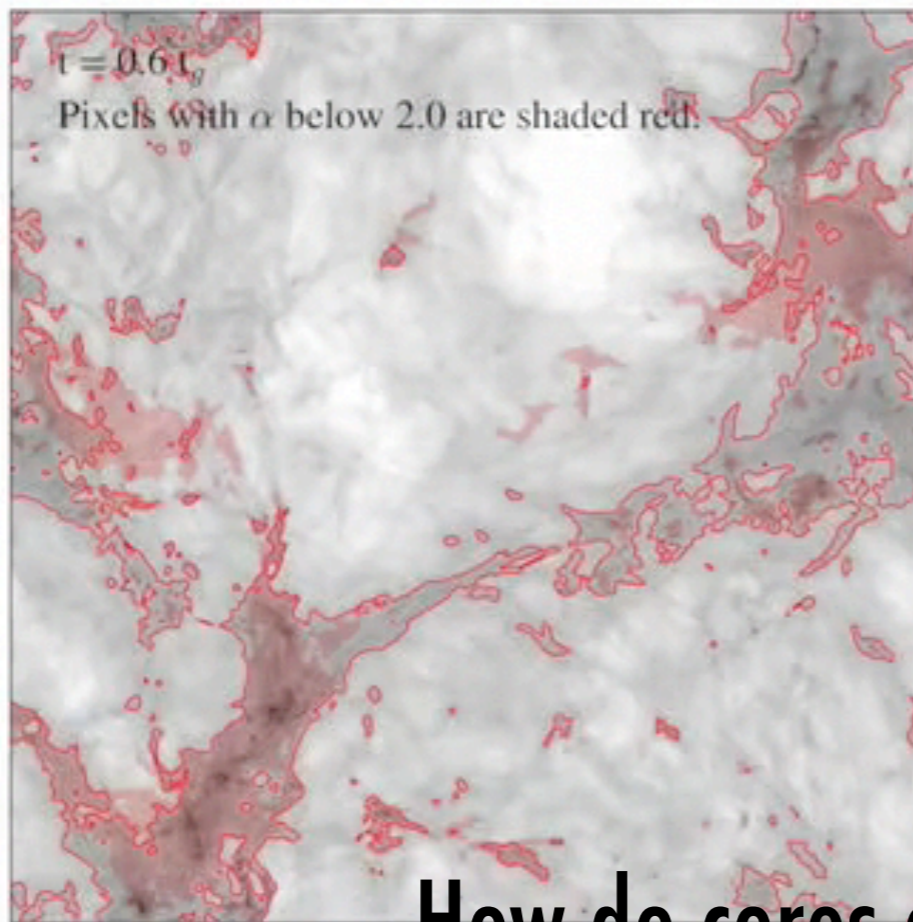
-  mm peak (Enoch et al. 2006)
-  sub-mm peak (Hatchell et al. 2005, Kirk et al. 2006)
-  ^{13}CO (Ridge et al. 2006)
-  mid-IR IRAC composite from c2d data (Foster, Laakso, Ridge, et al.)
-  Optical image (Barnard 1927)



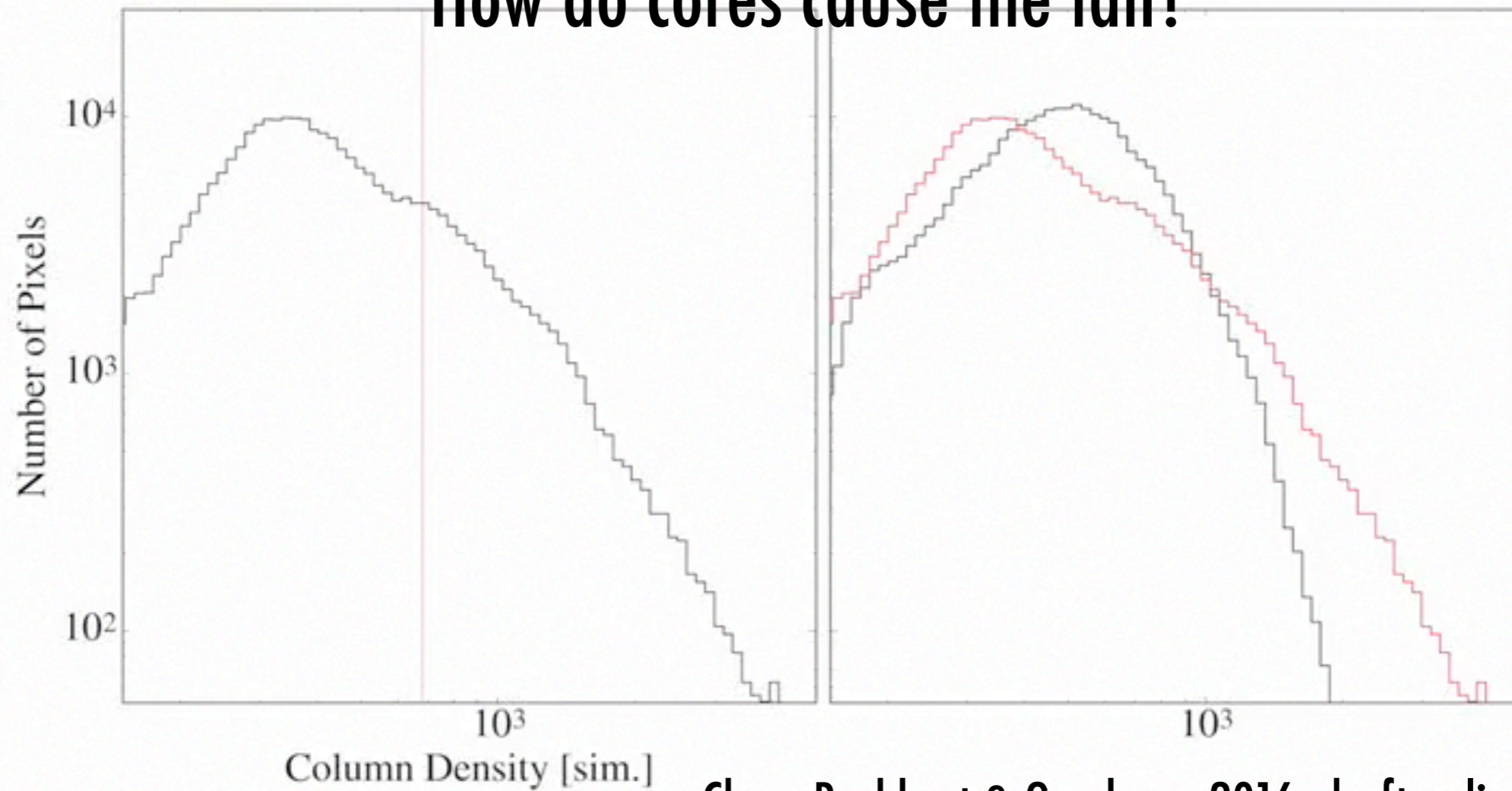
m: 1/249
Zoom: 227% Angle: 0

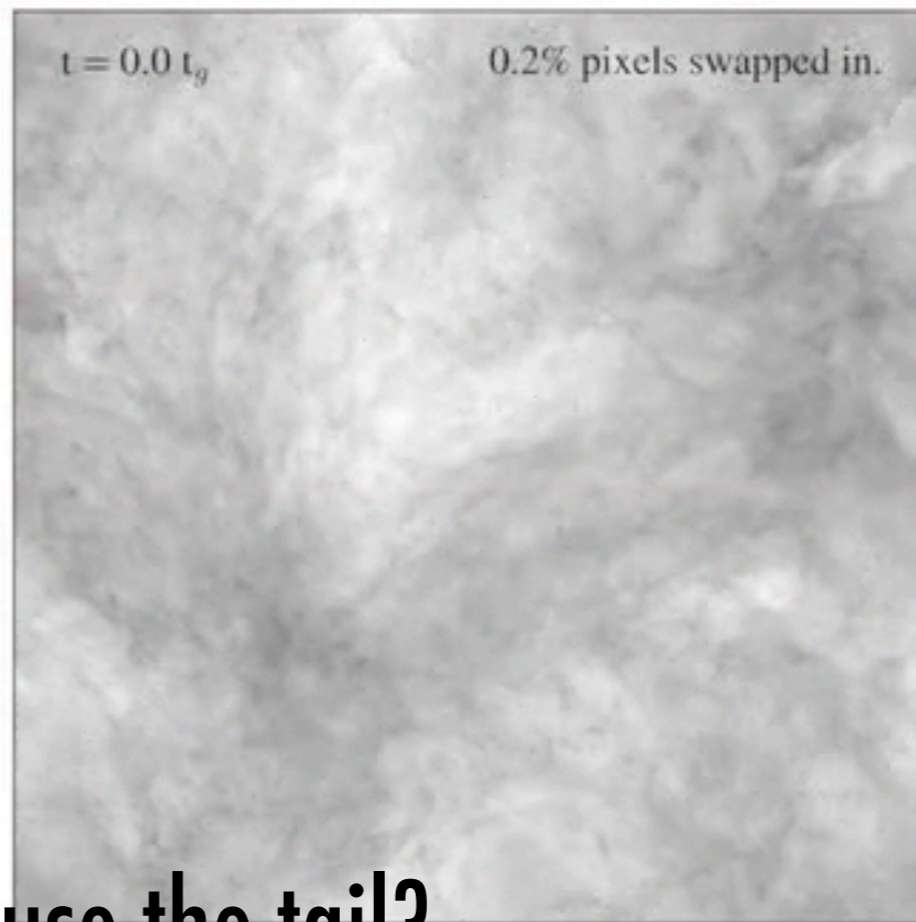
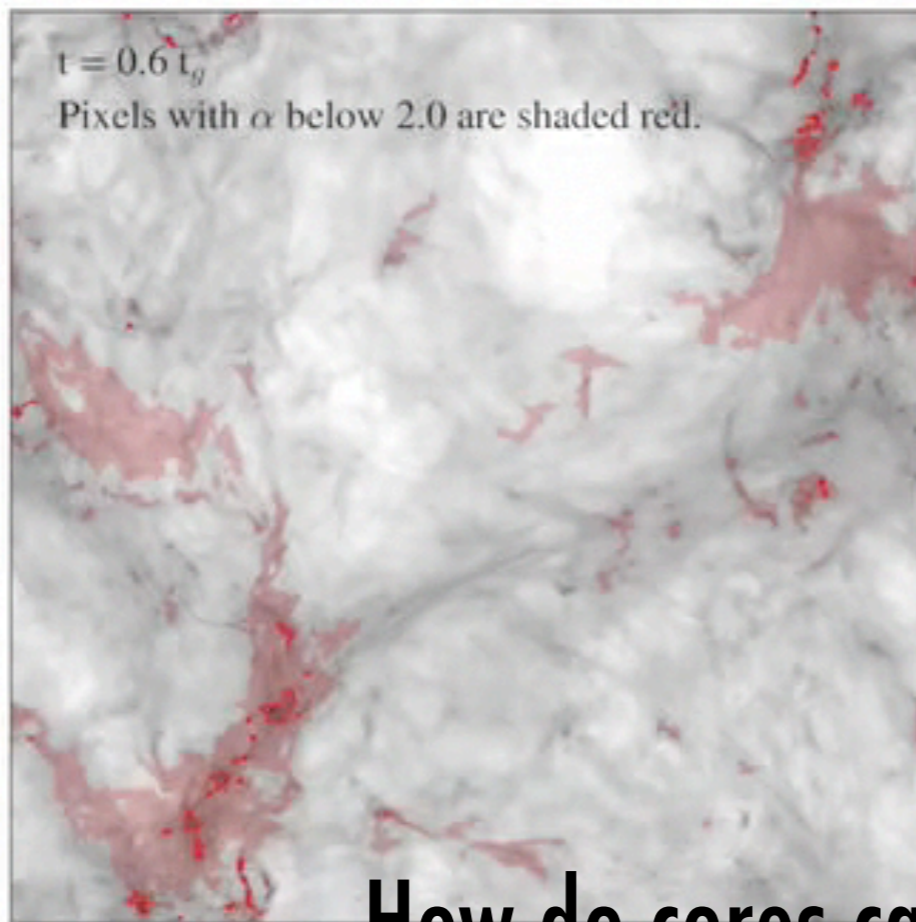


3D Viz made with VolView

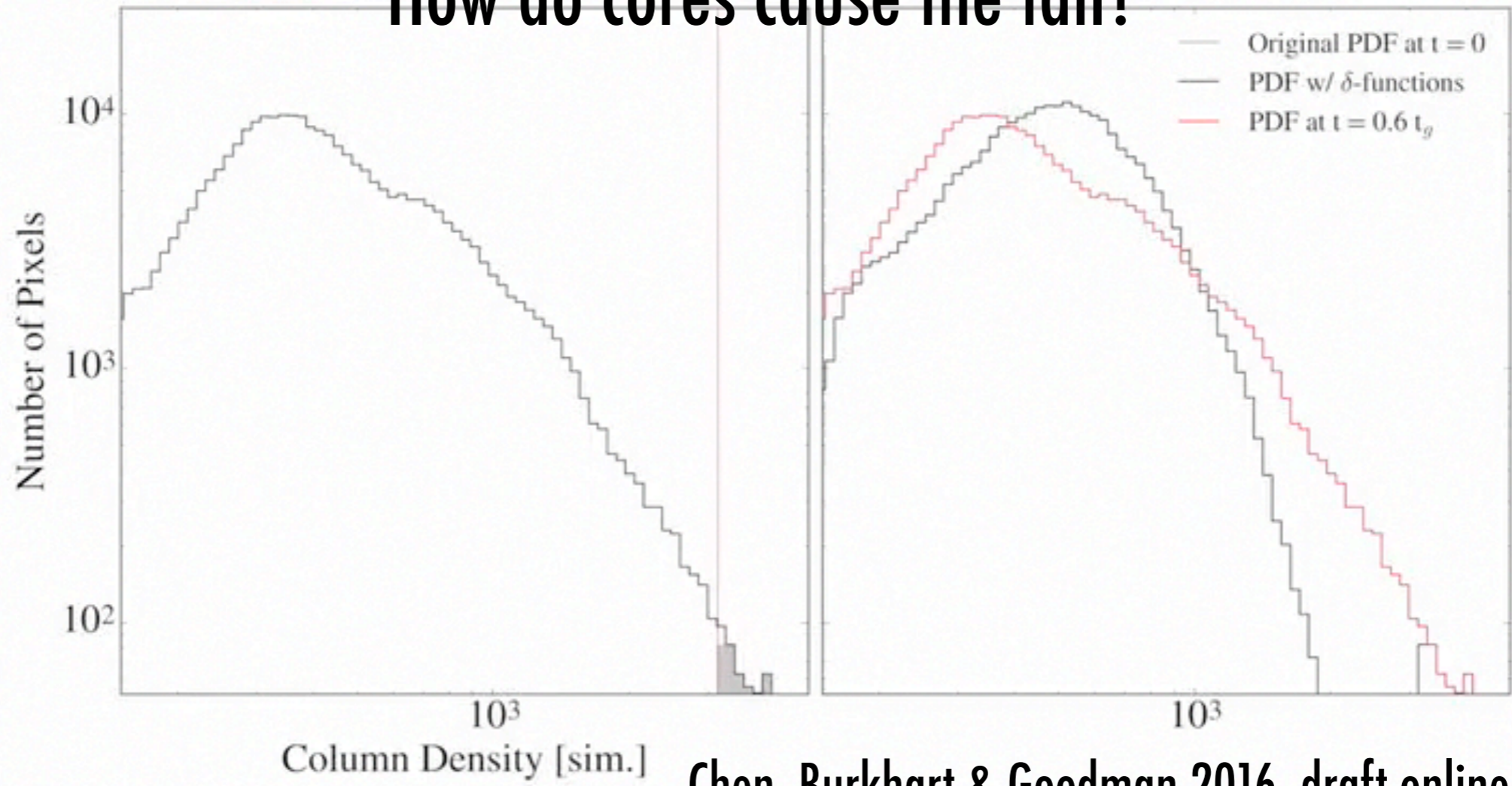


How do cores cause the tail?

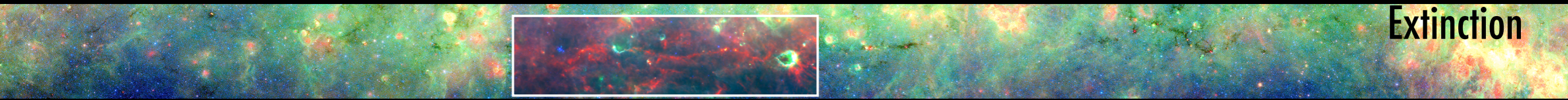




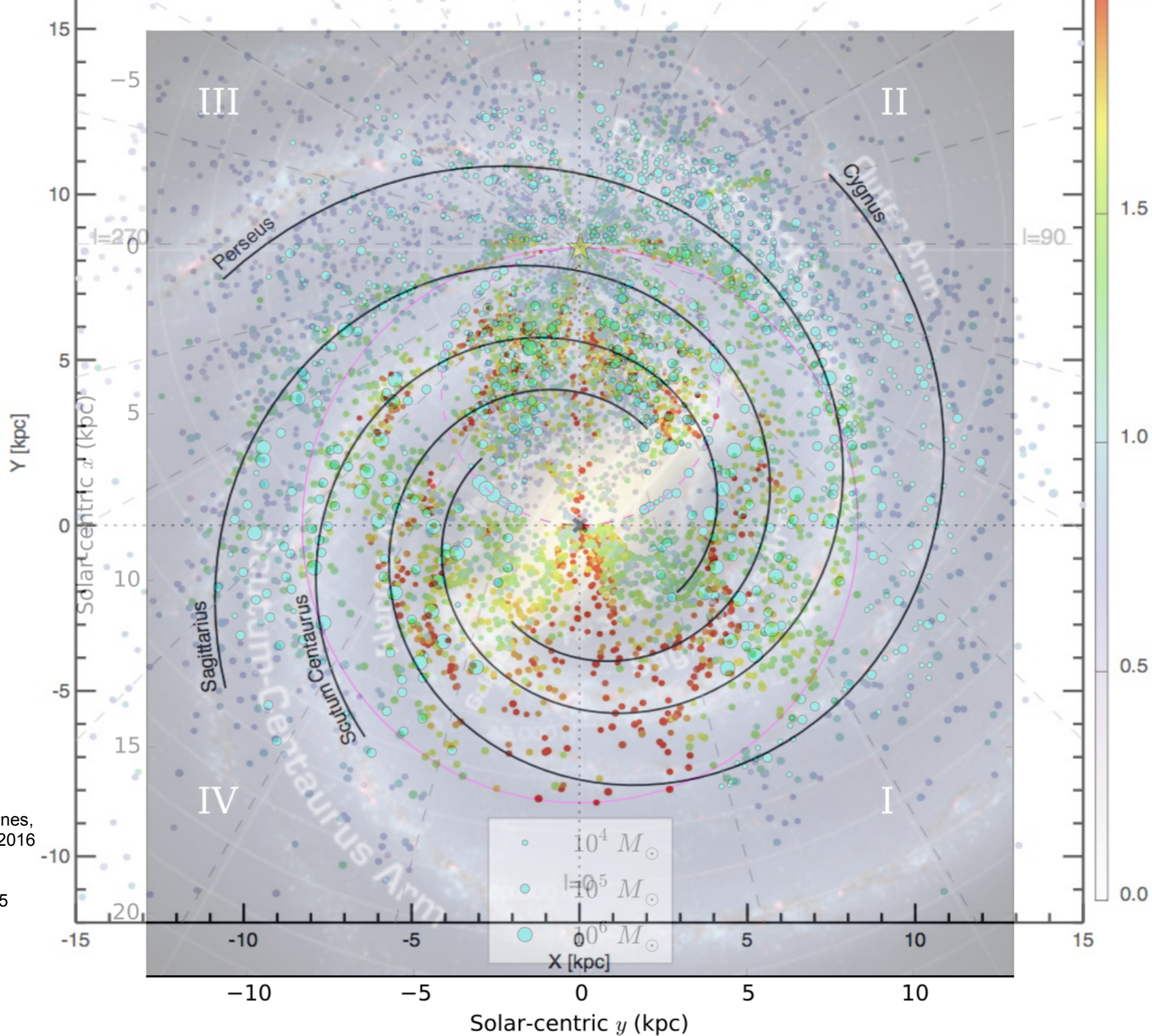
How do cores cause the tail?



NESSIE



Bottom panel: **Red**=column density from Herschel, **green**=70 micron data from Herschel, and **blue**= 8 micron data
image courtesy of Cara Battersby



Miville-Deschênes,
Murray & Lee 2016
(transparent)

Rice et al. 2015
(colored)